Power and Fuel Economy Optimization of Unthrottled Spark-Ignition Engines Using Highly Flexible Hydraulic Variable Valve Actuation System

by

Yangtao Li

A thesis
presented to the University of Waterloo
in fulfillment of the
thesis requirement for the degree of
Doctor of Philosophy
in
Mechanical and Mechatronics Engineering

Waterloo, Ontario, Canada, 2018

Examining Committee Membership The following served on the Examining Committee for this thesis. The decision of the Examining Committee is by majority vote.

External Examiner	NAME: Ming Zheng
	Title: Professor, Mechanical, Automotive and Materials Engineering
Supervisor(s)	NAME: Amir Khajepour
	Title: Professor, Mechanical and Mechatronics Engineering
	NAME: Cécile Devaud
	Title: Professor, Mechanical and Mechatronics Engineering
Internal Member	NAME: Roydon Fraser
	Title: Professor, Mechanical and Mechatronics Engineering
Internal Member	NAME: Zhongchao Tan
	Title: Professor, Mechanical and Mechatronics Engineering
Internal-external Member	NAME: Nasser Lashgarian Azad
	Title: Associate Professor, Systems Design Engineering

AUTHOR'S DECLARATION

This thesis consists of material all of which I authored or co-authored: see Statement of Contributions included in the thesis. This is a true copy of the thesis, including any required final revisions, as accepted by my examiners.

I understand that my thesis may be made electronically available to the public.

Statement of Contributions

Chapter 4, 5 and 6 are containing contents that are in an article published in Applied Energy on Sept. 4th, 2017, available online: https://www.sciencedirect.com/science/article/pii/S0306261917312412, by Yangtao Li (myself), Amir Khajepour (my supervisor), Cécile Devaud (my co-supervisor) and Kaimin Liu (visiting PhD student from Hunan University, China), "Power and Fuel Economy Optimizations of Gasoline Engines Using Hydraulic Variable Valve Actuation System". In which, Mr. Liu provided great support for building the GT-Suite model of the engine and helped with the experiments for model calibration.

Chapter 5 and Chapter 6 include some of the contents that are appeared in an article entitled "Realization of Variable Otto-Atkinson Cycle Using Variable Timing Hydraulic Actuated Valve Train for Performance and Efficiency Improvements in Unthrottled Gasoline Engines" by Yangtao Li (myself), Amir Khajepour (my supervisor), Cécile Devaud (my co-supervisor), which has been submitted to Applied Energy on the submission date of Dec. 25th, 2017 and has been accepted on the date of Apr. 5th, 2018. These above mentioned two articles were both written by myself and revised by my supervisors.

In Chapter 7, the experimental studies are accomplished as a teamwork. In which, the detailed contributions of all the involved team members are mentioned as follows. Matthew Chermesnok and Mohammad Sharif Siddiqui, fellow graduate students (Master), made improvements on the mechanical design of the HVVA system as well as involved in the manufacturing and assembly processes of the HVVA system and its test bench. Mitchell Terpstra, fellow graduate student (Master), participated in the assembly of the engine test bench and the experimental tests of the HVVA prototype engine. Jeff Graansma and Jeremy Reddekopp, lab technicians, offered a great deal of technical supports and advises on setting up the engine test bench and tuning the test equipment. I, myself, were involved in the designing, assembly, and tuning stages of the HVVA engine and its test bench. Furthermore, I was in charge of designing and conducting the specific experimental tests for validating the introduced HVVA engine operation strategies that are proposed in this research, and guided the team through the works of engine and equipment calibrations, bench test operations, and troubleshooting procedures.

Abstract

Variety of technologies along with the mechanisms for their implementations have been developed in order to pursue possible improvements in the performance and efficiency of gasoline engines. Yet, most of the commonly used techniques, such as the cam-based variable valve timings (VVT) and variable compression ratio (VCR), are realized by different kinds of complicated mechanisms, providing an extended but still relatively limited adjustability, for attaining improved valve timings and different engine cycles according to the varying working conditions of the engine.

The hydraulic variable valve actuation (HVVA) system, however, can provide greater freedoms to the engine valve motions than most of the traditional cam-based valve train systems do. By considering the characteristics of the HVVA system, the strategies of putting its outstanding flexibilities into use for further improving the performances of gasoline engines with respect to power and fuel economy are developed in this research. By utilizing the flexibility offered by the HVVA system, a set of new valve motion strategies is developed for realizing an unthrottled engine load control.

In this research, the late exhaust valve closure (LEVC) and early intake valve closure (EIVC) strategies are adopted at the same time for granting the engine an internal exhaust gas recirculation (IEGR) feature and together evolved into a tunable IEGR scheme for fulfilling the partial engine loads without throttling. Alternatively, the realization to the proposed variable Atkinson cycle (VAC), which is realized by late intake valve closures (LIVCs), can also achieve the same goal of unthrottled engine load control for partial load operations.

Moreover, an HVVA engine model is proposed and built in GT-suite, which is able to capture the interdependencies of the HVVA system and the engine operations, and is as well carefully calibrated by experimental data acquired from individual bench tests of the HVVA system and the baseline engine. The HVVA engine in this research is a converted from a baseline single-cylinder engine and is able to carry out a variable Otto cycle (VOC) at full engine load operations for achieving higher power performance while realizing a variable Atkinson cycle (VAC) or a tunable IEGR feature at partial engine load operations for gaining better fuel economy without having any further modifications or attaching additional components to the engine.

In addition, a set of genetic algorithm (GA)-based optimization schemes is also developed for identifying the proper operating parameters of the HVVA engine when adopting any of the proposed

engine operation schemes. A MATLAB-Simulink and GT-Suite coupling simulation structure is proposed for carrying out the GA approaches. Furthermore, these GA optimizers are designed to be capable of maintaining their proper functionality while non-linear constraints are taken into considerations.

By running the HVVA engine with the optimized operating parameters identified by the proposed GA optimizations, noticeable improvements on the engine outputs at full load operations and fuel economy at partial load operations are revealed. Benefited from the features of the HVVA system, the tunings of the HVVA engine can be flexibly customized to fulfill any requirements towards different desired engine characteristics.

At last, with the corresponding operating parameters be optimized by the proposed GA optimization techniques, all the proposed HVVA valve motion strategies are carried out by an actual prototype HVVA engine and are qualitatively validated by experiments. The experimental results are showing expected outcomes on the improvements to the engine's power and fuel economy performances under corresponding operations. A power improvement of 12.3% is noticed from the experiments by running the HVVA engine in the proposed VOC operation at the exemplary 1000rpm engine speed. In addition, comparing to the throttled operation of the baseline engine, the experiment studies show also the HVVA engine is able to run with leaner air-fuel mixtures to achieve the same desired partial engine load operations by adopting the IEGR scheme or the VAC operation. With an adopted air-fuel ratio (AFR) of 16.1 for the IEGR scheme and 16.3 for the VAC scheme, the engine could realize the same exemplary speed-load operation of 1000rpm/5.2Nm, while the baseline engine with throttling load control requires an AFR of 14.7 to achieve the same partial load operation.

Acknowledgements

I hereby want to express my sincere gratitude to my supervisors, Prof. Amir Khajepour and Prof. Cécile Devaud, for their patient guidance and precious opinions that helped me to proceed with my research. Also, special thanks are owed to Prof. Jing Yang and her research teams from both Hunan University and Chongqing University of Technology, China, who provided a great deal of technical support to this research and generously shared their experimental facilities.

At last, I wish to thank all my fellow graduate students and researchers in the lab, who have made my life during the study so colorful.

Dedication

This thesis is dedicated to my dear mother, who has raised and taught me into the person I am today. The accomplishment of this work would not have been possible without her. I would like to take this opportunity to thank her, for literally everything.

Table of Contents

List of Figures

xiii

xiv

Figures in Appendixes

List of Tables

Nomenclature

HVVA	hydraulic variable valve actuation
VVT	variable valve timing
VCR	variable compression ratio
(L/E)IVO	(late/early) intake valve opening
(L/E)IVC	(late/early) intake valve closing
(L/E)EVO	(late/early) exhaust valve opening
(L/E)EVC	(late/early) exhaust valve closing
IEGR	internal exhaust gas recirculation
(V)OC	(variable) Otto cycle
(V)AC	(variable) Atkinson cycle
GA	genetic algorithm
ANN	artificial neural networks
VE (or η_v)	volumetric efficiency
SI	spark-ignition
IC	internal combustion
SA	spark angle
AFR	air-fuel ratio
ECU	engine control unit

BSFC	brake specific fuel consumption
HPSV	high pressure spool valve
LPSV	low pressure spool valve
TPA	tangent position angle
CA	crank angle (degree)
ECR	effective compression ratio
EER	effective expansion ratio
VOAC	variable Otto-Atkinson cycle
BMEP	brake mean effective pressure
IMEP	indicated mean effective pressure
WOT	wide open throttle
P_e	effective engine power
n (rpm)	engine speed (revolution per minute)
T	engine output torque
W_i	indicated work
Q_{fuel}	total energy contained by the burnt fuel per cylinder per engine cycle
η_i	indicated thermal efficiency

P_m	mechanical power loss due to frictions
P_i	indicated engine power
γ	fuel consumption rate in grams per hour
T(F)DC	top (firing) dead center
BDC	bottom dead center
d	absolute distance between the centers of the spool and casing ports measured on the planarized surface of their relative motion
A_{flow}	instantaneous flow area of the spool valves
r	casing ports and spool ports radius of the spool valves
m	overall moving mass of per engine valve
x	engine valve lift
A_h	effective area of the hydraulic piston
P_h	pressure within the hydraulic cylinder
k	valve spring stiffness
$F_{pressure}$	resultant force on valve due to non-equivalent gas pressures on both sides of the valve head
$F_{contact}$	contact force between the engine valve and the engine body at both ends of the valve travel

$F_{preload}$	preload force of the valve spring
F_f	frictions to the valve motion
C	a designed pre-decided threshold lift
F_k	kinematic friction resulted from both the moving contacts between parts and the damping effects while the valve is in motion
F_s	static friction when the valve is stationary
SITurb	spark-ignition turbulent flame combustion model
u	vector for 4 considered GA variables
v	vector for 6 considered GA variables
KI_{LIMIT}	corresponding KI value calibrated to the engine knock limit
TPAHE	TPA timings for HPSV of the exhaust valve
TPALE	TPA timings for LPSV of the exhaust valve
TPAHI	TPA timings for HPSV of the intake valve
TPALI	TPA timings for LPSV of the intake valve
λ (Lambda)	air-fuel equivalence ratio
KI	knock index
$Torq$	resultant engine torque evaluated by the HVVA engine model
$\Lambda, \Psi, f_1, f_2, f_3, f_4, g_1, g_2, g_3, g_4$	designed GA penalty functions

$W_{KI}, W_1, W_2, W_3, W_4, C_1, C_2, C_3, C_4$	GA weighting factors
C_{KI}, P_{static}	designed GA constant penalties
BFM_{int}	accumulated mass of the gas backflow at the intake valve
BFM_{exh}	accumulated mass of the gas backflow at exhaust valve
$T_{desired}$	desired engine torque at the partial load operations
T_{tol}	pre-described acceptable tolerance to the resultant engine torque with respect to the desired torque
HRR	apparent heat release rate
EFI	electric fuel injection
DSI	digital spark ignition

Chapter 1

Introduction

1.1 Motivation

As is well known, the engine valve motions, both timings and lifts, play a significant role in the resultant engine performances. They bring direct influences to engine pumping losses, in-cylinder turbulence and cylinder charge, that can lead to a considerable impact on the engine outputs, efficiency, and emissions [30]. Since the motion of the engine valves determines the cycle pattern of the air flow, it has dominating impacts to the engine's air exchange process, which affects not only the resultant volumetric efficiency (VE) [28], but also the subsequent combustion process. Thusly, the adoption to a set of proper valve motions is considered as one of the most essential and direct ways for achieving the desired engine performances [51]. However, since most of the commonly used valve trains, which are mostly cam-based, are only accompanied with very limited and discontinuous adjustability or even completely not adjustable [33-38], the provided valve motions are incompetent to meet the requirement of being consecutively adaptive to the varying of the engine working conditions, which is crucial when trying to optimize the engine performances as much as possible in terms of any chosen aspect with respect to any current-running speed-load operation of the engine.

   With the development of the valve train technologies, the flexibility provided by the valve systems has become higher and higher, and transcended the quantitative changes into qualitative changes. With it, not only the air exchange process of the engine could be better optimized for traditional engine operations, but also different engine cycles and operating techniques could be realized. Hence, the engine performance should be able to be further improved in terms of power, fuel economy, and even emissions by properly taking advantage of the new features of highly flexible valve trains.

1.2 Research Objectives

With the most commonly used cam-based valve train systems, even functioned with a variable valve timing (VVT) feature, the valve opening timings and closing timings cannot be fully and simultaneously optimized in a continues manner across the entire engine speed range. Hence, the tunings of the engine can only lay single emphasis on or make sacrifices among different required characteristics of the engine. In another word, most of the these engines can only be designed for either achieving higher power performance or gaining better fuel economy, or most likely accepting a

1

balanced or favored tradeoff in between, via designing the accordingly fit cam profiles since the valve motions will restrictedly follow the cam profiles no matter if VVT or multiple cam sets are incorporated in the valve train systems. Hence, the engine performance is not able to be optimized to a full extent at all speed-load operating points and is only allowed to be tuned towards certain pre-determined engine characteristics.

Considering these limitations and knowing the unrevealed potentials of fully flexible valve train systems, the goal of developing a series of new engine valve motion strategies for achieving different and better-optimized engine performances from utilizing a fully flexible valve train is set for this research. Differ from the cam-based VVT systems, the hydraulic variable valve actuation (HVVA) system developed in [1] can provide a full flexibility in terms of alternations to the valve timings, opening durations, and even lifts in a continuous manner to better match the valve motions to the engine operations. These features gained from the variable valve actuations could not only bring benefits to the engines that are naturally-aspirated, but also to the turbo- and super- charged ones.

In this research, a single-cylinder spark-ignition (SI) 4-stroke gasoline engine is chosen as the exemplary test engine that mounted with the HVVA system for revealing and studying the potentials of the HVVA system on further improving the engine performances in terms of power and fuel economy. To achieve this main objective, the work of this research is to be carried out by accomplishing the sub-objectives that are sorted in the following:

- After acquiring sufficient understandings to the characteristics and all the potential benefits of the HVVA system, principle studies on how would the HVVA system and its flexibility help the engine to improve its performance will be conducted. In addition, by considering the dynamics of the HVVA system, the main differences between the resultant valve lift profiles and how the valve timings to be controlled from using the HVVA system and the traditional cam-based will be addressed.

- Base valve motion strategies will be proposed according to the above-studied principles and will be roughly checked in a qualitative manner via a set of preliminary simulations performed by a simplified volumetric efficiency (VE) estimation model. Although this VE estimation model is only able to simulate the gas exchange processes upon given valve lift profiles and may not be capable of capturing the system behaviours of the HVVA system, the simulation results will still be very much valuable for providing us preliminary inspections and tendency predictions over the

2

resultant pumping losses, cylinder charges, and etc., when adopting the proposed base valve motion strategies.

- The HVVA system and the test engine will be modeled, and together evolving into a converted HVVA engine with both the modeled HVVA system and the baseline calibrated test engine. The engine will be calibrated separately through a series of individual bench tests. Modeling of the converted HVVA engine is actually quite different from modeling the baseline engine, which uses a cam-based valve train, due to the interdependency between the HVVA system and the in-cylinder states of the engine needs to be reflected, which is one of the most different and unique features of the HVVA engine comparing to the cam-based engines.

- Different developed engine valve motion strategies, which are composed of the afore-validated base valve motion strategies, will be formed for pursuing better engine performances in terms of improving the engine output at full load operations and lowering the fuel consumption at partial load operations by carrying out adaptive valve motions and distinct engine cycles. Meanwhile, a set of model-based optimization procedures will be introduced and conducted for each of the proposed strategies to quantitatively identify the corresponding operating parameters of the HVVA engine.

- An actual prototype HVVA engine will be eventually built and be set on a configurable platform for the purpose of experimental validations. A full set of the HVVA system and the counterpart engine components will be re-designed and manufactured for meeting the requirements and quality standard of the designed experiments. For the sake of gaining the features of fulfilling full spark angle (SA) control and air-fuel ratio (AFR) control, which the baseline engine does not contain but are required for validating the optimized results, an electrical sparking module and an electrical fuel injection system will be replacing the default mechanical sparking system and the carburettor of the baseline engine. Optimized results will then be verified at several typical sampling points of the engine's operation.

Eventually, in terms of applications, the work of this research can be used for providing a set of developed strategies for unthrottled HVVA engine controls, as well as the optimization techniques for identifying the corresponding operating parameters. A set of look-up tables for all the considered operating parameters of the engine could be generated offline by the optimization approaches proposed in this research, and embedded into the engine control unit (ECU) for real-time implementations. This actually can grant the engine with a configurable feature in terms of its tunings

that could make the same type of engine be able to enclose multiple characteristics without making any physical modifications to the engine components for handling different implementations with distinct preferences and requirements over the engine's performances. In fact, it can also become much easier when the engine needs to update its current tunings and make possible of the engine to be further fine-tuned by switching among up to as-many-as-needed pre-tuned operating modes that are with only slight differences from each other over the desired characteristics. Furthermore, the HVVA engine is also capable of realizing different engine cycles or switching on-and-off over the internal exhaust gas recirculation (IEGR) functionality during its running by means of the highly responsive and fully adjustable valve motions.

1.3 Thesis Outline

To make a clear scope view to the structure of this thesis, all the 8 chapters and their core contents are briefly introduced as follows:

Chapter 1 gives a general introduction to the very primal motivation of this research along with the overall goal that is set according to it. This final goal is also elaborated and broken down into several sub-objectives that corresponded with further explanations.

In Chapter 2, starting with a brief background introduction, typical existing technologies of the valve trains and the HVVA system are introduced. Different types of valve motion strategies and their implementations for improving the engine performances are also presented along with the methodologies and optimization techniques for identifying the corresponding parameters.

Chapter 3 reveals and explains the potentials of the HVVA system, then accordingly, proposes and describes the base valve motion strategies for improving the engine performances from using the HVVA system. Feasibility validations over these proposed base valve motion strategies are also performed via a VE estimation model in this chapter. Subsequently, these base valve motion strategies are evolved into the proposed HVVA engine valve motion strategies for fulfilling un-throttled load control, which can grant the engine with better-optimized performances over its power and fuel efficiency for full load and partial load operations, respectively.

Chapter 4 presents a detailed explanation to the MATLAB-Simulink and GT-Suite co-simulation model of the HVVA single cylinder gasoline engine, which is not only designed with high configurability, but also built in such way for the purpose of being able to carry out the later-proposed optimization procedures to achieve un-throttled engine load control.

Chapter 5 introduces the proposed genetic algorithm (GA)-based optimization schemes for identifying the optimal considered HVVA engine operating parameters for full load and partial load operations. The optimizations are set towards the objectives of maximizing engine output at full load and minimizing the brake specific fuel consumption (BSFC) at partial load operations under different corresponding constraints.

Chapter 6 summarizes and shows the optimized results of the HVVA engine, and makes comparisons between the performances of the baseline engine and the optimized HVVA engine. Corresponding analyses are also provided with further explanations.

Chapter 7 shows the actual set-up of the HVVA engine test bench, which is built for verifying the proposed HVVA valve motion strategies, and demonstrates the collected results obtained from the experimental validations achieved by the optimized parameters.

At last, Chapter 8 draws the conclusions and discusses the future work.

Chapter 2
Literature Review

2.1 Background and Fundamentals

As is well known, the engine valve motions, both timings and lifts, play a significant role in the resultant engine performances. They bring direct influences to engine pumping losses, in-cylinder turbulence and cylinder charge, that can lead to a considerable impact on engine outputs, efficiency and emissions.

In modern engine valve systems, not only the valve trains have become more and more diverse in their designs and driven techniques, but also their flexibilities have been considerably improved together with their designs. A higher valve actuation flexibility, generally, means that the engine valves could acquire wider variations regarding their lifts, opening and closing timings, or even following different pre-designed valve lift profiles. A valve train with higher flexibility could provide the potential of a better matching between the valve motions and the engine demands under different working conditions with respect to power, fuel economy or emissions. The characteristics of the valve motions, however, are mostly determined by the nature and design of the valve train. To improve the engine performances, many researchers and scholars studied and developed different valve motion strategies restricted to the certain characteristics and flexibility limits of different valve trains.

For gasoline engines, the famous thermodynamic operating cycle, known as the Otto cycle (OC), has been widely used for 4-stroke piston-crank-mechanism engines, especially for civic automobile industries. However, due to the crisis of the global warming and depletion of the fossil fuels, the conventional OC engines are gradually wading into the situation of having poorer and poorer matches to the tightening demands of pursuing higher efficiency and lower emissions of the modern automobile industries.

The electrification of the vehicles, however, offers solutions to these demands. On one hand, for pure electric vehicles, despite their great advantages on lowing emissions and the use of renewable energy source, there are still many limitations, such as the relatively lower power density storage of the power bank and inadequacy of the infrastructures, extensive charging durations and high overall costs [2,3]. The hybrid vehicles, on the other hand, is a more suitable and cost-efficient solution to meet the reality of nowadays use [4]. The output from the electric motors of the hybrid vehicles can compensate the trade-off between the maximum power and optimum efficiency of the engine. In

another word, while maintaining or slightly sacrificing the desired maximum power of the overall output, the engine is allowed to optimize its efficiency at the most frequent operating load points at the cost of lowering its maximum power. Therefore, the goal of pursuing higher efficiency and reserving fuels is becoming more and more crucial for the engine industries nowadays, especially for those of the hybrid vehicles.

2.1.1 Gas Exchange and Combustion Processes of IC Engines

For the IC engines, diesel or gasoline, one of the most important factors that affect the engine performances is the in-cylinder gas exchange process. For full load operations, a better gas exchange process can be generally explained as a better exhaust performance to clear out the exhaust gas more completely during the exhaust process, and a better intake performance to fill the cylinder with more fresh charge during the intake process that could together contribute to a greater VE. For partial load operations, optimizing the gas exchange process could result in less pumping work losses from both the intake and exhaust processes, which would eventually lead to a higher engine efficiency and benefit in less resultant fuel consumptions.

Moreover, the gas exchange process not only has a direct effect on the engine performance, but also significantly influences the combustion process of engines, especially for those advanced combustion techniques that require accurate controls over such process [5]. As a matter of fact, beside the geometrical design of any IC engine, it is actually the combined behavior of these two processes that dominates the engine performances for the gas exchange and the combustion processes are closely bonded to each other. Hence, sufficient understandings to the combustion process are also required in this research for ensuring that there would be no violations to the combustion principles and no causes to abnormal combustions when trying to optimize the gas exchange process in the later part of this research.

As shown in Figure 2.1, a typical illustration to the relationship between the gas exchange process and the combustion process of a modern diesel engine that equipped with a variable valve actuation (VVA) feature is presented as an example [6] to better demonstrate the interdependency of these processes.

Although it can be seen from the figure that the gas exchange process might also be affected by some added external components, such as the variable geometry turbocharger (VGT) nozzle position and the EGR valve position, the valve motions, however, are remaining as the most crucial aspect to

the gas exchange process. Furthermore, it is also clear to notice that the engine performance, in terms of outputs, emissions, fuel economy and etc., are resulted by the overall outcome of the gas exchange and combustion processes. Therefore, due to the recognition to the importance of the gas exchange and combustion processes for IC engines, a lot of related research has been conducted.
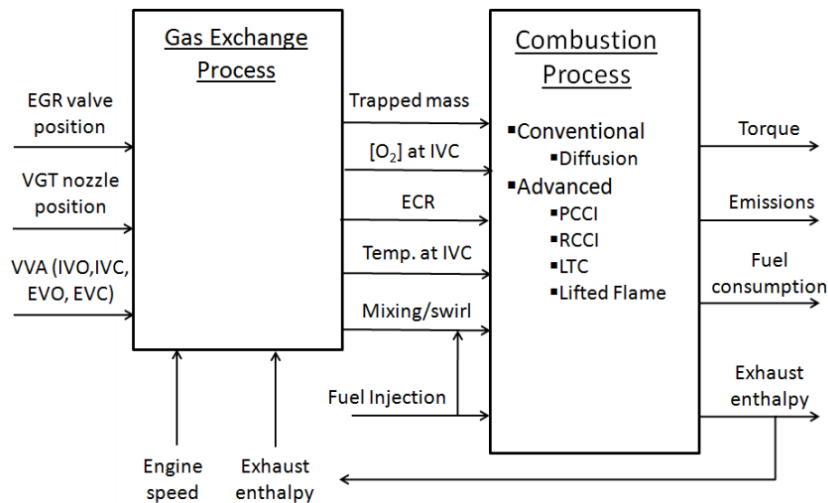
Figure 2.1 Illustration on relationship between the gas exchange process and the combustion process of a modern diesel engine [6]

On one hand, many studies were made on developing gas exchange models. Devesh Upadhyay [7] built a gas exchange model based on the sliding mode control technique, however, no solid validation from experiments was shown. J.Wang [5] also developed a control-technique-based model for describing the gas exchange process, but only performed very limited validations of the model under two prearranged test engine speeds. It should be noted that these two models are both not capable of modeling the gas exchange processes with variable valve actuations. R. Fairbrother et al. [8] proposed a combined model for gas exchange and combustion processes based on full engine cycle simulation under different valve timing. However, the experimental validation results they presented were coming from indirect measurements and the data was also very limited.

On the other hand, based on the fundamentals of the combustion process of IC engines [9,10], investigations on ignition and flame propagations were also widely conducted for studying engine combustion processes. Topics over the study of abnormal combustion processes and their causes are always the focus of research on spark-ignition (SI) engine combustion processes. In [11-14] the most

typical and common known abnormal combustion processes, namely the knocking and super-knocking combustions, were studied. These abnormal combustions are both caused by self-ignition of the pre-mixed air-fuel mixture due to the high temperature and pressure at a single or multiple discrete locations inside the cylinder [15]. Therefore, the knockings could be resulted from an inappropriate gas exchange process, especially when incautiously implementing the EGR technique [16]. The swirling flow can also affect the combustion process for IC engines, especially those direct fuel inject (DI) engines that require an organized swirl for making the fuel to be spread and better mixed with the charged air according to specific requirements [17].

2.1.2 Volumetric Efficiency Estimation

As the engine valve motions bring dominating impacts to the volumetric efficiency, which is considered as one of the most significant argument for evaluating the engine gas exchange processes and significantly affecting the engine performance, a lot of researchers dedicated their efforts on the VE modeling and estimations.

The volumetric efficiency was defined by Charles Fayette Taylor [18] as the actual charged mass of the charge mixture over its theoretical mass that fills up the piston displacement volume under the state of the intake manifold. Concerning the modeling and estimation to the volumetric efficiency, a variety of techniques and algorithms were studied in the past.

J. Chauvin et al. [19] used the experimental data from the engine tests and built up a 2-D lookup table for estimating the volumetric efficiency. The estimation results were found based on the two inputs of engine speed and the pressure within the intake manifold. Two years later, T. Leroy et al. [20] built a model for estimating the fresh air charge and residual gas fraction using three 2-D lookup tables that can capture the change of the air charge outcomes under different intake and exhaust valve closing timings. E. Hendricks et al. [21] used a function of engine speed, intake temperature, and pressure to model the volumetric efficiency while Ove F. Storset et al. [22] deduced their own function for the same task but for turbo-charged diesel engines. However, their model could not be implemented for engines with EGR features. Mrdjan Jankovic et al. [23] and G. De Nicolao et al. [24] developed a parametrical model that uses a polynomial function of fourth order to describe the volumetric efficiency based on the states of the intake manifold.

"Grey-box" or even "Black-box" models are also widely considered for volumetric efficiency estimation. Apart from the studies that use lookup tables as mentioned above, a multi-layer perception

neural network model was also implemented for volumetric efficiency estimation [24]. In 1986, Hamid B. Servati et al. [25] developed a regression model for volumetric efficiency estimation using 6 tunable parameters for an engine without VVT. An on-line estimation technique is used by Alexander Stotsky et al. [26], who introduced an input observer to better estimate the intake air mass. Also, other observer techniques were brought into this field of research. Gilles Corde et al. [27] used a Luenberger observer to estimate the air charge mass from observed charge dynamics of the engine.

A physically based approach was proposed by L. Kocher et al. [28], who developed a model that estimates the volumetric efficiency from an aspect of energy flow during the engine intake process. The energy flow from heat transfer and piston work were taken into their consideration. An analytical volumetric efficiency model for mean-value engine models was proposed by Turin, R. et al. [29]. Their model was designed for a cam-phasing VVA system and manages to estimate the volumetric efficiency according to the energy flow during the intake process.

2.2 VVT and VVA Systems

Research on the developments of the variable valve timing (VVT) and variable valve actuation (VVA) systems of engines has been conducted for many decades. It has been pointed out that better engine performance could be obtained if the valve timing could be adjusted and optimized according to the actual engine speed and load [30]. There are many different kinds of mechanisms that were developed for achieving the VVT or VVA. In the detailed review by Dresner, T. and Barkan, P. [31], a variety of valve timing changing and shifting mechanisms together with their features are well documented and classified. In this section, some typical VVT and VVA systems are reviewed, followed by the introduction to the HVVA system.

2.2.1 Common Types of the VVT and VVA Systems

For most of the cam-based VVT and VVA systems, the valve timing can be altered from a variety of different mechanisms that shift the cam-to-crank angle, and the valve lift can also be changed. However, these changes are limited from using axially varying cam profiles or switching different sets of cams [31,32]. Figure 2.2 demonstrates a group of well-known techniques and mechanisms that are cam-based for realizing VVT and VVA [33-38].
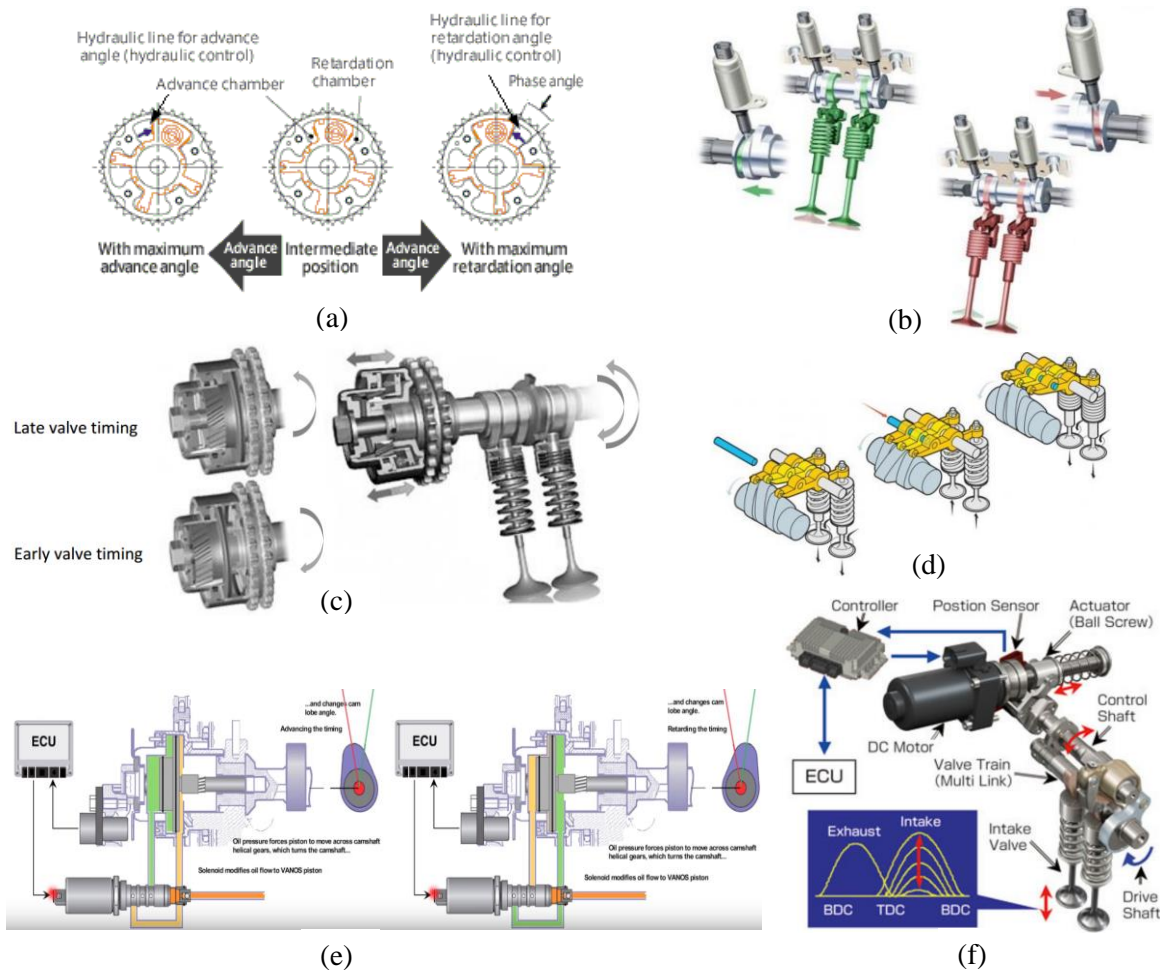
Figure 2.2 Typical cam-based VVT and VVA systems [33-38]

(a. Mitsubishi MIVEC [33] b. Audi Valvelift [34] c. VarioCam Plus [35]

d. Honda VTEC [36] e. BMW VANOS [37] f. Nissan VVEL [38])

Since these VVT and VVA systems are all cam-based, functioning by either cam switching or phase shifting methods, the flexibility they could provide is always limited due to the nature of the cam-based valve trains that the valve lift would always follow the contour of the engaged cam set. Hence they are not able to perform free alternations to the valve motions in terms of valve timings and opening durations in a continuous manner.

For camless valve trains, the flexibility of the valve motion events and the valve lift characteristics could be quite different based on their designs and driven methods [39,40]. For instance, the opening and closing profiles may appear to be more gradual from using the hydraulic or pneumatic valve systems than those from using the solenoid systems. However, the electromagnet valve actuation

11

systems may generally provide a quicker response and higher accelerations, while the system initiates any valve lift changes [41-44]. Figure 2.3 shows the examples of camless valve systems.

(a)

(b)
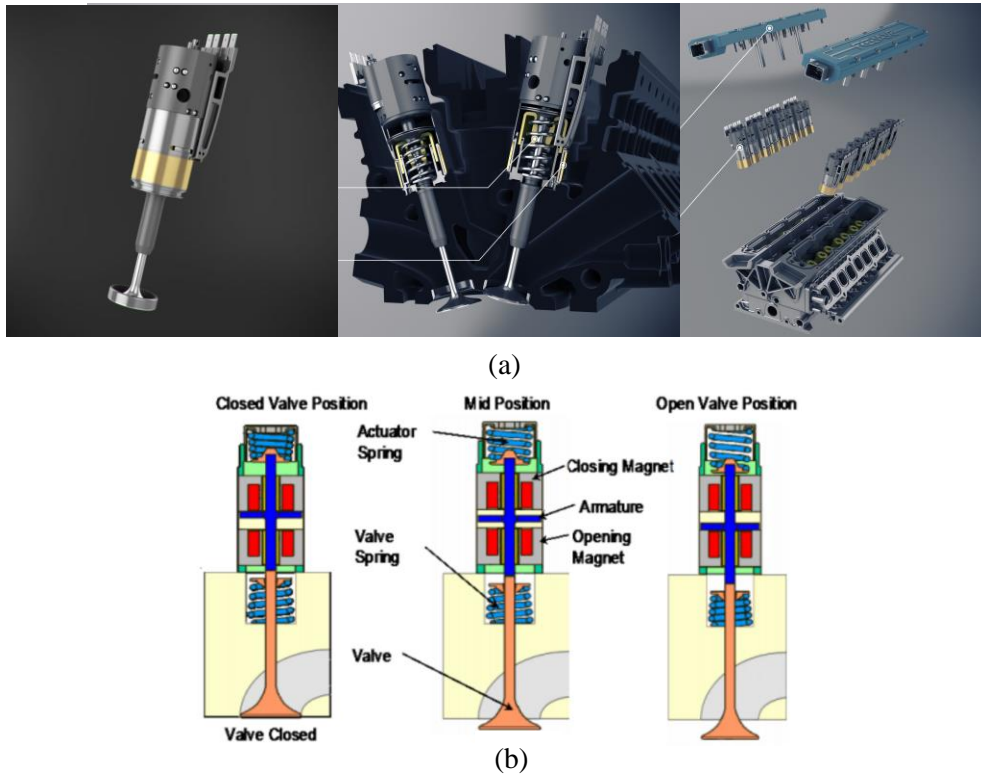
Figure 2.3 Exemplary camless valve systems [45,46]

(a. Electro-pneumatic FreeValve system [45] b. Electromagnet valve system [46])

2.2.2 The HVVA System

The hydraulic variable valve actuation system, which is adopted in this research for providing the valve motions with a full adjustability, was originally designed in [1,47], the inventors use a pair of spool valve mechanisms in cooperation of two phase shifters that each driven by a servo motor to control the timings of one engine valve at a full flexibility.

As shown in Figure 2.4 and Figure 2.5, the engine valve is attached to a hydraulic piston which is actuated by the pressurized oil that flows through the spool valves, while the spool shaft is driven by the pulley that obtains its rotary motion proportionally from the crankshaft of the engine. Once the spool port of the high-pressure spool valve (HPSV) reaches its tangent position angle (TPA) to the casing port, the HPSV is starting to open. It should be noticed that the TPA can be described with

respect to different references, but in this research, it is depicted in the corresponding crank angle (CA) degrees. The pressurized oil charges into the hydraulic cylinder through the casing port during the opening duration of the HPSV, and pushes the engine valve to open. The oil then traps within the hydraulic cylinder and the engine valve maintains its position once the HPSV is closed until the low-pressure spool valve (LPSV) opens. The engine valve starts to close as the LPSV gets to its TPA, the trapped oil will then be released from the hydraulic cylinder through the LPSV port by the returning spring of the engine valve. The angular position of the spool ports with respect to their casing ports can be freely changed by the E-motors, which grants the capability of altering the timing and opening duration of each single engine valve without interfering with those of the other valves. The valve lift is controlled by the pressure at the upper stream of the HPSV, and such pressure is built and maintained by an oil pump and an accumulator. With these features, this HVVA system can grant the engine with fully flexible valve motions in terms of valve timings, opening durations and lifts.
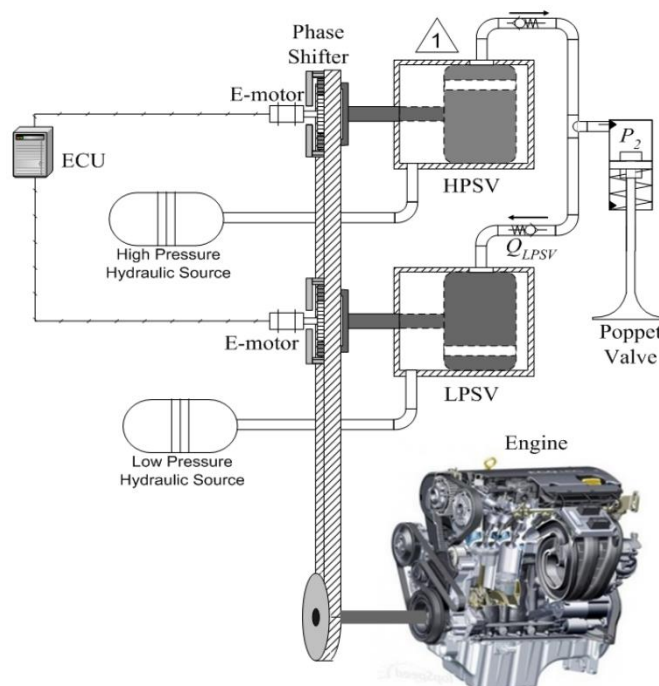
Figure 2.4 Schematic drawing of the HVVA system [47]

In addition, the hydraulic piston adopts an adjustable cushioning at both ends of its travel to shave the speed when contact with the hard stops. This grants the potential of letting the engine valves to travel at a higher maximum linear velocity without causing serious impacts and bouncing at their

stops. In another word, the rising and seating motions of the valves may take place within even shorter durations in terms of the crank angle degrees under any engine speeds.
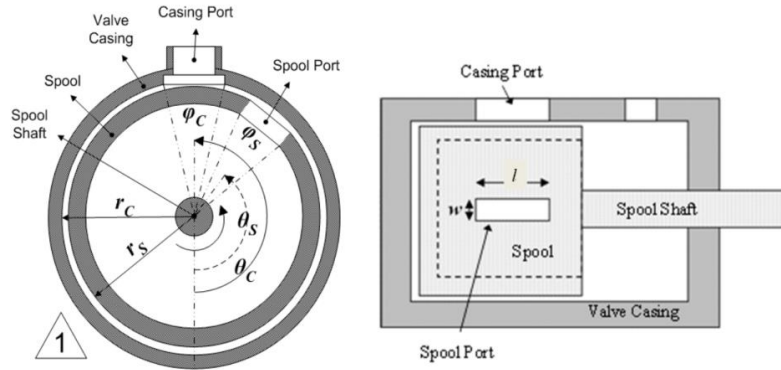
Figure 2.5 The rotary spool valve construction [47]

2.3 Techniques for Pursuing Better Engine Performances

The potential benefits that could be brought to the engine performance from adopting a VVT or VVA system can be mainly concluded in the aspects of power, fuel economy and emissions. Many researchers have deduced their own valve motion strategies for a specific type of the VVT or VVA system and investigated their practical improvements that could be contributed to the engine performance [48-50].

2.3.1 Implementations of Different Valve Motion Strategies

Over the past decades, different strategies to the intake valve lifts, timings and durations in order to improve spark-ignition (SI) engine performance from using VVA systems were studied and documented [51], with both theoretical and experimental results been investigated and presented [52], showing how different intake valve actuation configurations affect the residual gas fraction (RGF), intake gas velocity during the intake process and pumping losses etc. One of the most widely used technique is the multi-mode change-over VVT that the valve train consists of multiple sets of different cams. Hatano, K et al. [53] developed a multi-mode VVT engine, which can switch between cam sets that provide different valve timings, durations and lifts to reach a better engine performance under different working conditions. They claimed that the engine with this VVT demonstrates a fuel economy improvement up 16% during the Japanese test driving cycle.

Alternatively, the VVT systems that enable a consecutive motion to the cam phase shifting can further optimize the engine performance within a continuous range of engine speeds and loads [54,55]. Meanwhile, the features of the IEGR and the capability of performing different engine cycles are granted to the engines along with the improved adjustability to the valve motions [56]. As a matter of fact, the implementation of IEGR is proved to be effective on improving the fuel economy of the engine due to the bringing of the reductions to the pumping losses and the concessions to lean mixture combustions [57,58].
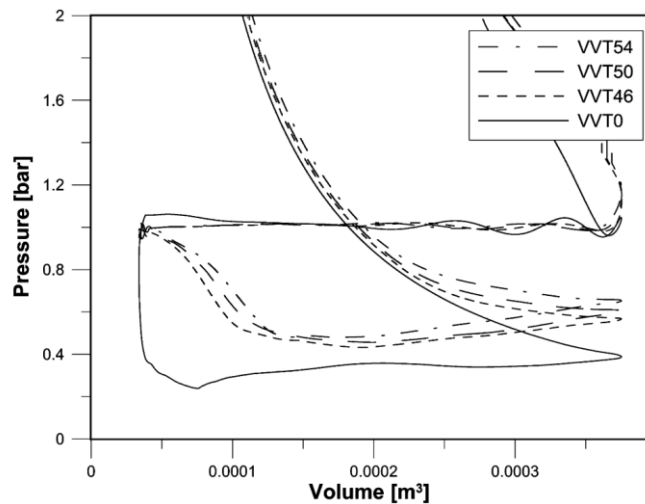
Figure 2.6 In-cylinder P-V diagrams for pumping cycle at different VVT configurations [54]
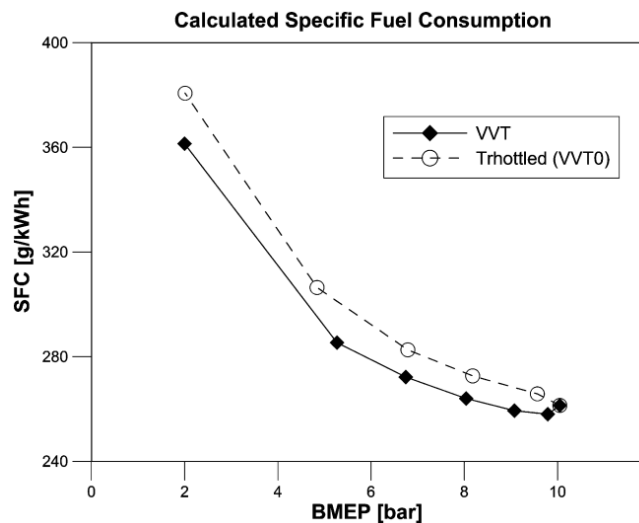
Figure 2.7 Calculated SFC comparison between pure throttle load control and throttle-VVT load control [54]

15

Seen from Figure 2.6 as an example, which shows the in-cylinder P-V diagram shown in the research conducted by G. Fontana et al. [54], it can be noticed that the pumping work has been decreased from implementing their VVT strategy under different retarding angles of the valve timings. The reductions on the specific fuel consumption (SFC) resulted by their throttle-VVT load control strategy are shown in Figure 2.7.

Similarly, in the research by F. Bonatesta et al. [55], a variable camshaft timing (VCT) strategy was proposed and been implemented on two small-capacity SI engines. A theoretical best strategy they found was able to reduce the BSFC by over 8% for the port fuel injection (PFI) engine while a maximum BSFC reduction was noticed at approximately 5% for the gasoline direct injection (GDI) engine. Their concluded graphical fuel-economy VCT strategies for the PFI and GDI engines are presented in Figure 2.8.
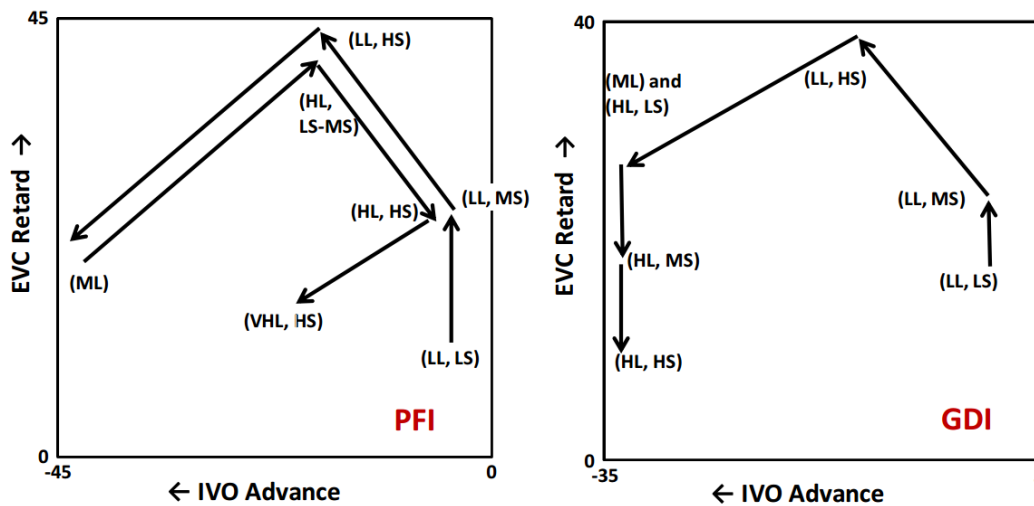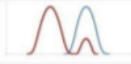
Figure 2.8 Graphical fuel-economy VCT strategies for the PFI and GDI engines [55]

The rebreathing strategies, on the other hand, grant a second opening to either exhaust or intake valves [60-62]. These strategies provide an IEGR process during the engine gas exchange strokes to let the engine breathe back a portion of the exhaust gas. The IEGR is formed by either the gas backflow at the intake valves during exhaust strokes or direct inspiration through exhaust valves during intake strokes. The results from applying these strategies show a tendency of the incomplete combustion losses could become higher as the IEGR rate increases. In the detailed research by Manuel A. et al. [62], major impacts obtained from implementing the rebreathing strategy are observed in their experiments showing fuel conservation has increased by 0.3-0.5%, and HC emission

has reduced by 10-20% over the FTP75 cycle. The summarized results showing the comparisons between the LIVC and the rebreathing strategies from their research are shown in Figure 2.9.

VVA		Major impacts		Benefits / Limitations					
Strategies Intake Exhaust	Profiles	FTP75 cycle fuel cons.	FTP75 cycle emissions.	NOx	PM	HC	CO	Comb noise	Exhaust temp
LIVC		1% * reduction	50% PM reduction	+	++	-	-	+	O
Internal EGR		0.3-0.5% increase **	~20% HC reduction	O	-	+	+	O	+

Higher FE potentialimprovement for LIVC including the benefit for increased DPF regen interval

*: Depending on charging capability
**: Compensation by warm-up strategy and aftertreatment impact

Key:
+ improved
o neutral
- worse

Figure 2.9 Comparisons over the summarized results between implementing the LIVC and the rebreathing VVA strategies [62]

Another VVA strategy, the pre-lift intake valve strategy, was proposed by V. De Bellis et al. [59] for the implementations on camless engines. This strategy introduces a constant small intake valve lift during the exhaust stroke and creates an increased valve overlap from utilizing a fully flexible VVA system, which reveals the potential of lowering the BSFC and gas-dynamic noises at partial engine load. The engine was then modeled by GT-Power and ModFRONTIER to see how their pre-lift strategy influences its performance.

As shown in Figure 2.10, the valve pre-lift height h and duration over crank angle degrees $\Delta\theta$ from their proposed strategy can be freely adjusted. Furthermore, due to the effective compression ratio (ECR) of the engine was increased from implementing the pre-lift strategy, higher delivered torque at full engine load could be achieved with less fuel consumption.
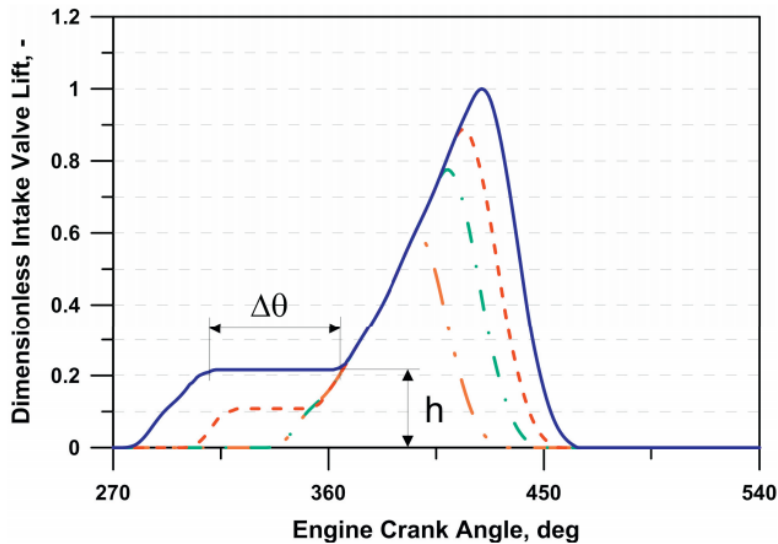
Figure 2.10 Valve Lift Profiles with Different Pre-lift Parameters [59]

In addition to the common strategies for throttled engines, studies on fulfilling partial engine load via using VVT and VVA systems instead of throttling are also one of the greatest focuses in developing VVT and VVA strategies. With all kinds of valve driven systems and mechanisms, a variety of valve motion strategies for achieving this goal have been compared and documented [63]. It has been pointed out that the engine load can actually be controlled by postponing the valve timings to carry out an IEGR or a reverse Miller cycle, which take effects as penalties to the resultant VE by the end of the intake process [54].

The IEGR effect can also be achieved by increasing the RGF from creating a negative valve overlap of the intake and exhaust valves that retains the burned gas within the cylinder during the exhaust stroke [64]. Cairns, A. et al. [65] implemented an internal and external combined EGR under partial load operations for improving fuel consumption. Also, by engaging the EGR, reductions on the CO_2 emission was noticed at up to 17% along with the HC and CO emissions been decreased by up to 80% under full load operations.

Alternatively, a more commonly used technique is to introduce an EIVC or an LIVC to the valve motions. An EIVC makes the engine take less fresh charge into the cylinder and results in a lower pumping loss, hence could help the engine to lower its BSFC at partial load. However, the HC emissions could become higher [66]. The LIVC operation allows a portion of the fresh charge to be pushed back into the intake manifold. This not only reduces the VE but also brings down the ECR

18

during the engine cycle and the temperature of the in-cylinder mixture before ignitions [67]. Although LIVC benefits in lowering pumping losses and nitric oxide emissions while receiving a similar HC emissions [68], the BSFC, for a multi-cylinder engine, might become higher under a low engine load with a high LIVC degree, due to the fact that the back-flowed flammable mixture within the intake manifold could be redistributed to other cylinders [69]. However, the LIVC shows advantages over the EIVC on preventing the engine from knock at high partial loads and achieving higher heat release rate at low partial loads [70]. Furthermore, the heat release rate and the combustion process could become relatively lower and slower, respectively, because of the turbulent motion of the charge could be significantly slowed down at low engine loads while employing an EIVC [71,72].

In order to put these strategies into use and understand the actual effects from their implementations on engines, a lot of studies and experiments were conducted. Tuttle, J. [66,68] conducted detailed research on controlling engine load with EIVC and LIVC strategies on the basis of a cam-based VVT system. The results showed that the indicated specific fuel consumption could be brought down by approximately 7% and 5% when adopting the EIVC and LIVC strategies, respectively, at 3.5-4 bars of the indicated mean effective pressure (IMEP). Similarly, by using a cam-less VVT system, R. Patel et al. [74] adopted both the EIVC and LIVC techniques for the load control of the engine and made a comparison. In their research, without causing a serious deterioration on the emissions, a 6% reduction on the indicated specific fuel consumption is realized. However, not only the intake valve timing matters to the engine performances but also the exhaust valve timing brings influences to the power and efficiency of the engine. In the theoretical study by E. Sher and T. Bar-Kohany [75], the engine could receive an increment of its maximum power by 6% and a decrement on the BSFC by up to 13% after optimizing both the intake and exhaust valve timings.

2.3.2 Realizations to VCR and Over-expansion Engine Cycles

Apart from the abovementioned valve motion strategies, the realizations to variable compression ratio (VCR) and over-expansion engine cycles via VVT are also considered as the most frequently used techniques nowadays for lowering the engine's fuel consumption [73].

Theoretically speaking, for OC engines, a greater compression ratio would lead to a higher thermal efficiency according to the thermal efficiency equation of the ideal OC [9]. In practice, however, the maximum compression ratio is capped for the reason of preventing knock while the engine is under full load or high partial load operations [76]. As a result, the engine efficiency would not be

considered as optimal if the compression ratio remains unchanged while it is allowed to be set at a higher value under low load. The VCR technology is developed to solve this problem and has provided solid evidence on improving the fuel efficiency under varying engine loads [77,78]. The VCR engines are able to adopt a higher geometric compression ratio to grant the engine a higher thermal efficiency at low load while having lower ones at high load to prevent the engine from knock [79]. According to the survey by T. Hoeltgebaum et al. [80], there are a variety of ways categorized in 7 classes for engines to implement the VCR. However, without the application of the VVT techniques, the Otto cycle VCR engines could not release the full potential of optimizing the engine efficiency. Hence, the implementation of the VVT, cam-based or cam-less, is as well an essential measure for improving the efficiency of the engines.

Apart from implementing the abovementioned VCR techniques and VVT strategies, performing different engine cycles is also a valid option that could result in contributing a higher engine efficiency. Comparing to the OC, an over-expansion cycle, which can be physically carried out by mechanisms or virtually realized by decreasing the ECR via altering the valve timings, is proved to be more thermodynamically efficient [81]. Different designs and strategies for realizing the over-expansion cycle have been well sorted and documented [73]. The very original and typical examples are the Atkinson cycle (AC) engine [82] and the Miller cycle (MC) engine [83]. The first AC engine utilizes a complex multi-linkage mechanism to make the travel of the piston longer during the expansion and exhaust strokes than that during the intake and compression strokes to form a greater geometric expansion ratio and a smaller geometric compression ratio within the same engine cycle. Alternatively, the MC engine maintains the geometric compression ratio and the geometric expansion ratio as equivalent as those of the OC engines but reduces the ECR by employing LIVC or EIVC events to appreciate the over-expansion process. In fact, as shown in Figure 2.11, the ideal MC is a thermodynamic cycle that shares the same principle of the AC, except that the over-expansion process does not expand to the atmospheric pressure as the ideal AC does [73]. However, a realistic AC engine would not adopt an over-expansion ratio that allows the in-cylinder pressure to expand to barometric due to the need of a long piston travel, which would lead to a greater mechanical loss and make conflictions toward the demand of downsizing. Besides, the work loss from the subsequent exhaust stroke would also become greater because the free exhaust stage would no longer exist at the beginning of the exhaust process [84]. Therefore, the MC is essentially identical to the practical AC, only that most of the MC engines are super- or turbo- charged while the AC engines are naturally aspired.

20
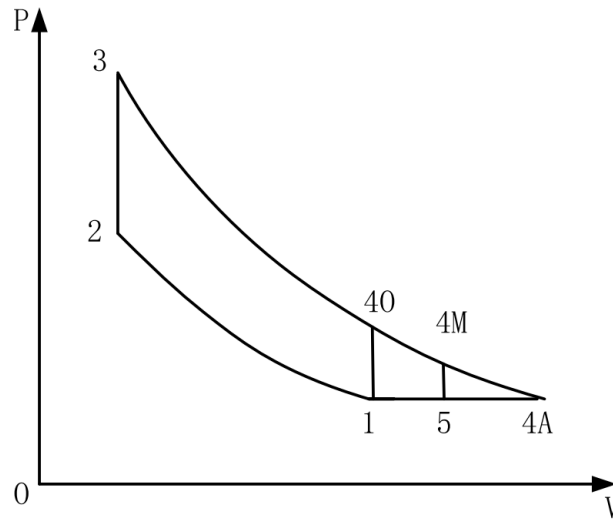
Figure 2.11 Illustrative P-V diagram for ideal Atkinson (1-2-3-4A-1),
Miller (1-2-3-4M-5-1) and Otto (1-2-3-4O-1) cycles [73]

A lot of experimental research had been conducted to reveal the actual benefits of the AC and MC for improving engine efficiency and fuel economy. Tie Li et al. [85] compared the results of realizing the MC by using EIVC and LIVC on a boosted gasoline engine. In their research, the BSFC can be reduced by 4.7% and 6.8% at high and low engine load, respectively, when adopting the LIVC. With the EIVC, the BSFC can be further lowered by another 0.6% at low load, however, no considerable improvement is noticed at high load. Feng, R. et al. [86] converted a conventional OC engine into an AC engine by increasing the geometric compression ratio and rearranging the valve timings. Through their experiment, the minimum BSFC is proved to be brought down to 234.5g/(kW·h) of the converted AC engine from the 250g/(kW·h) of the original OC engine. Moreover, the low fuel consumption area is also enlarged after converting the engine from OC to AC. Jinxing Zhao et al. [56] conducted a genetic algorithm (GA) based optimization with 5-variables for improving the fuel economy of a cam-based VVT AC engine. By optimizing the intake valve closing (IVC) timings and exhaust valve opening (EVO) timings along with the corresponding electrically throttle control valve, SA and AFR, the fuel economy of the AC engine can be resulted in a 7.67% reduction under a maximum simulation error of 8.5%.

As the AC engines are gaining better efficiency by compromising on its maximum power, the idea of an Otto-Atkinson cycle (OAC) engine is proposed and studied to overcome this trade-off [87]. The OAC engine operates as an OC and AC convertible engine, which runs on OC at full load in favor of

21

the power performance and switches to AC for attaining better fuel economy at partial load. In fact, there are several different solutions to compensate the fact that the AC engines have lower power density. As shown in Table 1, a group of typical technical measures for improving the engine's power density were listed by Jinxing Zhao along with the comparisons over their key features of advantages and drawbacks [73].

Table 1* Technical measures for improving power density [73]
Technical measures for improving power density.

Measures	Description	Advantages	Drawbacks
Intake boost (Miller cycle engine)	Partial load: Miller cycle; Full load: Turbocharged Miller cycle	1. No power loss; 2. Simple and suitable for mass production	1. Big turbocharger; 2. Need high efficiency intercooler
VCR (OA cycle engine)	Partial load: Atkinson cycle; Full load: Otto cycle	1. Constant ECR at partial load; 2. Optimum performance over the entire operating range; 3. Permit high GCR	VCR is too complex with bad dynamic response
Knock resistance (special OA cycle engine)	Partial load: Atkinson cycle Full load: improve knock resistance for approximate even full Otto cycle	1. Less power loss even increased power output; 2. Simple and suitable for mass production	1. Additional cost and time; 2. More measures for knock resistance

* Cited from [73]

Blakey, S. et al. [88] made an experiment of their design for carrying out the OAC on a cam-based multi-valve engine with two intake valves per cylinder. By applying an LIVC event to one of the intake valves via cam phase shifting and maintaining the normal event of the other intake valve, a greater equivalent curtain area of the intake valve openings is formed. In such way, the AC is realized along with the benefit of obtaining a greater degree of compatibility for a multi-valve engine. Boggs, D. et al. [89] modified a 1.6L OC engine into an OAC engine with fixed LIVC valve timings and increased geometric compression ratio. According to their experiment results, the BSFC can be reduced by 15% at 1500 revolution per minute (rpm) engine speed with 10% EGR and 2.62 bar brake mean effective pressure (BMEP) comparing to the baseline engine. Saunders, R. et al. [90] ran tests on a 4-cylinder OAC engine with load control by variable intake valve closures. It is concluded that the BSFC is able to be improved by a maximum of 13% from implementing the late valve closures only, and this improvement can be brought up to 20% while accompanied with variable clearance volume control which is known as one of the approaches to VCR.

2.4 Model-based Optimization Techniques for Engine Operating Parameter Identifications

Apart from the research on developing the designs and strategies of valve train systems, a large group of researchers also dedicated their efforts on modeling and optimizing the precise valve timings and valve motions along with other related aspects ruled by specific pre-chosen strategies, and through which to better utilize the extraordinary flexibilities awarded from the VVT and VVA systems.

The use of the physically-based valve system modeling [91] and 1D fluid dynamic modeling bring good insights for better understanding the gas exchange processes as well as the ensuing engine performance while altering the valve motions [92,93]. Besides, with a sufficient number of initial acquired input-output data, the engine performance can also be modeled and predicted from using artificial neural networks (ANN) [94,95]. It has been recognized and proved that with the assist of all kinds of artificial intelligence and optimization techniques, the operating variables of the engine, such as valve timings, SA and AFR can be efficiently optimized by either offline or online optimization techniques with respect to different objectives of interests.
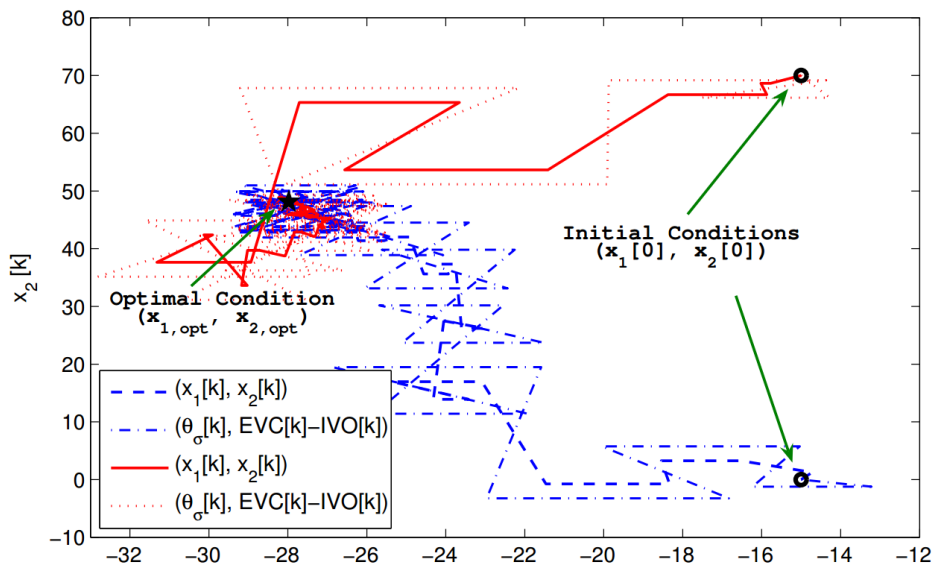
Figure 2.12 The Extremum Seeking control trajectory [96]

The Extremum Seeking algorithm, developed by Donghoon Lee et al. [96] and demonstrated in Figure 2.12, allows the optimizer to conduct an on-line optimization under steady states of the engine working conditions, and reach to an optimum convergence of valve timings and SA within 60 seconds. George Thomas et al. [97] performed a biogeography-based optimization (BBO) to improve

the engine's fuel economy and concluded a 1.7% improvement from using the variable camshaft timing system. They declared that the best search configuration they found for their BBO is with the settings of population at around 200 and mutation probability at approximately 0.05. In the study of E. Sher et al. [75], a 6% increment and a 13% decrement on the maximum engine power and BSFC were shown, respectively. They optimized the valve timings by a proposed predictive model that consists of all the considered aspects of the engine operations, e.g. gas exchange process, combustion process, emissions and etc., in the form of mathematical descriptions. K. Atashkari et al. [98] introduced an evolutionary algorithm for the optimal design of the ANN engine model with VVT and performed a GA-based multi-objective optimization to generate a set of Pareto fronts and investigate the results of two competitive objectives, e.g. engine torque versus fuel consumption.

Since that the optimizations to the engine performances are mostly a multi-variable global optimum problem with highly non-linear constraints, the optimization technique of GA is quite frequently adopted for dealing with these problems [56,93,98,99,100,101,102].

Y.G. Li et al. [101] proposed a GA-based non-linear design-point performance adaptation approach for estimating unknown engine model parameters of gas turbine engines. The performance of this GA optimization was also proved to be more robust when compared with the Influence Coefficient Matrix (ICM) based approach from their research. The exemplary processes of the GA-based and ICM-based approaches are shown in Figure 2.13 and Figure 2.14, respectively.
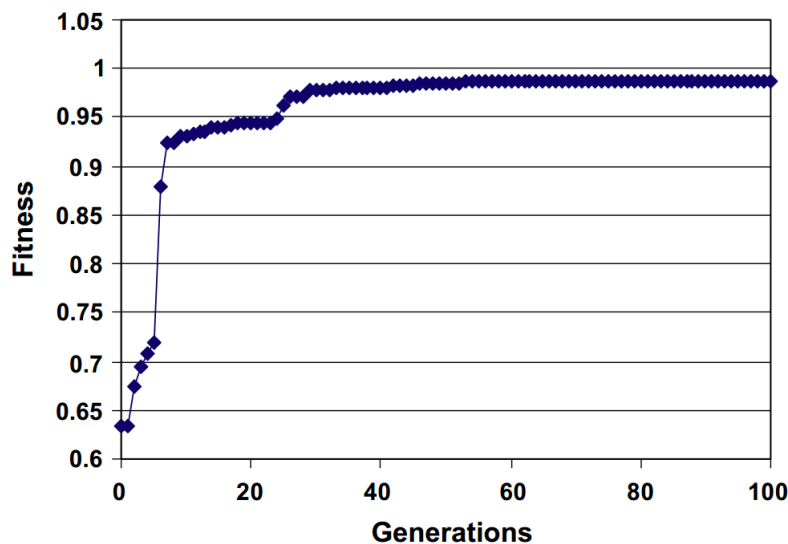
Figure 2.13 The GA-based adaptation searching process [101]
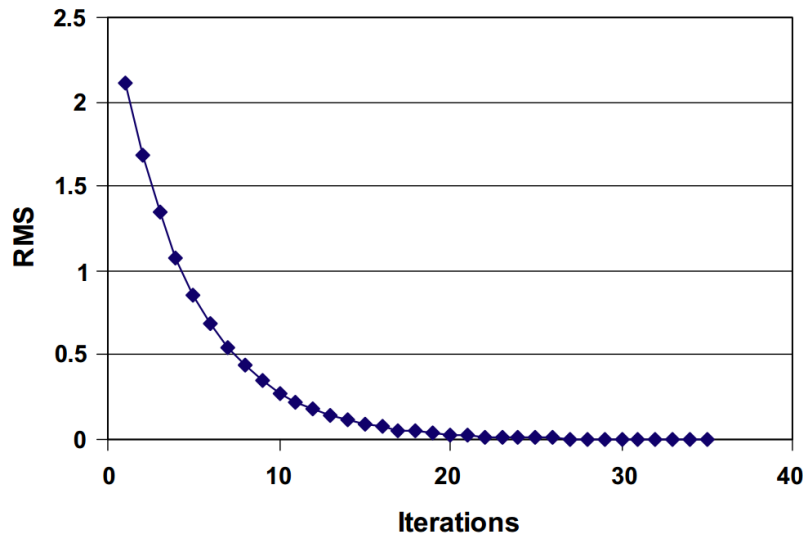
Figure 2.14 The convergence process of the ICM-based adaptation [101]

(RMS: root mean square)

In the research of G. D'Errico [93], both single- and multi- objective optimizations were performed using GA. The valve timings and throttle angle were considered as variables for optimizing BSFC and NOx emissions. Jinxing Zhao et al. [56] employed a GA optimization to seek for the optimum combinations of the valve timings, throttle opening, SA and AFR under a specific partial load of an Atkinson cycle engine. They used a parallel computation technique among multiple workstations to hasten the pace of the MATLAB and GT-Power coupling optimization procedure. Necla Togun et al. [99] proposed a genetic programming approach based on the traditional GA approach but more efficient for predicting the engine performances in terms of torque and BSFC. Prediction results from their approach yielded to a good agreement between the experimental data and the results generated by the neural network. Furthermore, a hybrid approach of GA and ANN was developed by Ugur Kesgin [100] to optimize the engine efficiency and NOx emissions. The ANN was used for capturing the characteristics of the engine and making predictions on the engine performance while the GA was engaged to perform the optimizations.

2.5 Summary

Although many valve train mechanisms and their accompanied valve motion strategies were studied as mentioned in above, the utilization of a fully flexible valve train, such as the HVVA system in this particular research, still hold strong potentials for further improving the engine performances by

adopting better optimized valve motion strategies that would put the flexibility and variability of the valve train into full use.

In addition, as also can tell from the aforementioned literature, the GA approach has been tested and proved to be one of the appropriate and viable optimizers for solving the complex optimization problems of engines. Therefore, in this research, by considering the dynamic of the HVVA system, the potentials of the HVVA system for further improving the engine performance upon different preferences will be revealed by proposing a set of new HVVA valve motion strategies and their corresponding GA-based optimization methodologies.

Chapter 3

Improving Engine Performances Using the HVVA System

In this chapter, a set of base valve motion strategies that could be realized by the HVVA system are introduced along with the explanations to the corresponding principles of how they could bring benefits to the engine performances via altering the gas exchange process. In addition, these base valve motion strategies are also checked by a valve-lift-profile-based gas exchange model (See Appendix A) for the purpose of acquiring qualitative validations to the principles.

3.1 Continuously-Engine-Speed-Adaptive Valve Motions for Improving Engine Output at Full Load Operations

As mentioned before, an optimized gas exchange process at full load operations could grant the engine with a greater VE and lead to an increased engine output. Theoretically, in order to receive a better gas exchange process, longer effective valve opening durations with respect to the crank angle degrees for both the intake and exhaust valves are required as the engine speed increases. However, for most conventional cam-based VVT systems, they can only shift the relative cam-to-crank angles to adapt to the varying engine speed with the same pre-designed cam profiles. Based on the nature of shifting, for both the intake and the exhaust valves, it can only optimize either their opening or closing moments depending on whichever affects more to the whole gas exchange process, but is not capable of optimizing both at the same time. In this section, one of the implementations of the HVVA system is proposed below in order to further improve the gas exchange process by adjusting the valve opening and closing timings individually and continuously according to the engine speed, and eventually lead to a better power performance of the engine at full load operations.

The engine characteristics at full load operations for gasoline engines are referring to the resultant engine performances in terms of output torque, effective power, BSFC and etc., under the condition of the throttle is fully opened, or known as the wide open throttle (WOT) operation conditions. The best power performance of the engine under a certain engine speed is achieved when the engine is running at full load. Thus, the power performance of the engine can be improved by pushing the limit of the maximum output torque at all engine speed.

Since that the effective power of the engine P_e can be expressed as a function of the engine output torque T and engine speed n [103] as:

$$P_e = \frac{2\pi nT}{60} \times 10^{-3} = \frac{nT}{9550} \tag{3.1}$$

also, it is known that the engine output torque is generally direct-proportional to the VE (See Appendix B), denoted by η_v, that:

$$T \propto \eta_v \tag{3.2}$$

it then can be concluded from Eq. (3.1) and Eq. (3.2) that a better gas exchange process, or actually a greater VE, can result in a higher engine output torque and effective power.

Therefore, by simultaneously increasing the advancing angle and the retarding angle of both the intake and exhaust valves as the engine speed increases, which the conventional cam-based VVT systems cannot do, the HVVA system is able to provide a further optimized gas exchange process by taking the advantage of its continuously variable valve motions. As a result, superior power performances of the engine at all engine speeds can be achieved.
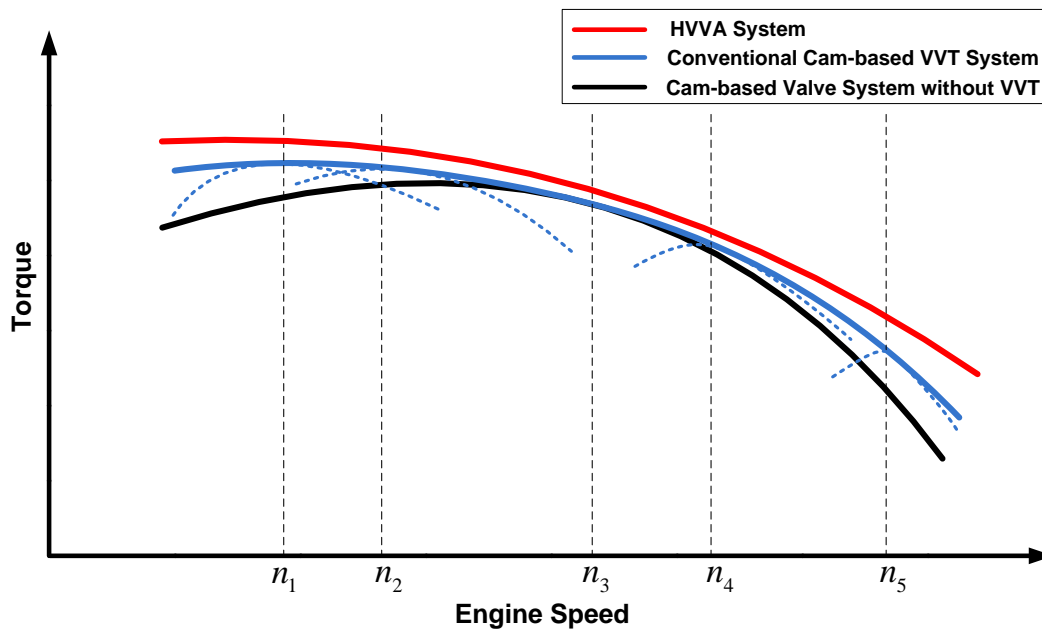
Figure 3.1 Comparison on the engine full load characteristics from using different valve systems

Figure 3.1 shows a set of illustrative torque profiles at full load operations over a random-chosen engine speed range from using different valve systems. Also, it is assumed that the cam profiles,

28

which are designed and optimized for working under the engine speed of n_3, are identical for all the cam-based valve systems shown in Figure 3.1.

As is known, the conventional cam-based VVT system can shift the cam-to-crank angles according to the real-time engine speed for receiving a better gas exchange process. The gathering of all the maximum torque points from all the torque curves resulted from the optimally shifted cam profile under different engine speeds forms the contour of the maximum torque at all engine speeds. In order to better explain this, four exemplary torque curves are shown in dashed lines in Figure 3.1 to demonstrate how would the torque looks like after the cams been shifted by different angles considered to be able to provide the optimum timing while under the engine speed n_1, n_2, n_4 and n_5 respectively. The conventional cam-based VVT system could output a higher torque over the engine working speed range in average compared to the conventional cam-based valves without a VVT system.

However, with the HVVA system, the maximum torque at all engine speeds can be further increased. This is because the system has the flexibility to optimize both the opening and closing timing for both intake and exhaust valves in a simultaneous, continuous and independent manner. Theoretically speaking, the more the speed that the engine is running at deviates from n_3, the more obvious the improvements could be. In addition, even the maximum torque under the engine speed of n_3 could still be greater than that with the other two mentioned valve systems, for the adoption of the HVVA system could actually eliminate the throttle body from the engine and grant the engine with the capability of performing load control without throttling. Thusly, the intake process will no longer suffer from the pressure loss at the throttle body which exists even at WOT operations. Hence, by summarizing the potential benefits mentioned above that could be provided by the HVVA system, the resultant VE could be increased in a global scale across the entire speed range while the engine runs at full load operations.

3.2 Unthrottled Load Control for Improving Engine Fuel Economy at Partial Load Operations

With the air-fuel ratio remain unchanged, the engine load is controlled by managing the amount of the fresh charge during the intake process. At partial load operations, the engine output resulted from such intake process should just be able to match the desired load. This is controlled by the opening angle of the throttle in conventional gasoline engines. However, since there would be no need for a

throttle body when adopting the highly flexible HVVA system, a set of HVVA valve actuation strategies are proposed in this section for realizing unthrottled engine load control. With these newly proposed valve actuation strategies, the engine would not only be able to control the amount of the fresh charge, but also would receive a reduced pumping loss due to the elimination to the throttling effect, and hence, become more fuel efficient.

3.2.1 Better Fuel Economy Due to Pumping Loss Reduction

For partial engine load operations, if the same amount of fresh charge was taken into the cylinder by the end of the compression stroke from implementing the conventional engine load control via throttling and the proposed unthrottled HVVA engine load control, it is reasonable to assume that the resulted engine outputs by these two approaches would be relatively identical. Then, the decrements on the overall pumping loss work, which is accumulated from both the intake and exhaust processes, would lead to a positive increment to the indicated work W_i, or the indicated power P_i, of the engine. As it is known, the indicated work W_i can be written as

$$W_i = Q_{fuel}\eta_i \tag{3.3}$$

where Q_{fuel} indicates the total energy contained by the burnt fuel per cylinder per engine cycle, then from Eq. (3.3), it can be seen that the indicated thermal efficiency η_i is actually increased since W_i is increased while Q_{fuel} remains unchanged. In addition, since that

$$P_i = P_e + P_m \tag{3.4}$$

where P_m is the mechanical power loss due to frictions between parts and power distributions for driving other accessories, it is obvious that the effective power P_e would increase as P_i increases, for P_m would be considered as constant for steady state analysis. Then, according to the estimation equation to the BSFC of the engines, which is

$$BSFC = \frac{\gamma}{P_e} \tag{3.5}$$

where γ is the fuel consumption rate in grams per hour (g/h), it can be comprehended as either the engine could produce more effective power under the same fuel consumption rate, or the engine could output the same power with less fuel consumption, if the engine's pumping loss could be reduced. In another word, the reduction to the pumping losses can lead to a lower BSFC while delivering the

30

same required engine output, which means that the engine would gain a higher fuel efficiency and thus become more fuel economic.

Since the HVVA system can change both the IVC and EVO independently without interfering the IVO and EVC, the intake and exhaust processes (known as the pumping cycle) can be optimized simultaneously in terms of the overall pumping loss during the full engine cycle.

3.2.2 Valve Motion Strategy for Intake Pumping Loss Reduction

For gas engines, the conventional way to reduce the amount of the intake fresh charge when the engine runs at partial loads is to let the throttle open less. However, due to the increased throttling effect from doing so, a higher vacuum would form within the cylinder when the piston reaches its bottom dead center (BDC) by the end of the intake stroke. This generally means that the engine suffers more from the pumping loss during the intake processes as the throttle opening angle becomes smaller, especially for low partial engine load operations.
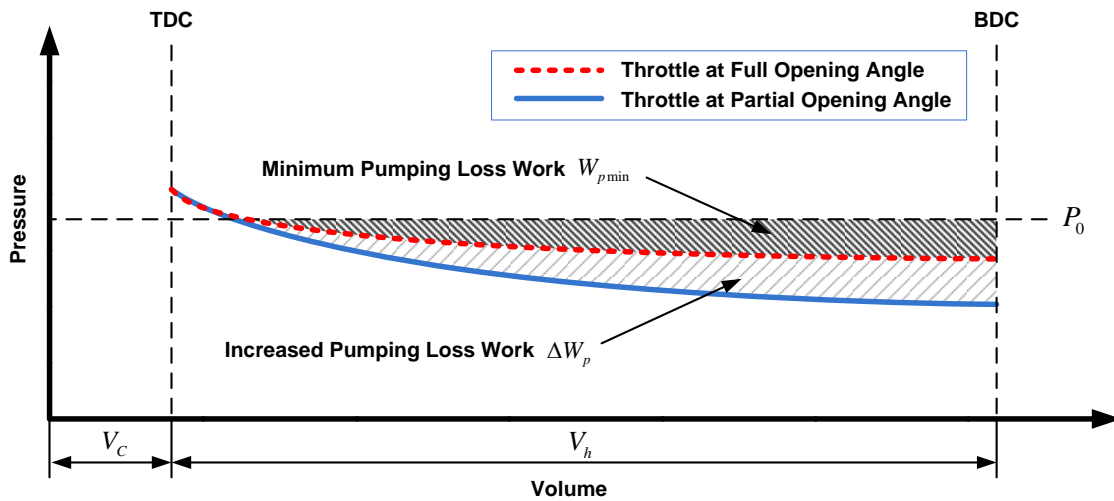
Figure 3.2 Illustrative in-cylinder P-V diagram for intake pumping loss demonstrations under full opening and partial opening of the throttle

As can be seen in Figure 3.2, when the engine runs at full load under WOT condition, the pumping loss work during the intake stroke is considered as the minimum at that engine speed. By denoting $W_{p\min}$ as the minimum pumping loss work, it can be represented and quantified by the heavy shaded area shown in Figure 3.2. While the engine runs under the same engine speed but at a partial load with the throttle opens partially, the in-cylinder gas mass and pressure by the end of the intake

31

process will be less than those of the WOT working condition. As a consequence, the actual pumping loss work would be increased. By denoting the increased pumping loss work as ΔW_p, shown as the light shaded area in the figure, the resultant intake pumping loss work under any partial engine load can be then expressed as $W_{p\min} + \Delta W_p$.

However, with the HVVA system, the overall pumping loss during the intake process can be reduced under all partial engine load operations.

For reducing the intake pumping loss work, the very principle is to minimize the in-cylinder vacuum rate during the intake stroke, which means to let as much as possible gas to be taken into the cylinder to fill up the in-cylinder volume. However, this violates the fact that less gas should be taken into the cylinder to comply with the desired partial engine load. Thus, with the illustration shown in Figure 3.3, a new unthrottled engine load control scheme is proposed by adopting LIVCs.
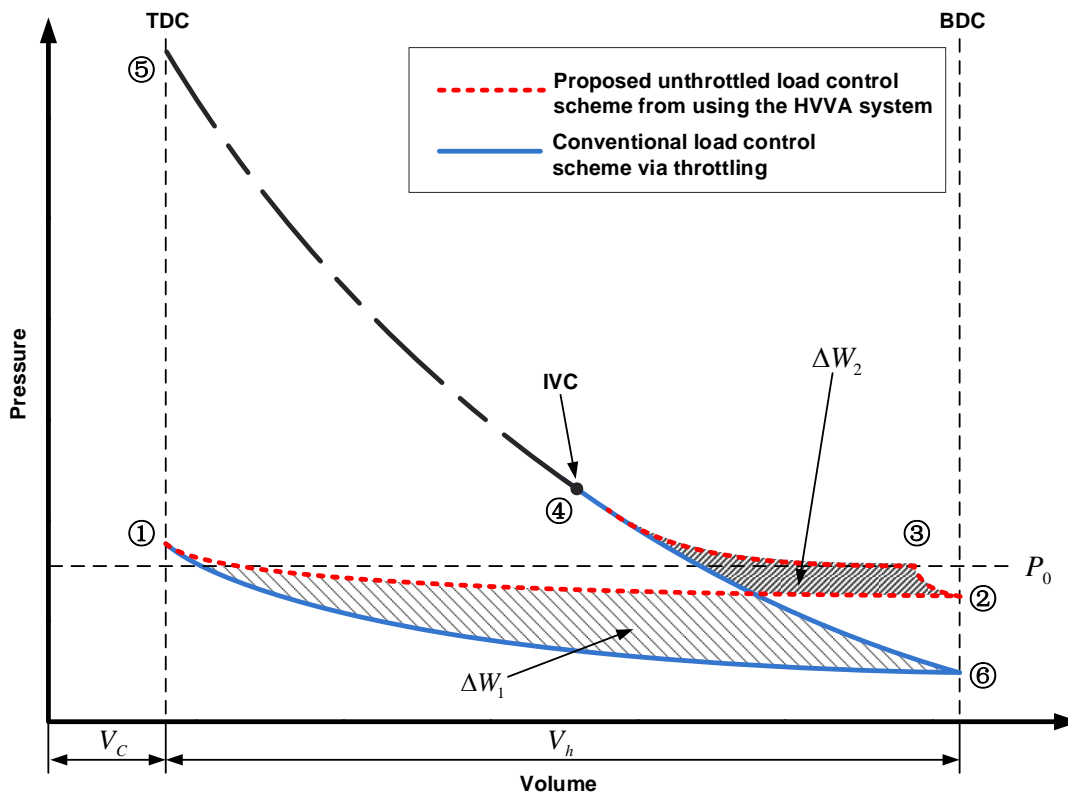
Figure 3.3 Comparison on the intake and compression processes between the conventional and the proposed schemes when the engine runs at the same partial load

As shown in Figure 3.3, the conventional way of making the engine run at any partial load is to use the throttle to reduce the air charge during the entire intake stroke (from ① to ⑥), followed by the compression process from the BDC all the way up to TDC (from ⑥ to ⑤). However, the in-cylinder vacuum would become higher and higher as the engine load reduces. This would result in a greater work loss from the pumping.

Now, as shown by the dashed red curve in Figure 3.3, the HVVA system will change the intake and compression processes into the following steps to make the in-cylinder charge to be the same by the end of the compression stroke as those from using the conventional scheme via throttling:

1. During the intake stroke, the intake valve opens to its maximum lift to let as much as fresh gas charge into the cylinder, so that the pumping loss during the intake stroke could be minimized (from ① to ②).

2. Once the piston reaches the BDC, the intake valve is maintained at its maximum lift. As the piston moves up during the compression stroke, those excessive amounts of the intake gas would be pushed back into the intake manifold. Theoretically, the in-cylinder pressure would be rapidly increased from below the atmospheric pressure P_0 to above because of the reversed motion of the piston at BDC and the fact that the cylinder would still be under charging process at the very start of the compression stroke due to the momentum of the incoming fresh charge as well as the restriction of the valve (from ② to ③). Then, the intake valve will start to close at a certain moment that would result in an IVC that the in-cylinder states would coincide with that resulted from the conventional throttled scheme (from ③ to ④).

3. After the intake valve is fully closed, the remaining gas within the cylinder will endure the same compression process as that of the conventional scheme from ④ to ⑤.

Furthermore, as shown in Figure 3.3, apart from the areas that represent the shared pumping loss work resulted from both the schemes, by denoting ΔW_1 and ΔW_2 as the individual pumping loss work that only applies to the conventional scheme and the proposed HVVA scheme, respectively, the intake pumping loss work saved from using the proposed scheme can be represented as:

$$\Delta W_{int} = \Delta W_2 - \Delta W_1 \tag{3.6}$$

Thus, whenever the ΔW_{int} is greater than zero, the proposed HVVA scheme is viable and would bring increment to the indicated work W_i while consuming the same amount of fuel.

33

By visualizing the in-cylinder pressure changes during the intake and compression strokes for both the conventional and the proposed schemes, a clearer and more direct illustration to the above processes is shown in Figure 3.4. In which, both schemes would have the same volumetric efficiency during the intake process by controlling the intake gas mass from using the throttles and the HVVA system, respectively.
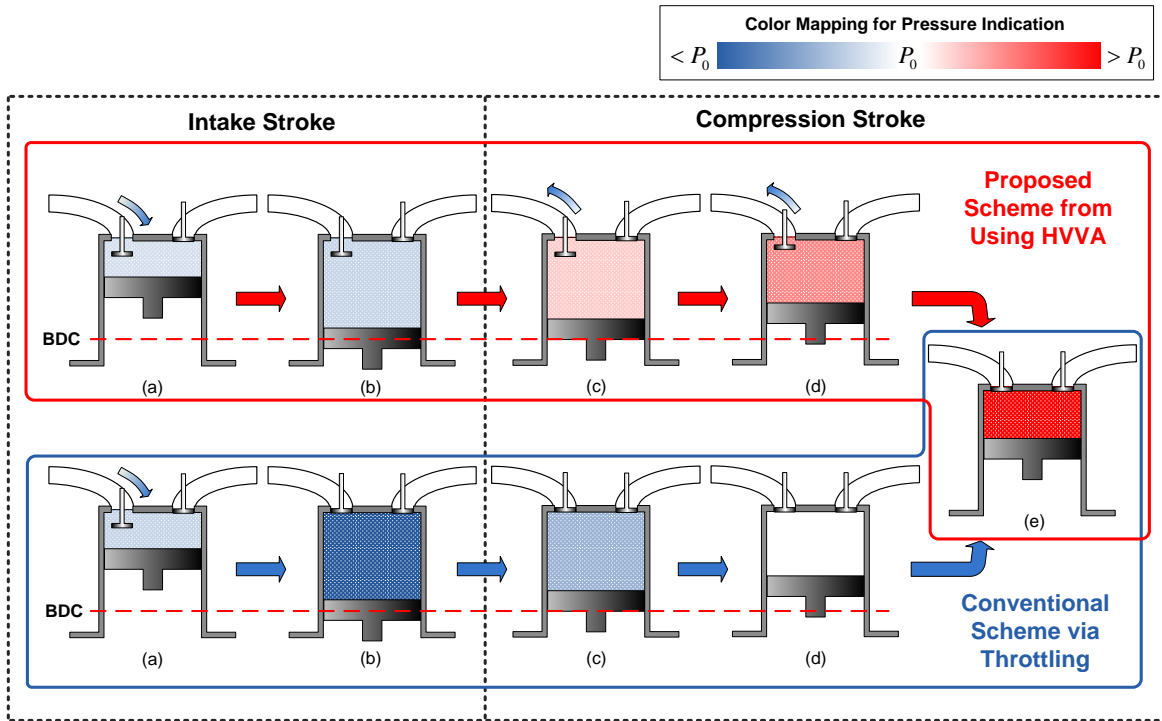
Figure 3.4 Illustration on intake processes for both the conventional and the proposed schemes for realizing the same engine load

3.2.3 Valve Motion Strategy for Exhaust Pumping Loss Reduction

In addition to the intake pumping loss reduction, the decrements on the exhaust pumping loss can also take essential effects on increasing the indicated work of the engine. An HVVA strategy for reducing the exhaust pumping loss is introduced in this section. By further advancing the EVO for a certain degree in terms of the CA, the initial exhaust pressure can be considerably reduced. Furthermore, thanks to the high flexibility provided by the HVVA system, the advancing degree of the EVO is able to be adjusted freely and continuously according to the required speed-load operations of the engine. This can be explained by the two exemplary cases illustrated by the in-cylinder P-V diagram in Figure 3.5.
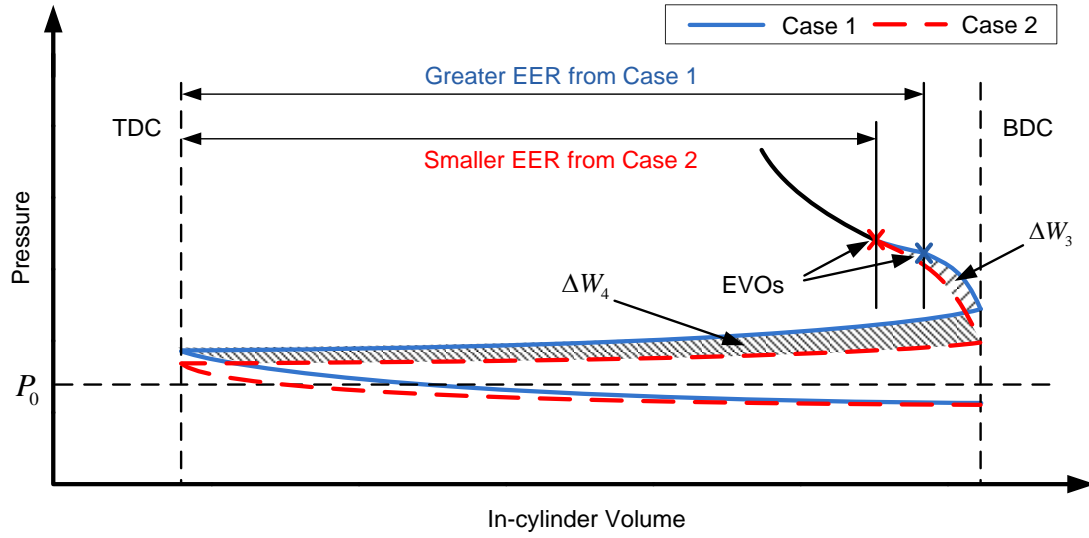
**Figure 3.5 Demonstrative in-cylinder P-V diagram of the two exemplary cases
with different exhaust pumping losses**

With a more advanced EVO, as of the Case 2 comparing to Case 1 in Figure 3.5, a smaller effective expansion ratio (EER) as well as a lower in-cylinder pressure at the exhaust BDC can be realized. It can be seen from the given illustrative examples, adopting a smaller EER would lead to a portion of work loss, denoted as ΔW_3 in Figure 3.5. This is because less positive work will be converted from the power stroke for driving the piston due to the earlier depressurization process within the cylinder caused by the more advanced EVO. At the same time, however, the in-cylinder pressure at the beginning of the exhaust stroke is brought down to a lower level, which can reduce the pumping loss from the subsequent passive exhaust process [84]. The saved pumping loss work, denoted as ΔW_4, could be considered as a compensation to the previously mentioned work loss, ΔW_3, from the aspect of the overall indicated work. As a matter of fact, with optimized EERs according to the different speed-load operating points of the engine, the work trade-off between ΔW_3 and ΔW_4 could always reach to an optimal by maximizing:

$$\Delta W_{exh} = \Delta W_4 - \Delta W_3 \tag{3.7}$$

where ΔW_{exh} stands for the saved pumping loss work from implementing the proposed strategy. It also should be noticed that this proposed strategy for reducing the exhaust pumping loss work is applicable to both full load and partial load operations.

35

3.2.4 Tunable IEGR Feature

Another proposed implementation of the HVVA system is the realization to a tunable IEGR feature. This proposed tunable IEGR feature is realized by the adoption of the late exhaust valve closing (LEVC) strategy, which makes the engine breathe back a portion of the exhaust gas from the exhaust manifold during the intake stroke to form the EGR functionality. However, the adoption to the proposed tunable IEGR feature should obey the following rules:

- Avoid exhaust gas back-flow into the intake manifold during the exhaust process to eliminate the risk of scorching or even igniting the intake manifold. The IVO should be set properly. However, a properly set IVO with even an advancing angle would not cause exhaust gas backflow at the intake valve, for the pressure difference on both sides of the intake valve would be balanced out quickly enough while the piston approaching to its TDC at a relatively slow travel speed. In addition, there would be also a huge discharging effect under the tiny openings of the intake valve. With such small openings of the valve, it is quite hard and unlikely to form a flow through the intake valve by canceling and redirecting the incomparable moment of the in-cylinder gas that is currently running through the exhaust valve.
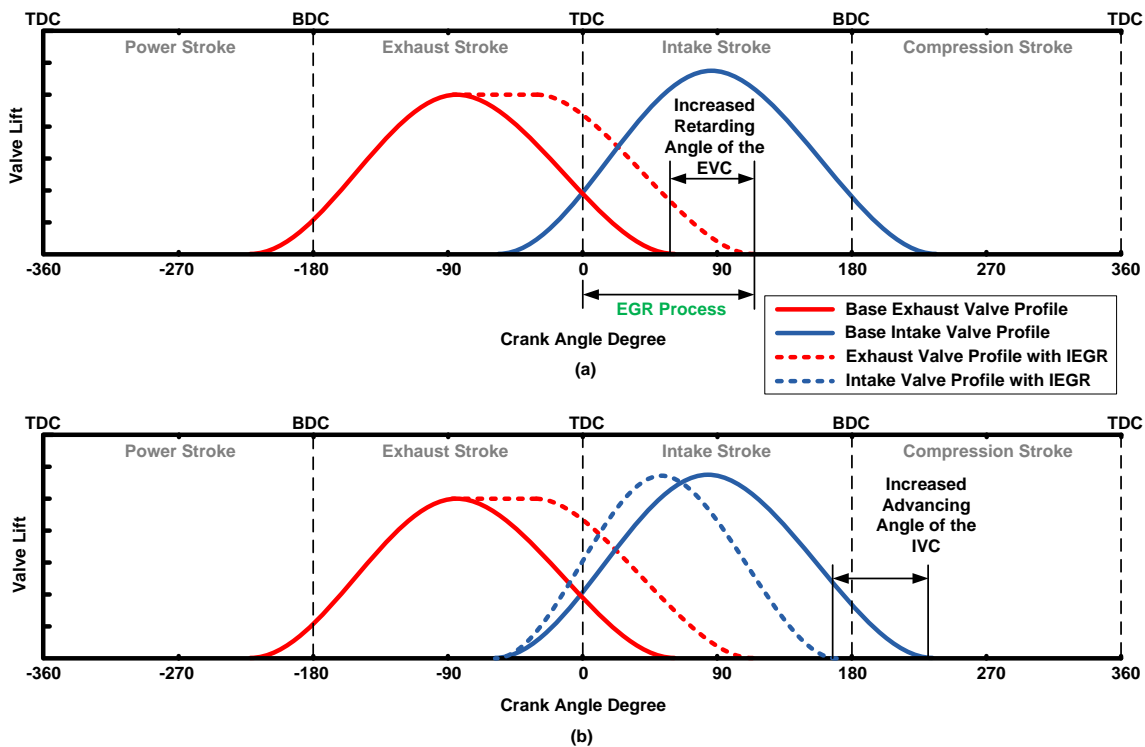
Figure 3.6 Illustration of the IEGR feature from using the HVVA system

36

- The IEGR process can only take place during the intake stroke, which means the amount of the exhaust backflow should only be adjusted by the retarding angle of the EVC (seen from Figure 3.6a).

- Under the circumstances that the engine would still take in an excessive amount of fresh charge besides the amount it needs to comply with the current engine load even if the maximum allowable EGR rate has been reached, the HVVA system will then perform an EIVC to regain control of the expected volumetric efficiency (seen from Figure 3.6b).

With the proposed tunable IEGR feature, whenever the engine runs at a partial load and the cylinder would not be completely charged by fresh gas, a certain portion of the rest volume will be filled by the exhaust gas. This could actually bring an increment to the effective thermal efficiency of the engine. To better demonstrate this from the perspective of the entire engine cycle, an illustrative P-V diagram is shown in Figure 3.7 for further explanations.
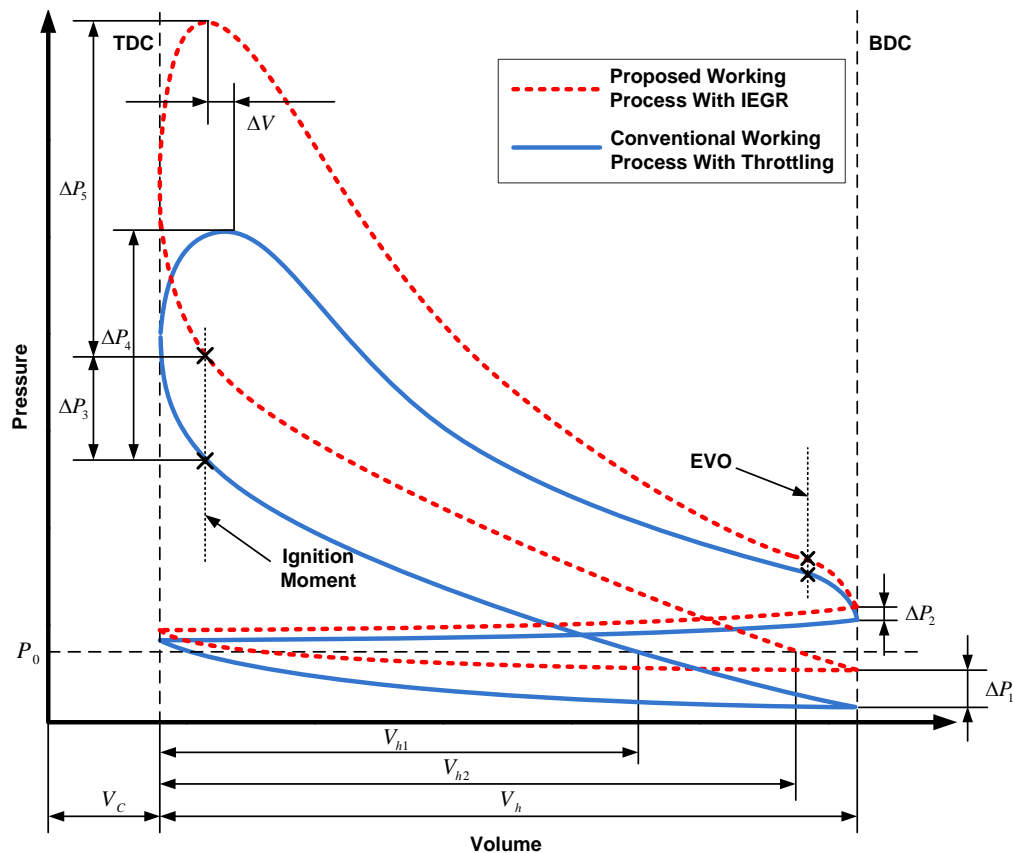
Figure 3.7 Illustrative P-V diagram showing both the full engine cycles from running in the conventional throttled scheme and the proposed unthrottled scheme with IEGR

As can be seen from Figure 3.7, while under the preconditions of the same engine load with synchronized ignition and EVO timings, the in-cylinder pressure with the IEGR at the intake BDC would be higher than that of the conventional working process by the amount of ΔP_1. This is because a portion of the in-cylinder vacuum generated from the intake process was filled by exhaust gas. After experiencing the adiabatic compression process during the compression stroke the initial pressure difference ΔP_1 would be scaled to ΔP_3 right before the ignition. Also, with the marked-out effective compression displacements, V_{h1} and V_{h2} for both schemes, it can be easily observed from the figure that the effective compression displacement with the IEGR is greater. In addition, due to the higher in-cylinder pressure and temperature resulted from implementing the IEGR, the in-cylinder energy density at the ignition moment could become much higher than that of the conventional scheme. As a result, although the amount of the injected fuel was the same, the flame propagation and pressure burst speed after ignition would be faster. In another word, the maximum eruptive pressure could be reached sooner and more close to the top firing dead center (TFDC) moment, and the maximum pressure could apply over an additional volume duration ΔV comparing to the scheme that without the IEGR.

Moreover, since the combustion process could happen within a shorter period in terms of the in-cylinder volume, the maximum pressure bursts generated from the IEGR scheme, denoted as ΔP_5, would be much higher than that from the conventional scheme, which is denoted as ΔP_4, under even the same amount of heat release from the combustions. Therefore, it can be seen that the IEGR scheme can provide a higher effective thermal efficiency and produce more work over the power cycle.

In addition, by comparing the two schemes, it is clear to see from the figure that the intake pumping loss could be reduced by implementing the IEGR. However, with the same EVO timings, the exhaust pumping loss might turn out to be increased due to the in-cylinder pressure difference at the exhaust BDC, denoted as ΔP_2, when adopting the IEGR scheme.

Fortunately, benefited by the nature of the HVVA system, the EVO timing could also be adjusted and optimized to minimize the pumping loss work during exhaust process from implementing the proposed exhaust pumping loss reduction strategy from the previous section. Hence, the overall exhaust pumping loss work resulted from implementing the IEGR could actually be brought down to an even lower level than that of the conventional scheme.

In this research, however, an inevitable step before implementing the tunable IEGR feature to different engines is to determine the maximum feasible EGR rate for every specific engine, since the EGR rate could vary significantly under different HVVA valve timings. The principles for determining a feasible EGR for any specific engine are elaborated as follows.

- *The exhaust gas recirculation during the intake process must not cause an ignition within the cylinder.* As mentioned in above, the exhaust gas will be coming into the cylinder during the intake process when the IEGR is implemented. Then, for those engines with indirect fuel injection techniques (port injection), there could be a chance that the incoming air-fuel mixture might be ignited by the exhaust gas that bears an extremely high energy in the form of heat if the EGR rate were set over too high. However, with a proper EGR rate that allows only an acceptable amount of the exhaust gas circling back into the cylinder, this intolerable situation can be prevented from happening. The reason can be explained by the nature of combustion process explained in below.

    As is known that for the engine combustion processes, the ignition process can be divided into the following steps from a micro perspective of view [105,106]:

    First, one or more chemical bonds were broken by the received energy that is sufficient for initiating the bond breaking process, and release heat from such reaction. Over time, once the energy reaches a certain level of density from heat accumulation, more and more nearby chemical bonds would be broken and release more heat. Then, if such heat accumulation is always faster than the speed of energy spread, this chain-reaction would keep reacting and eventually lead to complete combustion.

    Now, it is certain that the high-temperature exhaust gas carries a huge amount of energy that is more than enough to cause the abovementioned bond breaking process. At some discrete locations within the cylinder, the energy density may reach the level for breaking the chemical bonds of the fuel. However, due to there is also low-temperature fresh air coming through the intake valve during this period, the high-speed turbulence would depress the heat accumulation with respect to any random location within the cylinder. Thus, if the heat accumulation speed is not high enough to suppress the energy drain caused by the in-cylinder turbulence at a certain location, the chain-reaction of ignition process will be interrupted. Therefore, the in-cylinder gas would not be ignited if the EGR rate is controlled under a secure level. Yet, for those engines with the direct fuel injection techniques, the maximum tolerable EGR could be set higher, for

there is no fuel coming into the cylinder during the intake process and thus eradicates the risk of flaming up.

- ***During the power stroke, knocking must be avoided [105,107].*** Since with the IEGR, the in-cylinder temperature and pressure by the end of the compression process could become much higher due to the additional gas mass and energy brought by the exhaust gas. In particular, when the engine runs at a medium-high load, an over set EGR rate may result in a high temperature and pressure by the end of the compression process that could cause knocking during the power stroke, which is a typical abnormal combustion process and is strictly prohibited.

- ***The flame propagation speed during combustion should not be slowed down dramatically***. As been explained in above, a light EGR may actually help and accelerate the combustion speed and gain a higher effective thermal efficiency of the engine. But an excessive EGR may result in the opposite [108]. It is known that except for the heat brought and the resultant in-cylinder pressure increments, the exhaust gas itself is actually a resistance to the combustion process for it consists of inflammable substances that would dilute the air-fuel mixture. Therefore, an over performed EGR may slow down the flame propagation speed and make the effective thermal efficiency of the engine drop.

Hence, in order to perform the tunable IEGR feature and develop the corresponding feasible HVVA valve motion strategy for a specific engine, the abovementioned principles should be satisfied simultaneously by identifying the maximum feasible EGR rate for different engines via experiments. Yet still, by setting EGR rate to be zero, this proposed tunable IEGR feature can be completely turned off whenever it is not needed.

3.3 Summary

In this chapter, a group of fundamental strategies for the HVVA system applications on engines is proposed. With the high flexibility HVVA system, by adopting the proper or a combined strategy from the above-proposed valve actuation schemes, the engine could gain better performances and is able to switch between different features according to the actual demands without making additional changes or adding additional parts to it. Furthermore, the partial engine load operations could no longer be realized by throttling but are controlled via only the valve motions.

For actual implementation of these proposed HVVA base valve motion strategies, the engine performances could be benefited from adopting the proper ones for achieving different engine performance preferences in terms of power, fuel economy and emission performances.

By categorizing all the above-proposed base valve motion strategies into

Approach 1: Maximizing VE via continuously-Engine-Speed-Adaptive Valve Motions;

Approach 2: Pumping loss reduction;

Approach 3: Tunable IEGR feature,

the possible choices of adoption upon different performance preferences are shown in Table 2.

Table 2 Base HVVA valve motion strategy options for different engine performance preferences
Base HVVA valve motion strategy options for different engine performance preferences

Engine Performance Preferences	Power	Fuel Economy	Emission
Feasible Options	Approach 1	Approach 2	Approach 3*
	Approach 2	Approach 3	

* Even though the IEGR was uncooled comparing to most of the external EGR configurations, it could still bring benefits to lowering the engine emissions, especially for NO_x reduction, only that the effectiveness may not be able to reach as high as from implementing an external EGR.

Chapter 4

Modeling of the Unthrottled HVVA Single-cylinder Gasoline Engine[1]

In this Chapter, the HVVA system and the test engine are physically modeled and carefully calibrated in order to capture the overall behavior of the converted HVVA engine. Also, the key features and characteristics of the HVVA system and the Baseline Engine are individually presented.

4.1 The HVVA System

Firstly, for the HVVA system, the spool and casing ports for all the four spool valves have been redesigned in this research. The original rectangular ports that shown in Figure 2.5 have been modified into circular shapes that are identical and with a radius of r .

As shown in Figure 4.1, by denoting d as the absolute distance between the centers of the spool and casing ports measured on the planarized surface of their relative motion, the instantaneous flow area of the spool valves, A_{flow} , is calculated by:

$$A_{flow} = \begin{cases} 2\left[\left(\arccos\dfrac{d}{2r}\right)r^2 - \dfrac{d}{2}\sqrt{r^2 - \dfrac{d^2}{4}}\right] & when \quad (0 \le d \le 2r) \\ 0 & when \quad (d > 2r) \end{cases} \tag{4.1}$$
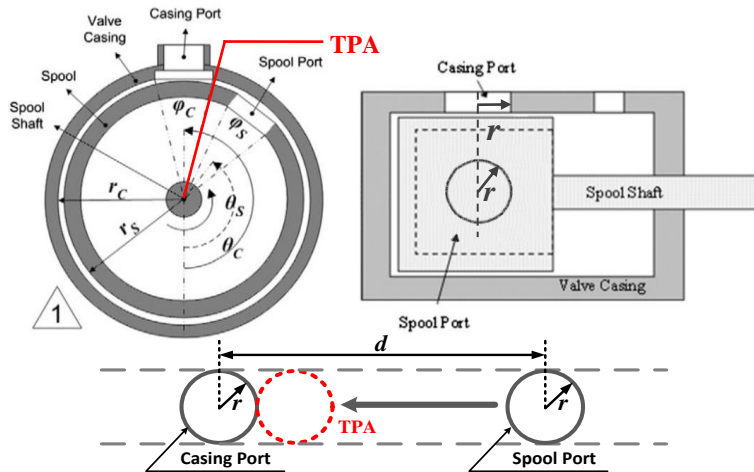
Figure 4.1 The modified rotary spool valve (modified from the original design in [47]) and the illustration to the relative motion between the spool port and the casing port

---

[1] Refer to the "Statement of Contributions" for authorship details of the contents in this chapter.

Secondly, the hydraulic piston adopts an adjustable cushioning device, as shown in Figure 4.2, to significantly shave its traveling speed when reaching close to the contacts at both ends of its travel. This grants the potential of letting the engine valves to travel at a higher maximum linear velocity without causing serious impacts and bouncing at their stops. In another word, the rising and seating motions of the valves may now be able to take place within even shorter durations in terms of the crank angle degrees under any engine speeds.
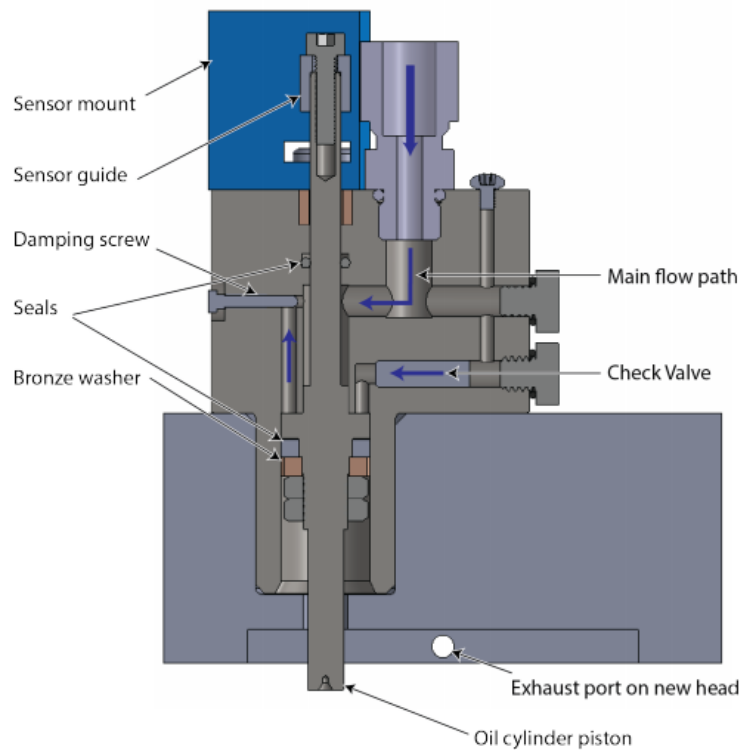
Figure 4.2 The section view of the cushioning device [109]

Besides the modifications made to the HVVA system for this research that was mentioned in above, it is also very important and necessary to point out the major differences between the valve motion controls of the HVVA system and the conventional cam-based valve trains.

For cam-based valve trains, the motions of engine valves follow the exact pre-designed cam profiles regardless the engine speed and the in-cylinder pressure. Moreover, the actual valve timings, namely the IVC, IVO, EVC, and EVO, are fixed to the certain cam designs and are directly altered by phase-shifting the cams in specific degrees when VVT is engaged.

However, unlike the cam-based valve trains, the actual valve timings of the HVVA system cannot be directly controlled. Instead, the HVVA system controls the opening timings for each spool valve, known as the TPA timings, to indirectly manage the opening and closing timings of the engine valves. The opening timing of the spool valves is determined by the relative angular positions of their spool ports and casing ports.

In another word, whenever the spool port spins to the angular position that tangent to the casing port, as marked out in Figure 4.1, the spool valve is considered as starting to open at that TPA moment. The oil will be then allowed to flow through the ports during the entire opening duration of the spool valve. The TPA timings for all the spool valves can be freely altered by changing the angular positions of their casing ports without interfering with each other, and eventually resulting in the variations of the actual valve timings.

To better demonstrate how the actual valve timings are related to the TPA timings of the HPSV and LPSV for both the intake and exhaust valves, an illustration is shown in Figure 4.3.
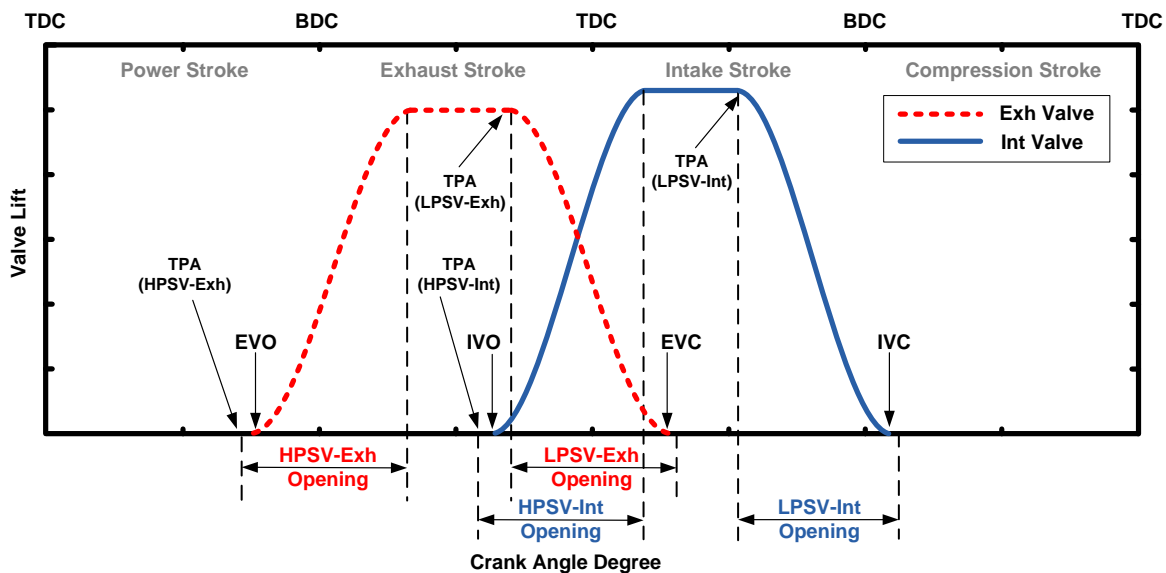
Figure 4.3 Demonstration of the TPA timings and engine valve timings

Seeing from Figure 4.3, the following explanations are given for providing better understandings to the characteristics of the HVVA system. With the same pressure built up within the accumulator at the upper stream of the hydraulic circuit, the engine valve would take a longer duration in terms of CA degrees to open to a certain valve lift at higher engine speeds than that at a lower engine speed. And this fact applies when the engine valves are to be closed and seated as well, for the releasing of

44

the pressure within the hydraulic cylinders also takes longer CA durations as the engine speed increases. In addition, whenever an HPSV has come to its TPA moment and ready to open, a delay on the actual valve opening timing would be noticed with respect to the corresponding TPA timing. This is because it would take time for the hydraulic cylinder to build up a pressure that could overcome both the preload force of the valve spring before driving the engine valve to move.

An HVVA assembly for a single set of the engine valve is firstly modeled in GT-Suite and calibrated by a set of HVVA bench tests. The hydraulic circuit is modeled from a stabilized high-pressure source, namely a point within the hydraulic circuit at which the pressure is retained by the accumulator, all the way to the oil outflow port that connected to the hydraulic fluid reservoir. However, the oil pump and the accumulator are not modeled in this system due to the redundancy and unnecessary complexities of modeling these components which are beyond the scope of this research.

For performing the HVVA system testing and model calibrations, Figure 4.4 shows the assembled test bench of the modeled single-valve-set HVVA system while the key specifications are listed in Table 3.
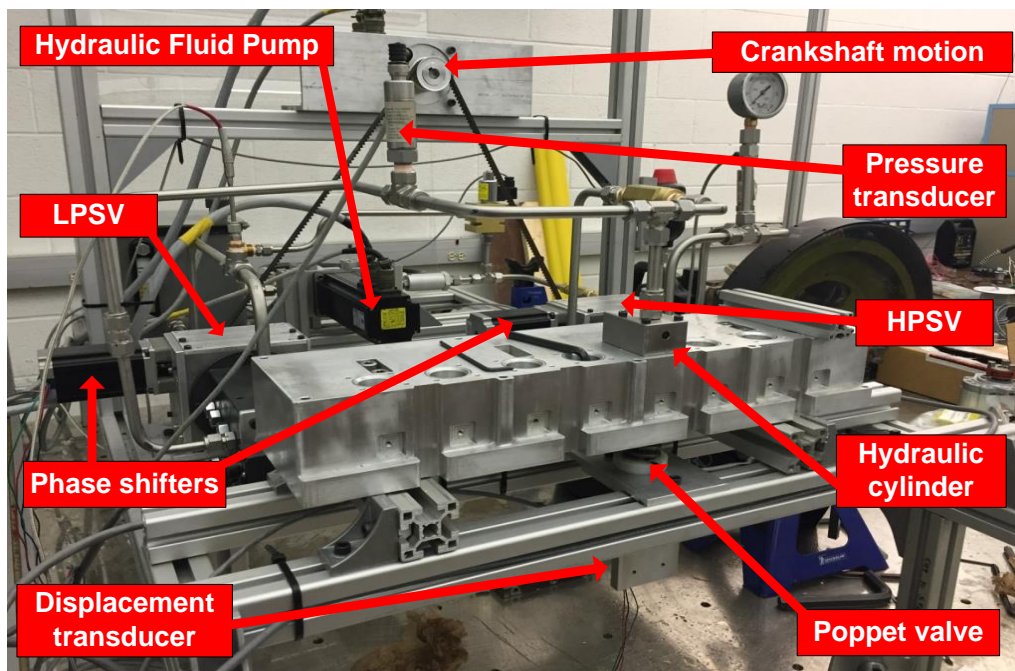
Figure 4.4 Test bench of the HVVA system (Single-valve-set assembly)

Table 3 HVVA system specifications
HVVA system specifications

Oil pressure at high pressure source	39 bar
Hydraulic piston diameter	15 mm
Spool valve diameter	35 mm
Spool valve port/casing port diameter	10 mm
Valve spring stiffness	40 N/mm
Valve spring preload	280 N
Diameter of the oil pipelines	7.8 mm

As shown in Figure 4.5, with the key parameters been calibrated by the experiments, such as the damping coefficients of the hydraulic piston, discharge coefficients at different openings of the spool valves and etc., the model of the HVVA system is also verified via bench tests showing good predictions to the actual profiles of the engine valve motions.
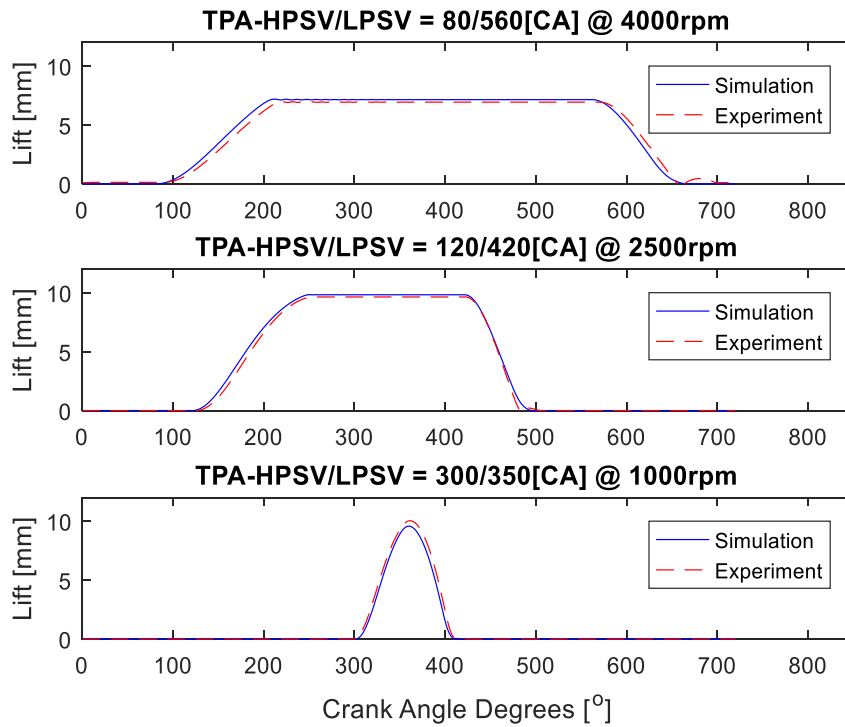
Figure 4.5 Calibration results of the HVVA system

4.2 The Baseline Engine

In this research, an OC single-cylinder gasoline engine is used as the baseline engine and modeled in GT-Suite, with its specifications listed in Table 4.

Table 4 Baseline engine specifications

Baseline engine specifications	
Displacement	196 cm^3
Bore	68 mm
Stroke	54 mm
Geometric compression ratio	8.5:1
Working Speed range	2000 rpm-3600 rpm
Number of valves	1 intake/1 exhaust
Throttle type	Butterfly
Net torque	12.4 Nm @ 2500 rpm
Net power	4.1 kW @ 3600 rpm
Valve motion events (EVO/EVC/IVO/IVC)	(129/413/345/620) CA^o
Maximum valve lift (intake/exhaust)	(5.59/5.63) mm

As shown in Figure 4.6 and Figure 4.7, a GT-Suite model of the baseline engine is built by taking cautiously measurements to its geometrics and carefully calibrated by using the data collected from the bench tests. In addition, all the prerequisite parameters that are required by the component modules of the GT-Suite are also acquired experimentally via separated pre-tests.
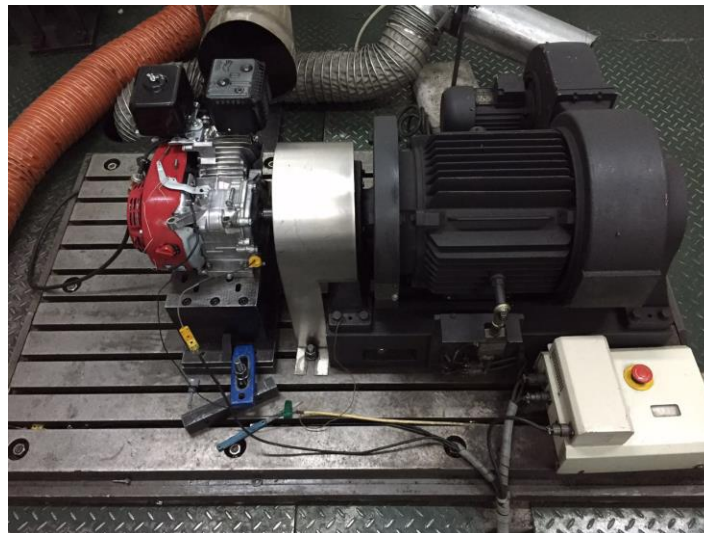
Figure 4.6 Bench test set up of the baseline engine for performance testing
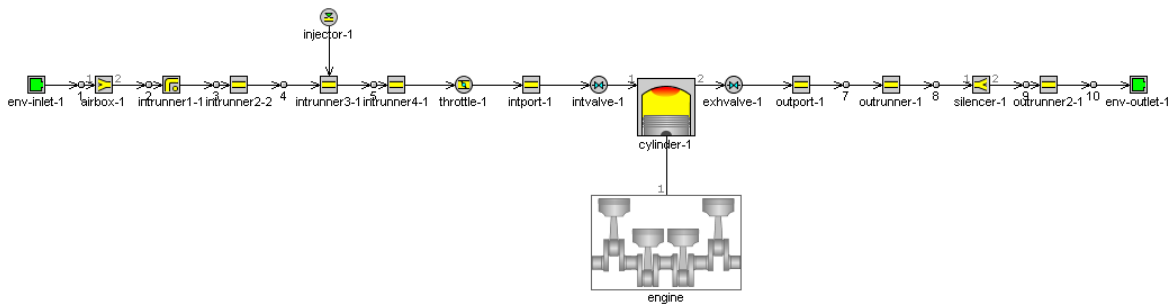
Figure 4.7 GT-Suite model of the baseline engine

As shown in Figure 4.8, one of the pre-tests for identifying the lift-dependent forward and reverse discharge characteristics for both the intake and exhaust valves, which are required by the GT-Suite model as the prerequisite parameters for the engine valve modules, is presented. The acquired flow coefficient tables are presented in Figure 4.9.

Figure 4.8 Cylinder head inlet and outlet flow tests for flow coefficient
identification at different valve lifts

48
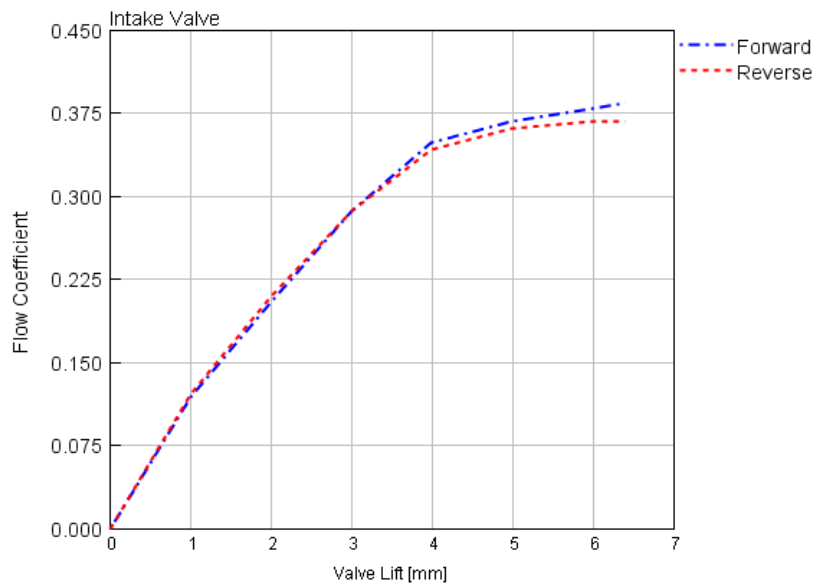
(a)
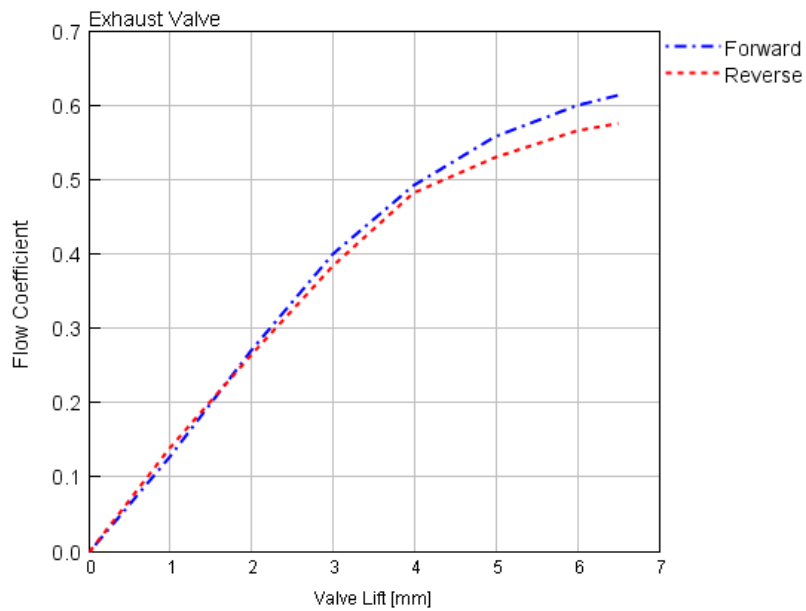
(b)

Figure 4.9 Acquired valve-lift-dependent flow coefficient tables for both the intake (a) and exhaust (b) valves

By performing all the related experiments, the GT-Suite model of the test engine is properly calibrated, and the calibration results are shown in Figure 4.10.

49
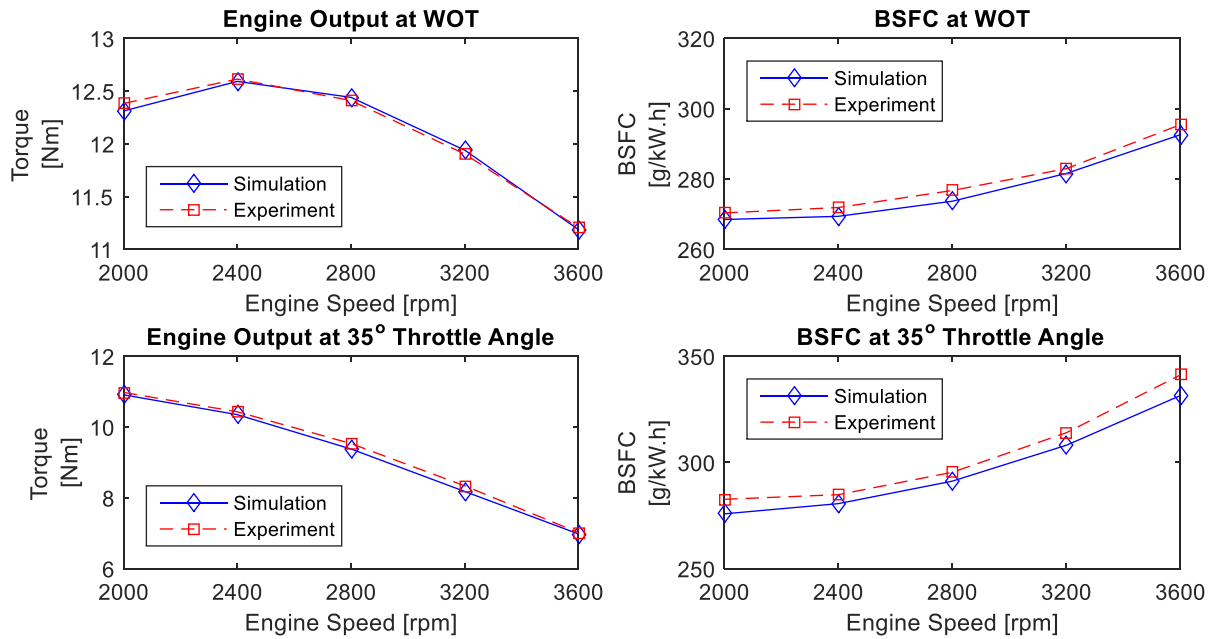
Figure 4.10 Calibration results of test engine model

4.3 GT-Suite and MATLAB-Simulink Co-simulation Model of the Converted Unthrottled HVVA Engine

As explained from above, the resultant valve motions of the HVVA system are different from those of the cam-based valve systems due to the completely different driven techniques of these two types of valve trains. Apart from considering this fact, however, it also should be noticed that one of the major differences of modeling the HVVA engine from modeling a cam-based engine is the interdependent behaviors of the valve system and the engine cycles are needed to be reflected.

This is because the valve motions would be affected by the in-cylinder pressure, which could be varying significantly during a full engine cycle and is dependent on the outcome of the engine combustion processes. Therefore, an indispensable term of $F_{pressure}$, which stands for the force that applies on the engine valve head due to the in-cylinder pressure, is needed to be considered while deriving the motion equations of the HVVA engine valves.

With the parameters defined in Table 5, while letting $x = 0$ indicate the position where the valve is completely seated and assigning the positive motion direction as the same direction as the valve's

opening motions, the valve lifts x for both the intake and exhaust valves are physically modeled based on the governing equation of

$$m\ddot{x} = A_h P_h - F_{preload} - kx - F_f - F_{pressure} - F_{contact} \tag{4.2}$$

Table 5 Definitions to the parameters in Eq. (4.2)

Definitions to the parameters in Eq. (4.2)

m	Overall moving mass
x	Valve lift
A_h	Effective area of the hydraulic piston
P_h	Pressure within the hydraulic cylinder
k	Valve spring stiffness
$F_{pressure}$	Resultant force on valve due to non-equivalent gas pressures on both sides of the valve head
$F_{contact}$	Contact force between the engine valve and the engine body at both ends of the valve travel
$F_{preload}$	Preload force of the valve spring
F_f	Frictions to the valve motion

However, $F_{pressure}$ does not apply as a constant force to the engine valve heads during the entire motion of the valves, it would dissipate rapidly after the valve opens to a certain tiny lift, at which the pressures at the top and back of the valve heads are equalized. Thus, in this research, $F_{pressure}$ is modeled as to exist while the valve lift is no greater than a pre-decided threshold lift C, and disappears while the valve lift exceeds the threshold. For different engines, the threshold lift C is always needed to be tuned and determined through model calibrations by experiments. Accordingly, the $F_{pressure}$ is estimated by

$$F_{pressure} = \begin{cases} P_c A_v - P_c' A_v' & when \quad (x \le C) \\ 0 & when \quad (x > C) \end{cases} \tag{4.3}$$

with P_c and P_c' representing the transient pressures within the cylinder and the inlet (or outlet for exhaust valve), A_v and A_v' as the corresponding effective areas at the front and back of the poppet valve head, while C indicates the pre-decided threshold lift.

Furthermore, the overall friction to the valve motions, F_f, and the contact force between the valve and the hard stops at both ends of the valve travel, $F_{contact}$, are found as

$$F_f = \begin{cases} sign(\dot{x})F_k & when & (\dot{x} \neq 0) \\ F_s & when & (\dot{x} = 0 \quad and \quad x = 0) \\ -F_s & when & (\dot{x} = 0 \quad and \quad x = x_{max}) \end{cases} \tag{4.4}$$

and

$$F_{contact} = \begin{cases} A_h P_h - F_{preload} - kx - F_f - F_{gas} & when \quad ... \\ \\ 0 & else \end{cases}$$

$$\tag{4.5}$$

$$\begin{array}{ll} ... & (x = 0 \quad and \quad A_h P_h < F_{preload} + kx + F_f + F_{pressure} \\ or & x = x_{max} \quad and \quad A_h P_h > F_{preload} + kx + F_f + F_{pressure}) \end{array}$$

respectively, where F_k stands for the kinematic friction resulted from both the moving contacts between parts and the damping effects while the valve is in motion, and F_s is the static friction when the valve is stationary.

Based on the abovementioned features of the HVVA system, the proposed HVVA engine model in this research is built in a way that is capable of capturing the characteristics of the HVVA system and realizing the interdependency of the HVVA system and the engine. The modeled throttle-less single-cylinder engine mounted with the HVVA system in GT-Suite is shown in Figure 4.11.

In addition, it is worth to mention that this HVVA engine model simulates the HVVA valve motions and the engine cycles under the same frequency and is capable of realizing the interdependency between the HVVA valve motions and the engine performance. Also, the simulation results are only to be retrieved and considered as valid after both the engine cycles and the HVVA valve motions have reached a steady state.

As shown in Figure 4.11, the major sub-components of the model have been marked out and listed in below along with the elaborations to their main features.

- The engine: The single-cylinder SI gasoline engine is modeled in this block. However, since the engine load will no longer be controlled via throttling, the throttle body module is removed from the baseline engine model that was introduced in Figure 4.7.
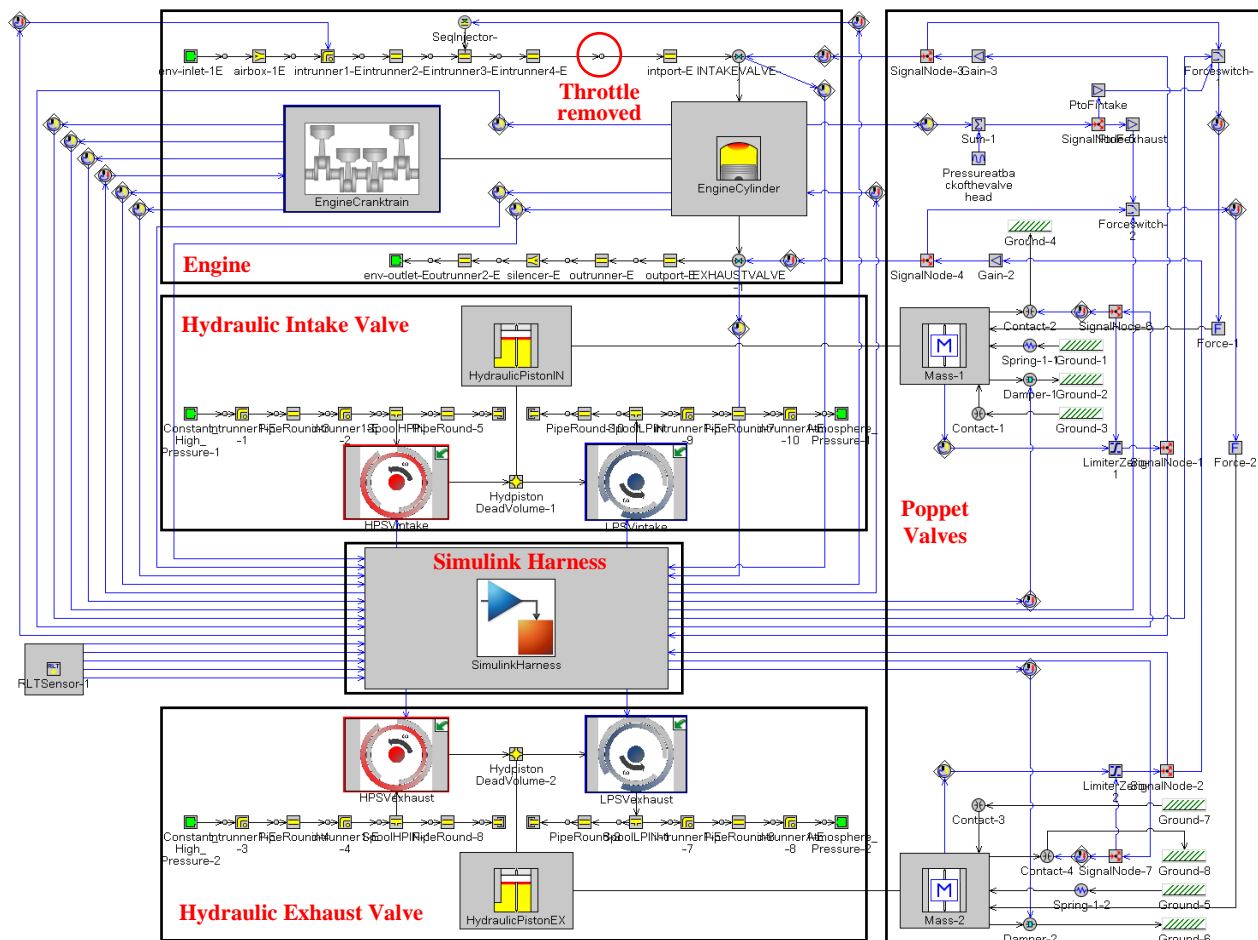
Figure 4.11 The GT-Suite model of the HVVA engine

- The hydraulic intake/exhaust valves: As the same as the single-valve-set HVVA system modeling that was mentioned in the previous section, the hydraulic circuits for both the intake and exhaust valves are modeled individually.

- The poppet valves: According to the governing valve equations of Eqs. (4.2-4.5), the resultant forces, as well as the displacements of the poppet valves, are modeled in this block with the maximum lifts of the intake and exhaust valves are capped at those of the original cam-based engine.

- The Simulink Harness module: The Simulink Harness serves as a bridge for real-time data exchange between the GT-Suite model and the Simulink model in MATLAB. In fact, the simulation of the HVVA engine is initiated from the MATLAB-Simulink environment, in which, not only the GT-Suite model is initialized and called to simulate the engine performance, but also

53

the retrieved GT-Suite data are post-processed to compute the desired information, such as the IEGR rate, gas backflow at intake or exhaust valve and etc. Furthermore, this module grants the model the capability of performing the later-proposed GA optimization schemes that will be elaborated in the next chapter.

Moreover, it is also essential to mention and explain the choice on the combustion model that is adopted in this research. Since that the engine performance is dependent on the overall outcome of the gas exchange process and the subsequent combustion process, a suitable combustion model that is capable of predicting the combustion scenarios resulted from different HVVA strategies is required. With the highly flexible valve motions provided by the HVVA system in this research, the turbulence intensity of the cylinder charge could be varying noticeably upon different valve timings, which would affect the subsequent combustion process and bring impacts to the engine performance. This is mainly because that the change of the in-cylinder turbulence takes an important role on the air-fuel mixing process and the flame propagation speed during combustion, which are straight related to the overall burn rate of the fuel and the combustion duration.

Generally speaking, a stronger in-cylinder turbulence could lead to a better mixed air-fuel mixture and a shorter combustion duration, which would be eventually reflected by the resulted engine performance, e.g. higher engine output at full load operations, or less fuel consumption at partial load operations. As a result, the commonly used Spark-Ignition Wiebe Combustion Model (SIWiebe) for simulating the combustion process of SI engines turns out to be not suitable for use when modeling the HVVA engine in this research because of the impacts to the combustion process brought by the different motions of the HVVA system, such as the resultant changes in the in-cylinder turbulence intensity, residual gas fraction and etc. can hardly or even not be able to be reflected by a SIWiebe combustion model. The Spark-Ignition Turbulent Flame Combustion Model (SITurb), on the other hand, takes into account the in-cylinder air motions, fuel properties, SA, locations of the spark plugs when predicting the combustion process [110], hence, is considered as a more appropriate and capable option for modeling the combustion process in this research.

By providing the geometry of the combustion chamber, the SITurb combustion model is fed with the turbulent intensity of the in-cylinder gas flow, which is evaluated by the embedded 'EngCylFlow' sub-model [110], together with the specified SA, AFR, spark locations and etc. when predicting the subsequent combustion process. This makes the SITurb combustion model capable of reflecting the resultant variations in the heat release rate, burn rate and knock intensity caused by different

conditions of combustion. Moreover, for performing more accurate model predictions to a specific engine, the internal parameters of the SITurb combustion models, such as the Flame Kernel Growth Multiplier, Turbulent Flame Speed Multiplier, Taylor Length Scale Multiplier and etc., can even be fine-tuned with the technique proposed in [56] through further calibrations if the detailed experimental data of the combustion processes are available. Therefore, the SITurb combustion model can provide a good estimation to the combustion process for realizing the engine performance resulted from the highly variable valve motions of the HVVA system, and is thusly proper for this research.

4.4 Summary

In this chapter, after conducting a series of prerequisite experiments along with the bench tests of the HVVA system and the baseline engine, the HVVA engine model is developed and calibrated. This model is able to realize the interdependency of the HVVA system and the engine cycle. In addition, the adoption of the SITurb combustion model can make the HVVA engine model to be able to reflect the impacts on the resultant engine performance caused by the variations of the valve motions and other considered operating parameters, which is a very essential and indispensable feature of the proposed HVVA engine model.

Moreover, this proposed model is developed for performing GT-Suite and MATLAB-Simulink coupling simulations, which makes it compatible to the later-introduced GA optimizer functioned by MATLAB codes.

Chapter 5

Model-based GA Optimizations for Improving the Power and Fuel Economy of the Unthrottled HVVA Engine[1]

5.1 MATLAB-Simulink and GT-Suite Coupling Model-Based GA Structure

The genetic algorithm (GA) is one of the most popular optimization methodologies among the big class of the evolutionary approaches. It is inspired by the natural selection of the nature that makes the fittest individuals survive throughout generations during the evolution and mutation processes of the breed. The GA is suitable for solving both the constrained and unconstrained global optimization problems despite the continuities of the objective (or fitness) functions. It also has been widely applied to the engine performance optimization problems [98-101]. Hence, the optimization strategies in this research are developed on basis of the GA approach.

In this research, since the designed GA optimizer is functioned by MATLAB while the engine performance is simulated in GT-Suite, a MATLAB-Simulink and GT-Suite co-simulation is required to perform the optimization procedures. For a more visualized and clearer demonstration to the build of the entire model of this research, Figure 5.1 shows the illustrated GT-Suite and MATLAB-Simulink co-simulation structure along with the data flow within.

Furthermore, the detailed flowchart of the GA optimization scheme carried out by the MATLAB-Simulink and GT-Suite co-simulation is shown in Figure 5.2, with the execution environments of each step being marked out as the icons shown next to the flow blocks. The detailed steps can be elaborated as follows:

a. The main body of the GA optimization approach is coded and executed in MATLAB. The MATLAB performs initializations to both the GA and the Simulink model, then generates the initial population with each contained individual carries a set of the variables that are within their corresponding domains.

b. All the individuals belonged to the current population are passed to the Simulink model one by one, in which the individuals are deciphered into the required input variables and fed to the GT-Suite model.

_____

[1] Refer to the "Statement of Contributions" for authorship details of the contents in this chapter.

c. The GT-Suite simulates the engine performance under the given parameters and exchanges the data with Simulink in real-time through the Simulink Harness Module. A module in the Simulink model observes the number of the current simulated engine cycle and retrieves the resulted performance data of the twentieth engine cycle from GT-Suite, which holds the effective information after the simulated engine and the HVVA system have both reached a steady operating state.

d. The real-time data received by the Simulink are post-processed to calculate those concerned objects that could not be directly retrieved from the GT-Suite model.

e. The core GA approach evaluates the fitness value of the current individual in MATLAB and passes out the next individual for repeating the steps from *b* to *e* until all the fitness values of the individuals in the current population are computed.
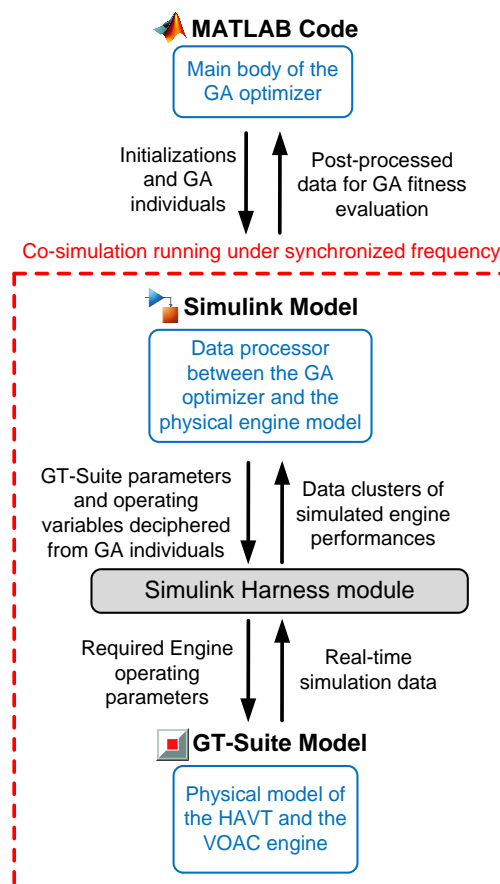
Figure 5.1 Illustration to the data flow within the GT-Suite and MATLAB-Simulink co-simulation structure

f. The selection, crossover and mutation procedures of the GA approach are carried out by the main optimization algorithm written in MATLAB for creating a new population of the next generation after all the individuals in the current generation have been evaluated. The new population will then go through the steps from *b* to *e* unless the GA termination criterion is satisfied and no further generation is needed to be produced.

g. The optimization procedure is completed when the termination criterion of the GA approach is met. The GA optimizer returns the best individual found in the progress and the optimum solution is considered to be identified.
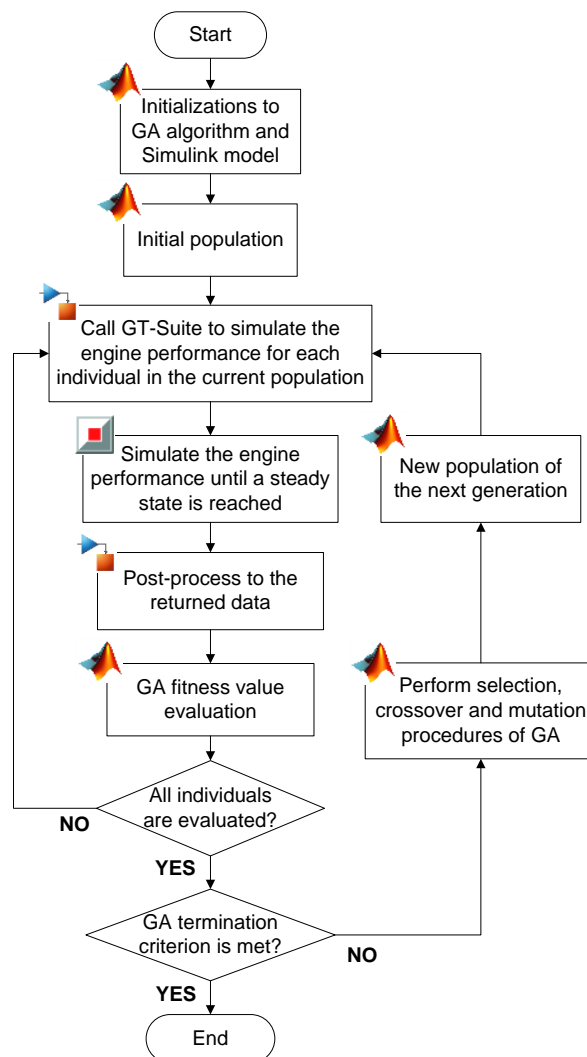
Figure 5.2 Flowchart of the MATLAB-Simulink and GT-Suite co-simulation based GA optimization scheme

5.2 Power Optimizations at Full Engine Load Operations via Realization to Variable Otto Cycle (VOC)

For full load engine operations, the adoption of the OC is favored over the AC due to the requirements of a full charge to the cylinder and a maximized ECR that could yield to the preference of greater engine output since the geometric displacement of the engine is fixed. With the cam-based valve trains, phase shifting VVT systems are commonly used to achieve a more satisfactory full charge to improve the VE according to the engine speed by shifting the cam phases to a more advanced or more retarded timing which would result in the same changes to the opening and closing timings to each of the valves.

However, as mentioned earlier, longer valve opening durations are required for maximizing the engine's power performance at higher engine speeds, hence the engine's maximum output at different speeds could actually be further improved since the cam-based valve trains are mostly incapable of providing continuous variations to the valve opening durations which limits the potential for improvements. With the HVVA system, by individually altering the timings for each of the HPSV and LPSV for both the intake and exhaust valves, not only the valve timings, but also the valve opening durations can be continuously adjusted in terms of the crank angle degrees, providing even better valve motion events than those achieved by the cam phase-shifting techniques, and could lead to a further optimized engine performance via performing a variable Otto cycle (VOC).

In order to better demonstrate the potential for power improvements at full load that could be achieved solely by optimizing the valve motions, which shows the importance of the valve motions and their impacts to the engine performance, and to identify the different resulting engine outputs from adopting the VOC and the original OC out of the same engine, the sparking angle and the air-fuel ratio are initially left to be unchanged during the power performance optimizations in this section for the purpose of providing a clearer explanation to the proposed GA structure and a more fair comparison over the two implemented engine cycles.

Since that the HVVA system can only control the TPA timings of the spool valves, by defining the vector $u = (\text{TPAHE, TPALE, TPAHI, TPALI})$ as a single individual in the GA population that carries 4 genetic genes, which represent the TPA timings for the HPSV of the exhaust valve, LPSV of the exhaust valve, HPSV of the intake valve and LPSV of the intake valve in terms of crank angle

degree, respectively, the designed approach for performance optimization at full load operations can be described as maximizing:

$$F(u, rpm) = Torq(u, rpm) \tag{5.1}$$

subject to:

$$80^{\circ} CA \leq TPAHE \leq 180^{\circ} CA \tag{5.2}$$

$$260^{\circ} CA \leq TPALE \leq 360^{\circ} CA \tag{5.3}$$

$$260^{\circ} CA \leq TPAHI \leq 360^{\circ} CA \tag{5.4}$$

$$480^{\circ} CA \leq TPALI \leq 560^{\circ} CA \tag{5.5}$$

$$KI(u, rpm) \leq KI_{LIMIT} \tag{5.6}$$

where the specified crank angle degrees are with respect to the corresponding crank angle of the engine piston at its TFDC, and *Torq* is the resultant engine torque evaluated by the HVVA engine model built in GT-Suite under the operating parameters contained by the corresponding individual of *u* and at the prescribed engine *rpm*. By using the method proposed by Douaud & Eyzat for calculating the induction time integral that is used for detecting cylinder knock [111], the knock intensity is then judged and evaluated by the knock index (KI), which is a phenomenologically-based crank-angle-dependent parameter developed by the Gamma Technologies [110] that is evaluated by Eq. (5.7) with all the parameters been defined in Table 6.

$$KI = 10^5 M \cdot \max(0, 1 - [1 - \Phi(CA)]^2) \cdot I_{ave}(CA)$$
$$\cdot \frac{V_{TDC}}{V_{cyl}(CA)} \exp\left(\frac{-6000}{T_{unburn}(CA)}\right) r_{unburn}(CA) \tag{5.7}$$

Table 6 Definitions for the parameter in Eq. (5.7)
Definitions for the parameter in Eq. (5.7)

Φ	Equivalence ratio of the unburned zone
M	KI multiplier
T_{unburn}	Bulk unburned gas temperature (K)
I_{ave}	Averaged induction time integral
r_{unburn}	Percentage of unburned in-cylinder gas mass
V_{cyl}	Transient cylinder volume
V_{TDC}	Cylinder dead volume

Therefore, as is described by Eq. (5.6), the knock probability should be always constrained within an acceptable domain by keeping the evaluated KI under the limit value of KI_{LIMIT}, which is the KI value that is calibrated experimentally to correspond to the scenario when noticeable gentle knock occurs.

Since that the non-linear constraint of Eq. (5.6) is needed to be eliminated in order to transform the current GA optimization problem into a non-constrained one, it is then paraphrased into an added penalty to the fitness function of Eq. (5.1). As a result, the appropriate GA approach for depicting this optimization problem is eventually designed and constructed in the form of minimizing:

$$F'(u, rpm) = \frac{1}{Torq(u, rpm)} + \Lambda(u, rpm) \tag{5.8}$$

subject to Eqs. (5.2-5.5), with Λ be found by

$$\Lambda(u, rpm) = \begin{cases} W_{KI} \cdot \max(\dfrac{KI(u, rpm)}{KI_{LIMIT}} - 1, 0) + C_{KI} & when \quad (KI > KI_{LIMIT}) \\ 0 & else \end{cases} \tag{5.9}$$

where W_{KI} and C_{KI} are indicating a weighting factor and a constant penalty, respectively.

In Eq. (5.8), Λ stands for the calculated penalty that corresponding to the non-linear constraint of Eq. (5.6) under the given parameters, which has not only been weighted by W_{KI}, but also been added with a constant penalty C_{KI}. The weighting factor W_{KI} is functioning after being properly adjusted for assuring the GA optimization would come to an effective convergence without ignoring the constraint. The constant penalty C_{KI} is designed for providing a noticeable increment to the fitness to make the GA optimizer capable of identifying the unfitted solutions that violate the constraint on the knock limit without being mistaken by the relatively small penalties from unqualified individuals when performing selections.

In addition, it is also worth mentioning that an over-wide search domain to the variables could result in a non-convergence to the GA approach or take an unnecessarily long time for the GA to identify the optimum throughout a huge number of redundant evaluations to the individuals that correspond to the valve timings do not even comply with the reality. Yet, an improperly tight domain would cause the real optimal solution to be never found. Thus, the domains of the variables in Eqs.

(5.2-5.5) are determined through multiple trials over reasonable guesses based on the comparison between the resultant valve timings and those from the common experiences.

By initializing the GA with a crossover rate of 0.8, population size of 50 and elite rate of 0.1 under a prescribed accuracy of per CA degree to all the variables, the GA approach could reach to a good convergence at between 40 and 60 generations from multiple trials of the optimization. Figure 5.3 and Figure 5.4 present the performance of the GA operation and the convergences of all the variables at 3600rpm engine speed, respectively.
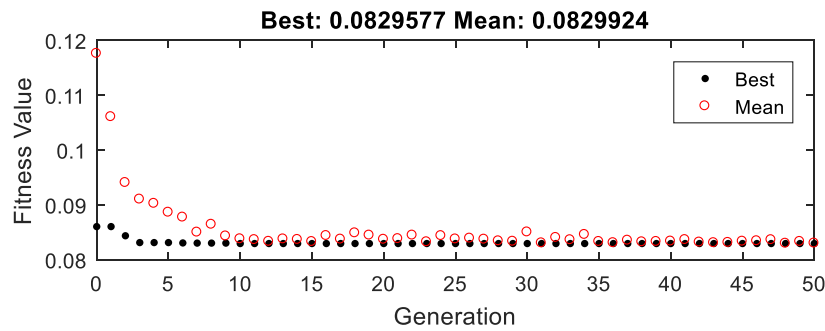
Figure 5.3 GA fitness convergence for performance optimization at 3600rpm
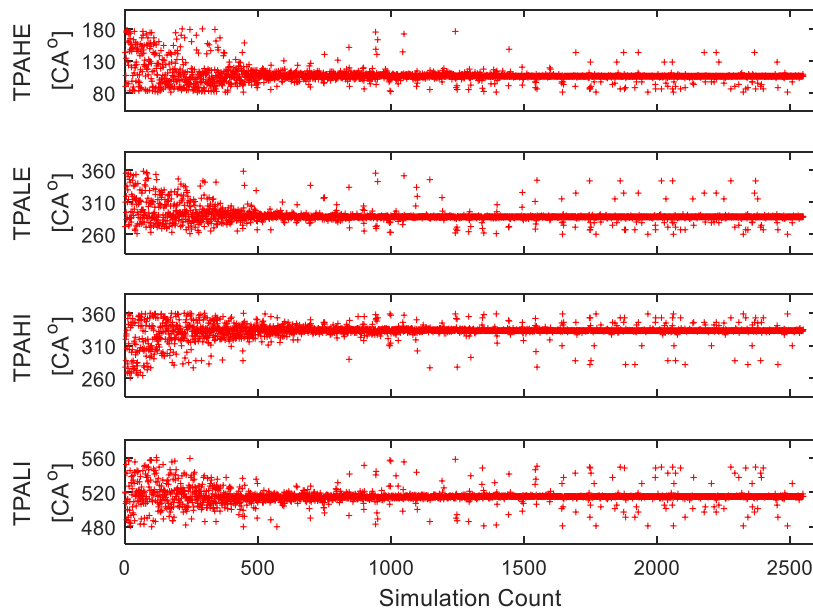
Figure 5.4 Convergence of the variables during GA operation for the power optimization at 3600rpm

62

5.3 Fuel Economy Optimizations at Partial Engine Load Operations

For the realizations to partial load operations, two different engine operation schemes are proposed in this section for improving the engine's fuel economy by performing unthrottled load controls. The corresponding GA optimizers are developed for identifying the considered operating parameters of the HVVA engine for both of the proposed engine operation schemes, and are elaborated in below.

5.3.1 Realization to Unthrottled Engine Load Control with Tunable IEGR

One of the proposed engine operation schemes for realizing the unthrottled engine load control of the HVVA engine is the adoption to the introduced Tunable IEGR feature. Although, theoretically speaking, the VE could be brought down significantly in order to achieve a desired low engine load from introducing a large IEGR rate to the engine cycles, the IEGR rate, however, can not be allowed to be over-set in reality. For those circumstances that the engine load cannot be guaranteed by operating the IEGR alone, an EIVC strategy is engaged to regain control towards the desired engine load.

According to the restrictions to the IEGR implementation that was mentioned in Chapter 3, an over performed IEGR, especially at low engine loads, may cause considerable impacts to the flame propagation speed during the combustion process and could cause very unstable running of the engine. Such impacts can result in an abnormal drop of the engine thermal efficiency, or even lead to ignition failures. Therefore, a maximum feasible IEGR rate should be identified through experiments and specified before implementing the tunable IEGR feature.

Moreover, due to the extremely high temperature carried by the burned gas could scorch or even inflame the intake manifolds, the gas backflow at the intake valves during the exhaust process is normally to be avoided for most of the engine cycle designs. Accordingly, the gas backflow at the intake valve is decided to be utterly prohibited over the entire engine cycles in this proposed engine operation scheme.

However, as the introduced IEGR could cause noticeable variations to the period of the inflammation retardation and the combustion speed, the air-fuel equivalence ratio λ (lambda) and the SA have to be optimized all together along with the valve motions in order to pursue greater improvements on the engine's fuel economy at partial loads. As can be seen from the definition of the lambda written in Eq. (5.10):

$$\lambda = \frac{AFR_{actual}}{AFR_{stoich}} \tag{5.10}$$

where the AFR_{actual} is stand for the actual AFR that is adopted by the engine, while AFR_{stoich} indicates the stoichiometric AFR, which is 14.7 for gasoline in this research, it is then easy to understand that when λ equals to 1, the flammable mixture is at stoichiometry, with greater than and less than indicating a lean and a rich mixture, respectively. More importantly, since the raised in-cylinder temperature and pressure by the IEGR could cause an increased knock probability to the engine combustion process [64], the prediction to the cylinder knock is also essential and needed to be taken into consideration in this section.

Therefore, for the optimization scheme of this section, 6 variables are contained by a single individual in the GA. The proposed GA approach for fuel economy optimization at partial engine load from implementing the tunable IEGR feature is designed and elaborated as follows.

By defining $v = (\text{TPAHE, TPALE, TPAHI, TPALI, SA, } \lambda)$ as the chromosome of the individuals in this GA optimization, the objective of optimizing the engine's fuel economy while taking account of the abovementioned constraints can be expressed by the GA optimization problem of minimizing:

$$H(v, rpm) = BSFC(v, rpm) \tag{5.11}$$

subject to:

$$IEGR(v, rpm) < IEGR_{\max} \tag{5.12}$$

$$KI(v, rpm) < KI_{LIMIT} \tag{5.13}$$

$$\left| Torq(v, rpm) - T_{desired} \right| < T_{tol} \tag{5.14}$$

$$BFM_{int}(v, rpm) = 0 \tag{5.15}$$

$$80^{\circ} CA \le TPAHE \le 160^{\circ} CA \tag{5.16}$$

$$330^{\circ} CA \le TPALE \le 520^{\circ} CA \tag{5.17}$$

$$280^{\circ} CA \le TPAHI \le 380^{\circ} CA \tag{5.18}$$

$$400^{\circ} CA \le TPALI \le 520^{\circ} CA \tag{5.19}$$

$$-50^{\circ}CA \leq SA \leq -10^{\circ}CA \tag{5.20}$$

$$0.9 \leq \lambda \leq 1.2 \tag{5.21}$$

where $T_{desired}$, T_{tol} and $IEGR_{max}$ are representing the desired torque at the partial engine load, a pre-described acceptable tolerance to the resultant engine torque with respect to the desired torque, and the maximum tolerable IEGR rate, respectively, while the BFM_{int} stands for the accumulated mass of the gas backflow at the intake valve over a single or multiple full engine cycles upon different preferences.

Similarly, by eliminating the non-linear constraints of Eqs. (5.12-5.15), the GA optimization problem described by Eqs. (5.11-5.21) is then re-interpreted into a new GA task of minimizing:

$$H'(v, rpm) = BSFC(v, rpm) + \Psi(v, rpm) \tag{5.22}$$

subject to Eqs. (5.16-5.21), with the $BSFC(v, rpm)$ to be found by Eq. (5.23) while r_{fuel} and P_{engine} representing the fuel consumption rate in grams per hour and the power produced by the engine in kilowatt, respectively.

$$BSFC(v, rpm) = \frac{r_{fuel}(v, rpm)}{P_{engine}(v, rpm)} \tag{5.23}$$

The Ψ in Eq. (5.22) is a designed overall penalty corresponding to the non-linear constraints resulted by the current individual, which is calculated by:

$$\Psi(v, rpm) = W \cdot \begin{bmatrix} f_1(v, rpm) & f_2(v, rpm) & f_3(v, rpm) & f_4(v, rpm) \end{bmatrix}^T + P_{static} \tag{5.24}$$

$$f_1(v, rpm) = \max(\frac{IEGR(v, rpm)}{IEGR_{max}} - 1, 0) \tag{5.25}$$

$$f_2(v, rpm) = \max(\frac{KI(v, rpm)}{KI_{LIMIT}} - 1, 0) \tag{5.26}$$

$$f_3(v, rpm) = \begin{cases} 0 & when \quad (P_{static} = 0 \quad and \quad |Torq - T_{desired}| < T_{tol}) \\ \left|\frac{Torq(v, rpm)}{T_{desired}} - 1\right| & else \end{cases} \tag{5.27}$$

$$f_4(v, rpm) = BFM_{int}(v, rpm) \tag{5.28}$$

65

$$P_{static} = \begin{cases} 0 & when \quad (f_1 = 0, f_2 = 0, f_4 = 0) \\ \dfrac{T_{tol}}{T_{desired}} W_3 & else \end{cases}$$ (5.29)

where W is a weighting matrix of $[W_1 \quad W_2 \quad W_3 \quad W_4]$ applies to $f_1(v, rpm)$, $f_2(v, rpm)$, $f_3(v, rpm)$ and $f_4(v, rpm)$, respectively. P_{static} is a designed static penalty for checking whether the constraints described in Eqs. (5.12, 5.13, 5.15) are satisfied, if not, a constant penalty that equals to the corresponding penalty value resulted from the actual torque at its maximum tolerance T_{tol} with respect to the $T_{desired}$ would be added to the fitness value. As a result, the compliance to all the constraints can be easily noticed by the GA approach for if any of the constraints is not satisfied, the Ψ would end up with a value that is at least greater than the static penalty $W_3 T_{tol} / T_{desired}$, hence a noticeable increment to the fitness is gained.

The reason for introducing the term P_{static} to the fitness function is to make the GA to be able to automatically pick out those solutions that do not satisfy the absolute restrictions of Eqs. (5.12, 5.13, 5.15) in case the sum of the penalties from Eqs. (5.25-5.28) is small enough to be neglected by GA and make the corresponding unqualified individual to be granted with a higher priority of survival over those qualified ones through generations. Moreover, the translated expression of Eq. (5.27) from Eq. (5.14) can further ensure the GA optimization procedure would stick to its true objective of minimizing the BSFC while the searching process of GA is coming to a final convergence with most of the survived individual have met all the constraints. This is because of the Eq. (5.27) holds the logic of letting the fitness value to be completely dominated by the $BSFC(v, rpm)$ and ignoring the meaningless computed penalty while the actual torque is already within the tolerance, hence avoiding the risk of the searching to the lowest BSFC being screwed by the undesired penalties when all the constraints have been satisfied.

Similar to the power optimizations from the previous case, the accuracies are set to per CA degree for the first 5 variables, but 0.001 for λ in this section. The T_{tol} is set to be 0.05 Nm while a weighting vector of $W = [1000 \quad 500 \quad 5000 \quad 50000]$ is determined as suitable based on many attempts and adjustments, and have proved that it could lead to a proper final convergence of the proposed GA approach. By increasing the population size to 70 and the generations to 100 instead of the 50 and 50 from the previous power optimization case, an exemplary GA performance for optimizing the BSFC

at 7Nm partial engine load and 3600rpm engine speed is shown in Figure 5.5, with the maximum IEGR rate and KI are set to be 0.32 and 100, respectively. Figure 5.6 shows the related convergences to all the variables during the GA optimization progress while the compliances to all the constraints are presented in Figure 5.7.

Best: 276.183 Mean: 319.194
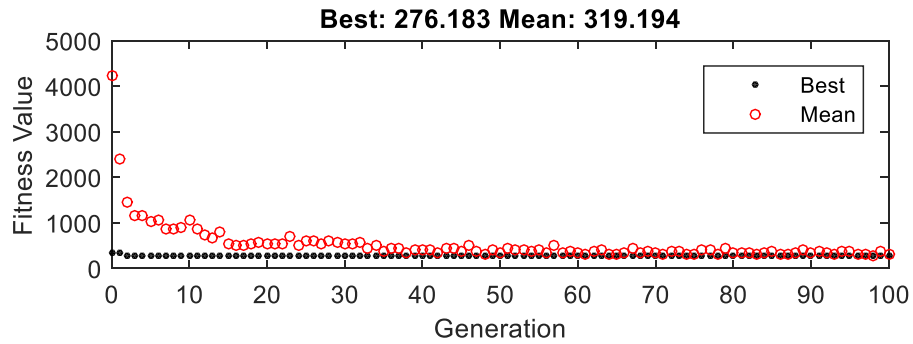
Figure 5.5 GA fitness convergence for fuel economy optimization at 7Nm/3600rpm
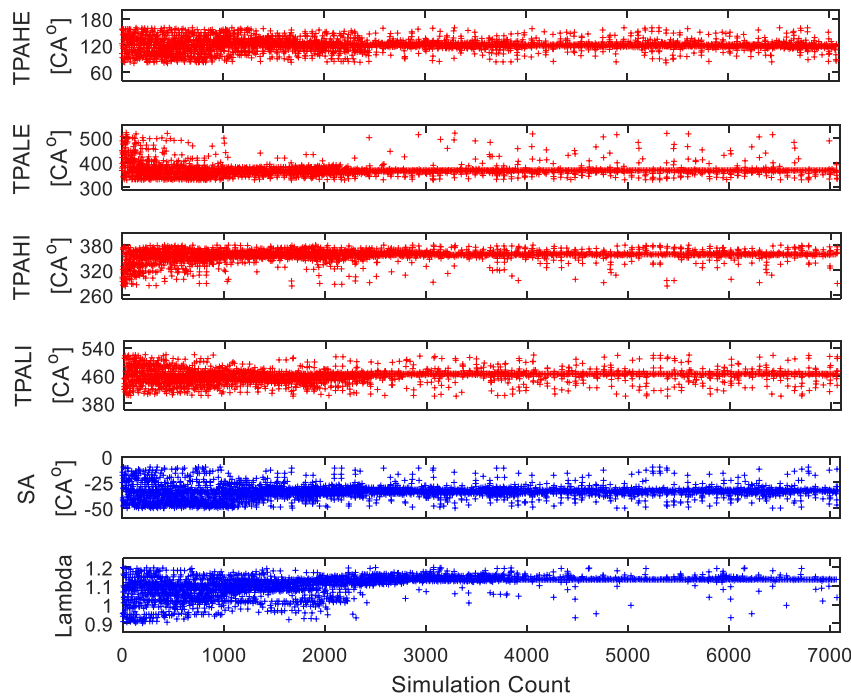
Figure 5.6 Convergence of the variables during GA operation for the fuel

economy optimization at 7Nm/3600rpm

As can be seen from the Figure 5.7, the GA convergence is strictly bounded by all the designed constraints of Eqs. (5.12-5.15), which shows and proofs that the set of the optimized solution to all

the considered operating parameters found by the proposed GA approach is feasible and qualified in terms of the limitations to the maximum IEGR rate and knock index, as well as the objective on achieving the desired engine output and the restriction to the gas backflow at intake valve.
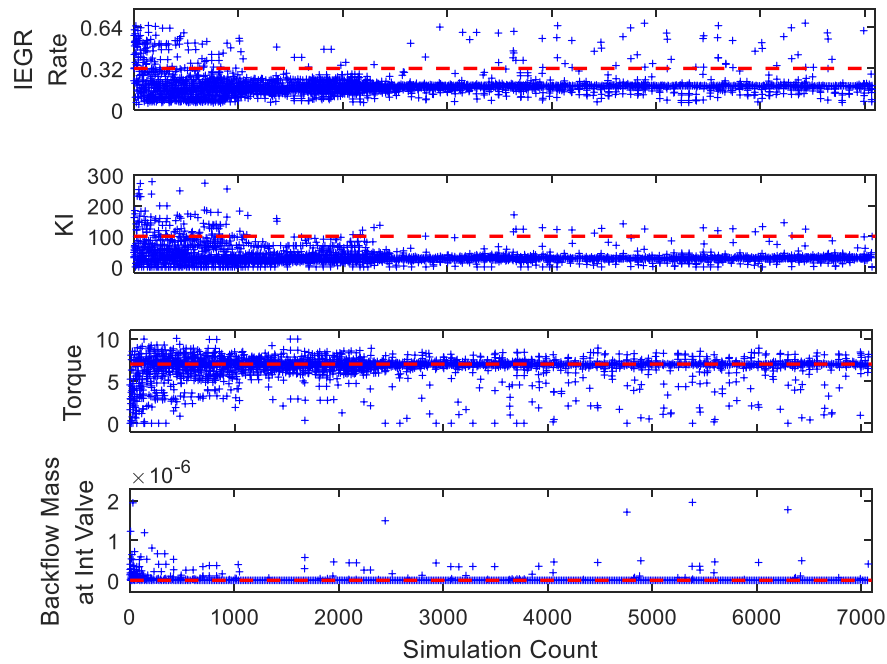
Figure 5.7 Constraint checks during the GA operation for the fuel economy optimization at 7Nm/3600rpm

In addition, a better demonstration on how does the introduced P_{static} penalty helps the GA to discriminate the unqualified individuals by zoning their corresponding penalties apart from those of the qualified ones is explained in Figure 5.8.
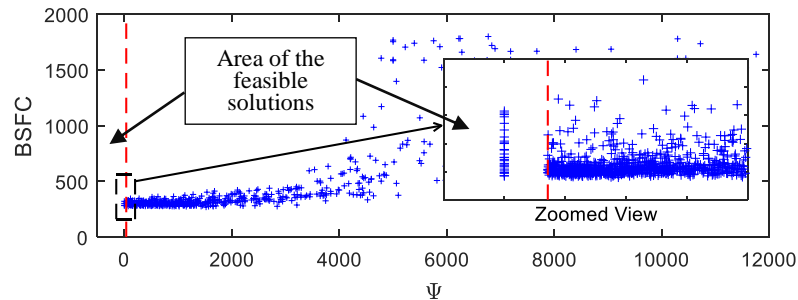
Figure 5.8 BSFC vs Ψ during the GA operation for the fuel economy optimization at 7Nm/3600rpm

68

5.3.2 Realization to Variable Atkinson Cycle (VAC)

Apart from the implementation to the tunable IEGR feature mentioned in above, the other introduced operation scheme for achieving unthrottled partial load control of the HVVA engine while improving the engine's fuel economy is the realization to a fully variable Atkinson cycle (VAC) that is proposed in this section.

In this proposed VAC operation scheme, the ECR and the effective expansion ratio (EER) can be adjusted simultaneously and consecutively to realize distinct ACs, which allows the engine to be able to attain different desired partial load at varying operating speeds without throttling. However, with the optimized ECR and EER, while taking the corresponding SA and AFR into consideration, the fuel efficiency can be increased so that the BSFC at the same speed-load operating point can be reduced comparing to that with the conventional throttled load control.

The variations of the ECR and EER are accomplished by altering the intake and exhaust valve timings, respectively. On one hand, the cylinder charge and the ECR are controlled via different LIVCs, which make the cylinder to take a full charge during the intake stroke since there is no throttling, and push out a portion of the charge back into the intake manifold during the compression stroke. As shown in Figure 5.9, with a greater delay on the IVC (a-b-e-f-g), a smaller VE and ECR would be resulted for achieving a desired lower engine load.

On the other hand, by changing the timings of the EVO, the EER is corporately adjusted along with the ECR, which makes the engine to always be able to adopt an efficient expansion process at any given load and speed, hence, higher thermal efficiency could be achieved. The principle to this was explained in the previous exhaust pumping loss reduction section in Chapter 3. Therefore, with the together-optimized EER and ECR, less positive work is needed to be produced during the power stroke for achieving the same required indicated work of the engine. In another word, a lower BSFC could be resulted by adopting the simultaneously optimized ECR and EER at any speed-load operating point of the engine while running in VAC.

As aforementioned, the proposed VAC adopts an LIVC for regulating the VE instead of throttling. However, differ from most of the existing VAC schemes that are realized by cam-based valve trains or other types of complex mechanisms, this proposed VAC from utilizing the HVVA system shows a greater potential on improving the engine efficiency at partial load operations since the ECR and EER can be easily adjusted by altering the valve timings and opening durations in a continuous manner, which enables the possibility of realizing different degrees of the Atkinson effects.
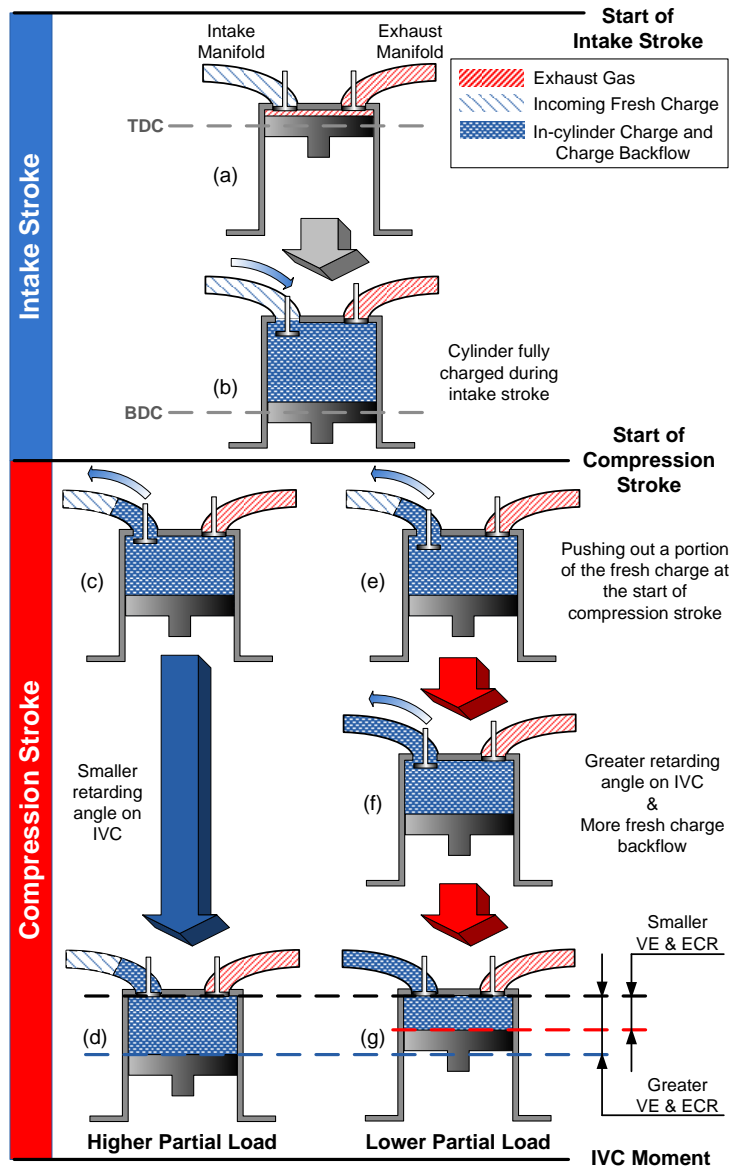
Figure 5.9 Illustration on achieving different VE and ECR for realizing unthrottled load control by running the HVVA engine in VAC

Similar to the introduced GA optimization scheme from the earlier section, by defining all the considered operating parameters as a vector of $v = \left(\text{TPAHE, TPALE, TPAHI, TPALI, SA, } \lambda\right)$, the corresponding GA optimization scheme for pursuing better engine fuel efficiency from realizing the VOC can be described as minimizing:

$$G(v, rpm) = BSFC(v, rpm) \tag{5.30}$$

subject to:

$$80°CA \leq TPAHE \leq 180°CA \tag{5.31}$$

$$280°CA \leq TPALE \leq 360°CA \tag{5.32}$$

$$280°CA \leq TPAHI \leq 360°CA \tag{5.33}$$

$$500°CA \leq TPALI \leq 650°CA \tag{5.34}$$

$$-50°CA \leq SA \leq -10°CA \tag{5.35}$$

$$0.9 \leq \lambda \leq 1.2 \tag{5.36}$$

$$\left| Torq(v,rpm) - T_{desired} \right| \leq T_{tol} \tag{5.37}$$

$$BFM_{int}(v,rpm) = 0 \quad (when \quad CA \leq 380°) \tag{5.38}$$

$$BFM_{exh}(v,rpm) = 0 \tag{5.39}$$

$$SA + 720°CA < IVC(v,rpm) \tag{5.40}$$

where the BFM_{exh} and IVC are the accumulated backflow mass of the gas at exhaust valve and the resulted IVC of the engine.

It can be noticed that the designed constraint for ensuring the knock probability would not exceed its limit is no longer needed in this section because the engine is very unlikely to knock while operating in VOC at partial load operations. Furthermore, since that the gas backflow at intake valve during exhaust processes is commonly prohibited for most of the engines due to the high-temperature exhaust gas may scorch the intake manifold or even inflame the air-fuel mixture within it, the Eq. (5.38) is thusly adopted as the constraint for such event by ensuring the accumulated backflow mass at intake valve, BFM_{int}, is supposed to be maintained at 0 during the exhaust process. In addition, since that the fresh charge is needed to be pushed out from the cylinder during the compression stroke for realizing the Atkinson effects at partial engine loads, and the rejected fresh charge is not supposed to be mixed with the exhaust gas from an IEGR effect in the VAC operations of this section, the exhaust gas backflow at exhaust valve is also forbidden over the entire engine cycle. This is reflected by the Eq. (5.39). More importantly, as the engine is running in VAC realized by LIVCs, it is also crucial to guarantee that the sparking event should always occur no sooner than the actual IVC, hence,

the constraint of Eq. (5.40) is indispensable in this optimization section for preventing the possible interferences between the SA and the actual IVC.

Likewise, by paraphrasing the non-linear constraints of Eqs. (5.37-5.40), this optimization problem can now be transformed into a designed GA approach of minimizing:

$$G'(v,rpm) = BSFC(v,rpm) + \begin{bmatrix} C_1 & C_2 & C_3 & C_4 \end{bmatrix} \cdot \begin{bmatrix} g_1(v,rpm) \\ g_2(v,rpm) \\ g_3(v,rpm) \\ g_4(v,rpm) \end{bmatrix} \tag{5.41}$$

subject to Eqs. (5.31-5.36). The functions of g_1, g_2, g_3, g_4 are corresponding to Eqs. (5.37-5.40), respectively, for calculating the related penalties if any of the constraints were not met, which are found by:

$$g_1(v,rpm) = \begin{cases} \left| \dfrac{Torq(v,rpm)}{T_{desired}} - 1 \right| & when \quad |Torq(v,rpm) - T_{desired}| > T_{tol} \\ 0 & else \end{cases} \tag{5.42}$$

$$g_2(v,rpm) = \int_{t=t_0}^{t=t_{380}} \max[-\dot{m}_{int}(v,rpm), 0] \, dt \tag{5.43}$$

$$g_3(v,rpm) = \int_{t=t_0}^{t=t_{720}} \max[-\dot{m}_{exh}(v,rpm), 0] \, dt \tag{5.44}$$

$$g_4(v,rpm) = \begin{cases} \dfrac{SA+720}{IVC(v,rpm)} - 1 & when \quad SA + 720°CA \geq IVC(v,rpm) \\ 0 & else \end{cases} \tag{5.45}$$

where $\dot{m}_{int}$ and $\dot{m}_{exh}$ are representing the gas mass flow rate at the intake and exhaust valve, respectively, while t_0, t_{380} and t_{720} are indicating the moments when the crank angle is at $0°$, $380°$ and $720°$, respectively. These calculated penalties of Eqs. (5.42-5.45) are then weighted by the multipliers of C_1, C_2, C_3, C_4 for ensuring all the constraints could be properly reflected in the fitness function of Eq. (5.41) without any of them being overlooked or become completely dominating when evaluating the fitness value, and eventually result in finding a set of feasible solutions throughout a natural GA convergence.

After many attempts for identifying the feasible multipliers for this VOAC test engine, a set of values of $\begin{bmatrix} 5000 & 50000 & 50000 & 120000 \end{bmatrix}$ is found as a proper set for the multipliers, which could

lead to good GA convergences to the proposed fitness function in this section while having the optimizations to be effectively bounded by all the considered constraints. With a prescribed population size of 70, the proposed GA approach is able to reach to a satisfactory convergence within around 100 generations. An exemplary result of the GA optimization procedure at 3600rpm with a desired engine load of 9Nm is shown in Figure 5.10.
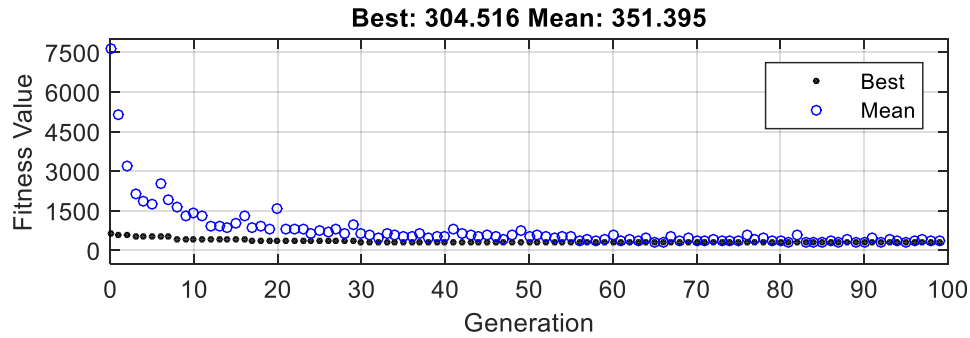
Figure 5.10 GA fitness convergence at 3600rpm/9Nm operation point

5.4 Summary

In this chapter, a VOC engine operations scheme is proposed for fulfilling full load operations of the HVVA engine. Also, for realizing unthrottled partial engine load control, two different engine operations schemes are developed, namely the implementation to a tunable IEGR feature and the realization to the VAC.

The GA optimization schemes for identifying all the considered HVVA engine operating parameters from adopting the introduced engine operation schemes are then proposed, which are carried out by the constructed MATLAB-Simulink and GT-Suite co-simulations. The proposed GA optimizers are designed towards the optimizations to the engine power performance at full load operations and fuel economy at partial load operations while considering the corresponding restrictions.

73

Chapter 6

Optimized Result Analyses and Discussions[1]

By adopting the aforementioned HVVA engine operation schemes and performing the corresponding GA optimizations, the simulated engine performances resulted from the optimized operating variables are demonstrated hereinafter along with their analyses and discussions.

6.1 Optimized Results for Improving Power Performance at Full Load via Implementation to the Proposed VOC

The power optimization results for the HVVA engine running at full load operations are presented in this section with the sampling points covering the entire engine working speed range of the test engine, 2000rpm to 3600rpm, with an interval of 400rpm.

Figure 6.1 and Figure 6.2 demonstrate the comparisons over the resultant engine outputs and BSFC at full load operations achieved by 3 exemplary cases, which are the baseline engine running with its original cam sets at WOT working conditions, the HVVA engine running in VOC with 4 optimized operating variables (4Var) of the TPA timings of the spool valves, and the HVVA engine running in VOC with 6 optimized operating variables (6Var) that has taken the optimizations of the SA and Lambda into consideration in addition to the previously mentioned 4 operating variables of the HVVA system, respectively.
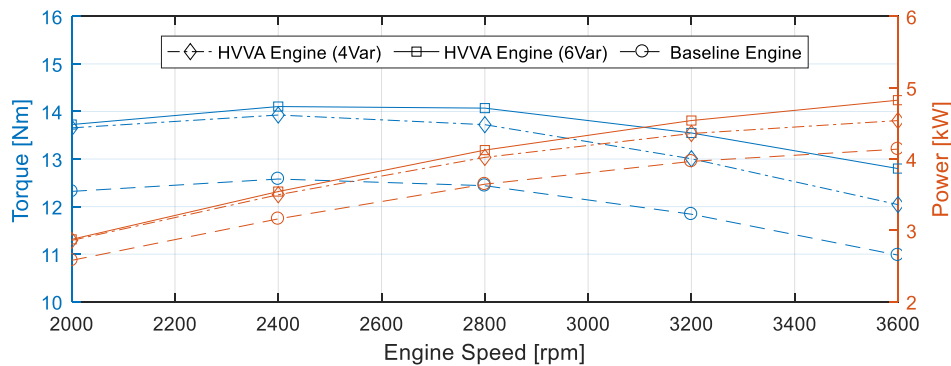
Figure 6.1 Comparisons over the engine output among the 3 exemplary cases at full load operations

_____

[1] Refer to the "Statement of Contributions" for authorship details of the contents in this chapter.
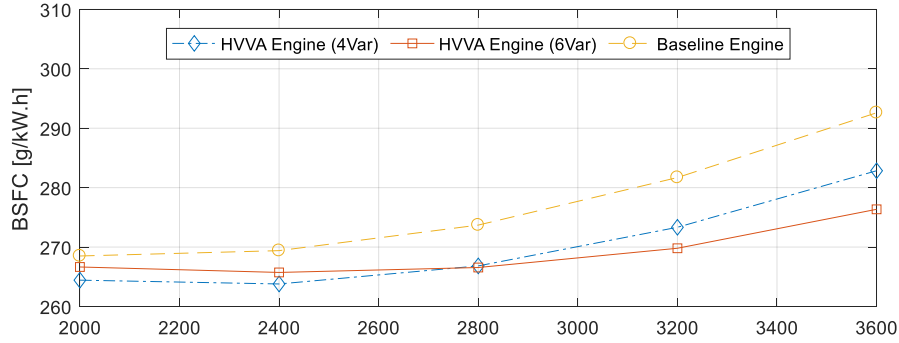
**Figure 6.2 Comparisons over the resulted BSFC among the 3 exemplary cases
at full load operations**

The GA optimization procedure with these 2 additional variables can be easily performed by declaring the corresponding parameter ranges of the SA and Lambda as additional constraints to the introduced full load GA optimization scheme described by the Eqs. (5.1-5.6), and increasing the population size to 70 with each individual carries 6 variables instead of 4. In addition, the calculated percentages of the improvements on the engine output and the resulted BSFC with respect to those of the baseline engine are summarized and shown in Figure 6.3.
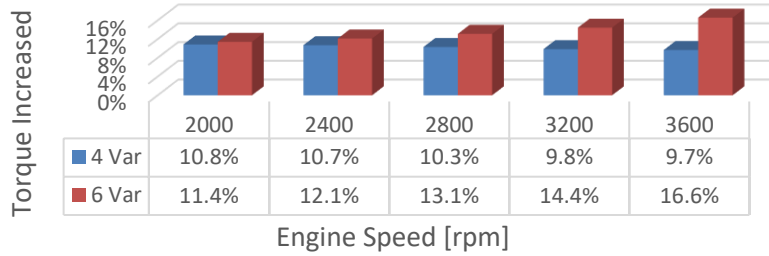
(a)
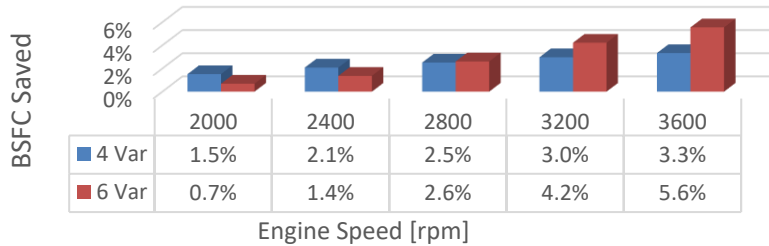
(b)

**Figure 6.3 Calculated percentages of the torque increments (a) and BSFC savings (b) with
respect to the baseline engine from adopting the VOC with 4 and 6 optimized variables**

75

As can be noticed from Figure 6.3, the power performance of the engine is increased across the entire operating speed range when running in VOC. Moreover, the corresponding BSFCs are not only maintained at the same level to those of the baseline engine, but also slightly lowered even, because of the actual valve timings are speed-dependently optimized to grant the engine with a greater VE, but simultaneously a smaller pumping loss over the entire engine speed range. In another word, the resulted VOC manages to deliver higher engine outputs in a more fuel-efficient manner comparing to the fixed OC of the baseline engine. In addition, with the 6Var optimization configuration, greater improvements of the engine output and fuel economy can be realized at higher speeds by 16.6% and 5.6%, respectively, at maximum. This is due to the optimized SA and AFR could adjust the combustion phase to be taken place within the most efficient combustion period according to the given engine speed, and make the combustion process more complete and more quickly. However, the BSFC improvements with the 6Var configuration at lower engine speed are less than that with the 4Var configuration. This is because the pursuit of greater improvements on the engine output at low engine speeds is achieved by sacrificing a portion of potential savings towards the fuel economy. Nevertheless, the optimized HVVA engine could still hold a better fuel economy than the baseline engine when running in VOC under full load operations while delivering noticeable increments to the engine output over the entire operating speed range.
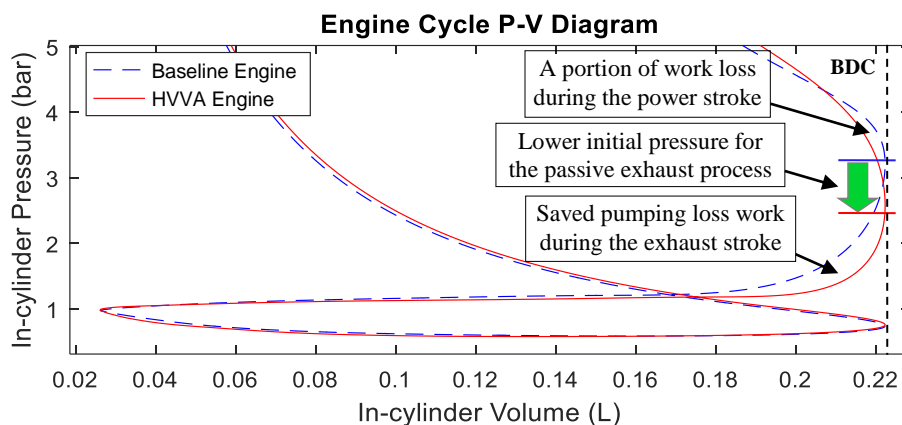
Figure 6.4 Zoomed pumping cycle view to the in-cylinder pressures of the baseline engine and the optimized HVVA engine under 3600rpm full load operations

Also, it is worth to mention that the optimization results for the 4 TPA timings of the HVVA system are identical from performing the 4Var and 6Var optimization schemes, which is because both of these optimization procedures are sharing the same objective of minimizing the cycle pumping

76

losses and maximizing the VE, simultaneously. In another word, the maximizations to the resultant output torque at full engine load are actually multi-objective optimization procedures that consist of these identical hidden sub-objectives no matter if the SA and Lambda were taken into consideration or not.

To further explain this, an exemplary pumping cycle P-V diagram is presented in Figure 6.4 which shows the in-cylinder pressures of the baseline engine and the optimized HVVA engine under the condition of full load operations at 3600rpm engine speed. As can tell from the figure, the resulted pumping loss work during the exhaust stroke of the optimized HVVA engine is less than that of the baseline engine. However, it can also be noticed that with a further advanced EVO, a portion of the positive work is lost due to the pressure drop during the power stroke. All these observed features shown in this P-V diagram actually verifies the explained principle of the exhaust pumping loss reduction strategy that was proposed in Chapter 3.

However, this can only be achieved by the capability of changing the opening durations of the valves, which, in this research, is granted by the HVVA system. If the EVO were advanced without extending the exhaust valve opening duration, by phase-shifting techniques of cam-based valve trains, for instance, the in-cylinder pressure would rise at the end of the exhaust stroke due to the fixed valve opening durations would cause a compulsive advance to the EVC, leading to a higher initial in-cylinder pressure for the intake process and a relatively greater exhaust pumping loss comparing to those from implementing the optimized HVVA valve timings.

Therefore, the optimized solution found by the proposed GA scheme is, in fact, an optimal set of the valve timings that would yield to an optimum balance between minimizing the overall pumping loss and maximizing the VE that could eventually contribute to a maximized engine output at any prescribed engine speed.

The optimized TPA timings for the HVVA system identified by the proposed GA approaches for fulfilling the VOC operations are depicted in Figure 6.5, along with the optimized SA and Lambda acquired from the optimization procedure conducted under a 6Var configuration. Furthermore, the resultant engine valve lift profiles are drawn in Figure 6.6. It can be noticed that both the intake and exhaust valve openings are prolonged in terms of CA degrees as the engine speed increases, which is benefit to perform a more complete exhaust process and bring in more fresh charge into the cylinder at higher engine speeds, even though the durations between their corresponding TPA-HPSV and

TPA-LPSV are shortened due to the characteristics of the HVVA system that the valve opening and closing durations would be elongated at higher engine speeds.
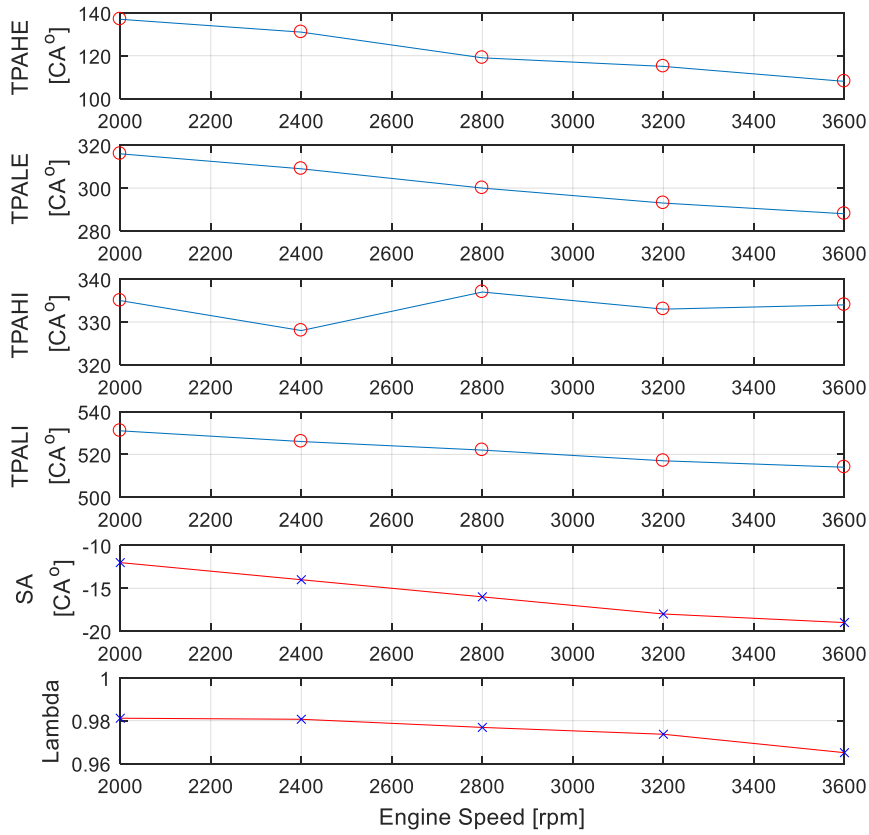
Figure 6.5 Optimized variables for full engine load operations when running in VOC
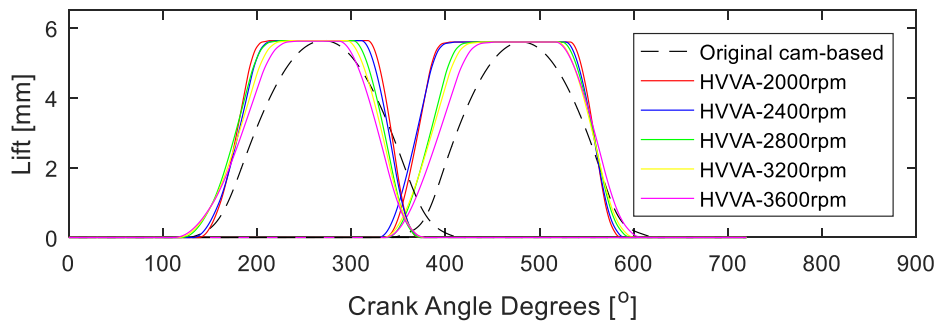
Figure 6.6 Resulted valve lift profiles of the HVVA engine and the baseline engine at full engine load operations

78

6.2 Optimized Results for Improving Fuel Economy at Partial Load Operations via Implementation to the Tunable IEGR Feature

For the fuel economy optimizations achieved from implementing the tunable IEGR feature, the resulted BSFC under the exemplary 7Nm load point, are compared in Figure 6.7 between the optimized HVVA engine and the original baseline engine at different sampling engine speeds. The reduction on the BSFC after optimization could reach up to 15.8% at 3600 rpm engine speed, with a computed average at approximately 13.1% over the entire speed range.
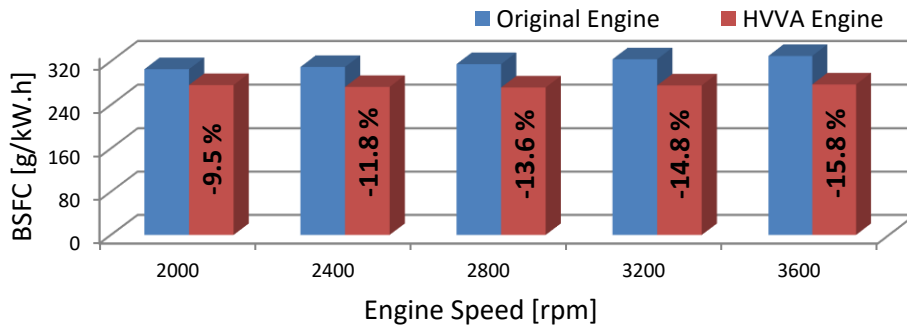
Figure 6.7 Comparison on the resulted BSFC between the HVVA Engine with IEGR and the original baseline engine with throttling at 7Nm load point

The corresponding optimized operating variables are given in Figure 6.8 along with their resulted valve lift profiles presented in Figure 6.9. As can be noticed, the BSFC reductions at higher engine speeds are greater than those at lower engine speeds. This is mainly because not only the pumping loss reduced by implementing the HVVA strategy is becoming greater and greater as the engine speed increases, but also the fuel efficiency is increased more from adopting the optimized AFR and SA while more diluted mixtures and more advanced SA are used at higher engine speeds. Besides, the decrease of the friction loss led by the cam-less HVVA valve train is also one of the facts that contribute to the improvements on the engine's fuel economy, and this fact brings more effect on the reductions to the BSFC at higher engine speeds due to the increment to the valve train's friction loss is less with the HVVA system comparing to that with the cam-based valve trains. To better understand this, the following explanations are provided.

For the HVVA engine, each spool valve is sitting on two bearings for supporting itself from both ends of its body with designed hydraulic lubrication at the contact surface of the spinning spool and its casing. Therefore, the friction loss of the HVVA valve system could be considered as coming from the almost "load-free" rotational motions of the spool valves since the motions of the engine valves,

79

or the corresponding variations on valve spring force, would not cause direct impact to the friction loss of the HVVA valve train. However, for the original baseline engine, the cam-based valve train suffers from the friction losses resulted from the camshaft, cam followers and other valve actuation mechanisms, such as push rods and rocker arms contained by the test engine of this research, which are the components that the HVVA system does not enclose at all. More importantly, the overall friction loss resulted by these components of the cam-based valve train would increase as the valve spring force increases whenever the engine valve gains an actual lift. In another word, the overall friction loss is also dependent to the external force that applies to the engine valve, which reveals the fact that the friction loss of the cam-based valve train was actually caused under the condition of being applied with external loads, hence, such overall friction loss could be significantly greater comparing to that of the HVVA system.
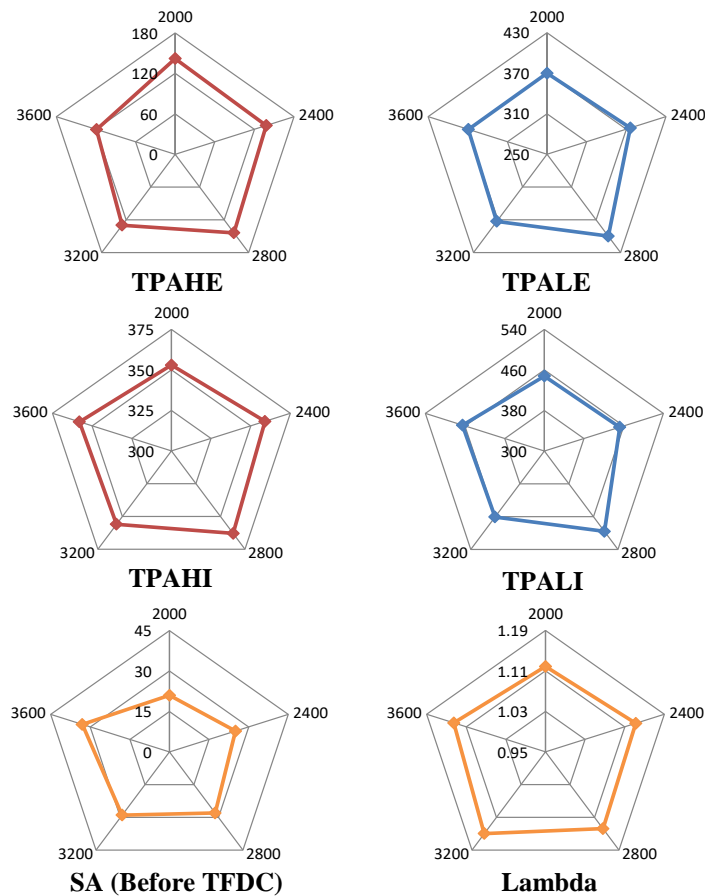
Figure 6.8 Optimized TPA timings, SA and Lambda of the HVVA engine running with IEGR for achieving the exemplary 7Nm partial load operations

80
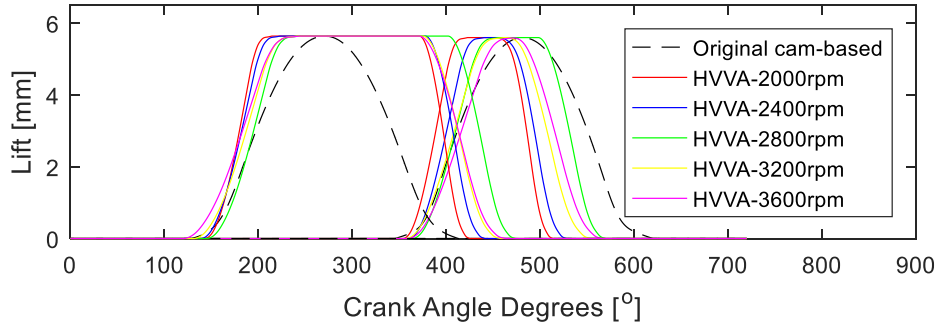
Figure 6.9 Resulted valve lift profiles of the HVVA system implementing the IEGR for achieving the exemplary 7Nm partial load operations

Furthermore, although that the friction losses of these two types of valve trains would both tend to increase as the engine speed increases, the friction loss increment of the HVVA system is still less than that of the cam-based valve train system. This is mainly because that according to the Newton's 2nd Law, the accelerations of the engine poppet valve and all its related moving parts would become greater at higher engine speeds, which would result in a greater force that applies in the same direction as the force of the valve spring. Therefore, this fictitious force caused by the increased accelerations of the moving mass from the cam-based valve system could be considered as an extra load, which would lead to an increased friction loss of the valve train due to the reason that the overall friction loss of the cam-based valve train is dependent to it just as mentioned above.

On the contrary, the HVVA system would not have this friction loss increment caused by the increased accelerations of the engine valves at higher engine speeds. Hence, this is also one of the reasons that the HVVA engine's fuel economy could be improved more at higher engine speeds comparing to that of the original engine.

Additionally, in order to provide further explanations on the reductions to the BSFC from using the optimized IEGR operation configurations of the HVVA engine, more illustrations for showing the details of the full engine cycles are drawn. It is obvious to see from Figure 6.10 and Figure 6.11 that, by adopting the proposed tunable IEGR strategy of the HVVA engine, not only the overall pumping loss of the entire engine cycle is significantly reduced, but also the flame speeds after ignition are increased while the injected fuel can be burned more efficiently to release the heat within a shorter CA degrees after the engine piston traveled beyond its TFDC. These improvements eventually lead to an increased ECR, reduced pumping losses and higher effective thermal efficiency of the engine. Therefore, less work is needed to be produced during the power cycle to reach to a desired partial

81

engine load. Moreover, in favor of the increased ECR that benefited from the IEGR feature, and the optimized SA, a leaner air-fuel mixture is allowed to be used, hence resulting in further reductions on the BSFC. The full engine cycle P-V diagram of Figure 6.12 provides an overall inspection to these facts and gives a more visualized comparison on the working processes between the HVVA engine and the baseline engine, which also directly shows a good agreement to the introduced principle of the IEGR feature that demonstrated in Figure 3.7.
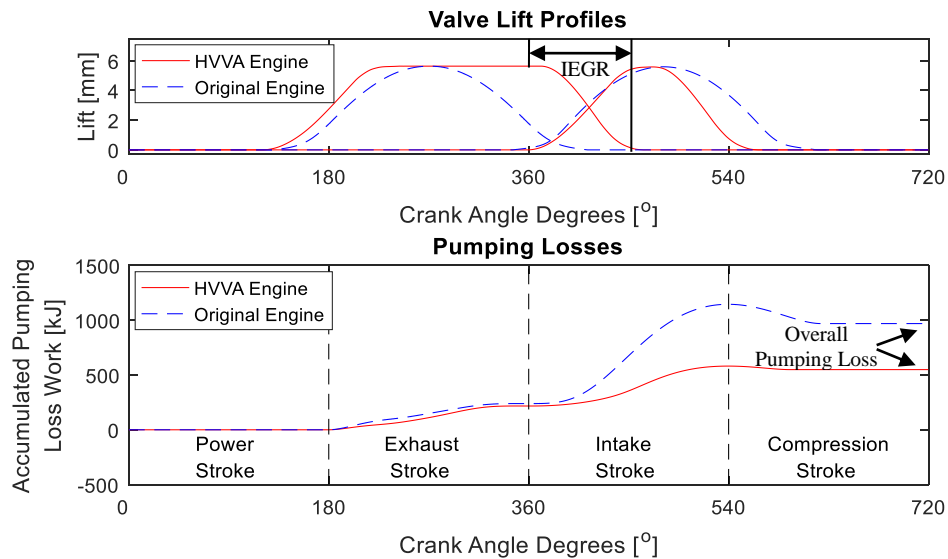
Figure 6.10 Comparison on the pumping loss at 7Nm/3600rpm achieved by the HVVA Engine with IEGR and the original baseline engine with throttling
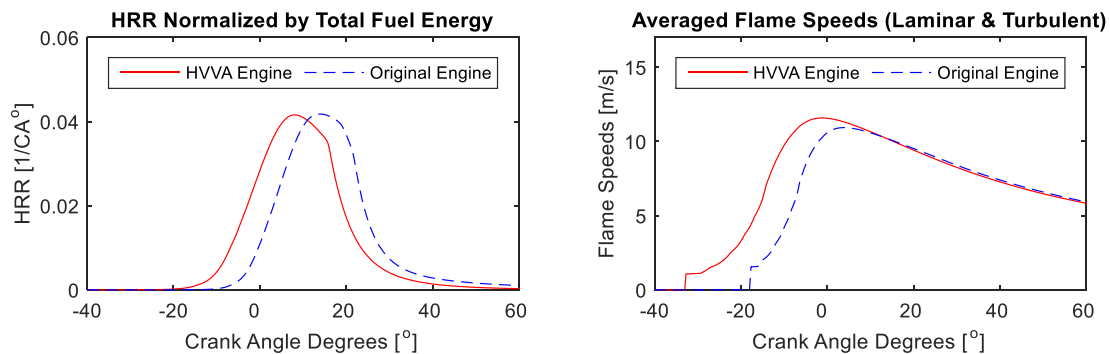
Figure 6.11 Comparisons on the corresponding apparent heat release rate (HRR) and flame speeds at 7Nm/3600rpm

It can be observed from Figure 6.12, with the more advanced SA and increased ECR of the optimized HVVA engine, the maximum in-cylinder pressure achieved from combustion is not only

82

increased by approximately 5 bars compared with the 25 bars of the original engine, but also appeared at a piston position more close to the TFDC. Moreover, seen from the zoomed view of the pumping cycle, it can be as well recognized that the pumping loss is reduced significantly by implementing the unthrottled load control strategy with IEGR. As a matter of fact, all these noticed differences are actually contributing to an increment on the thermal efficiency of the engine under partial load, hence making the engine to be more fuel economical.
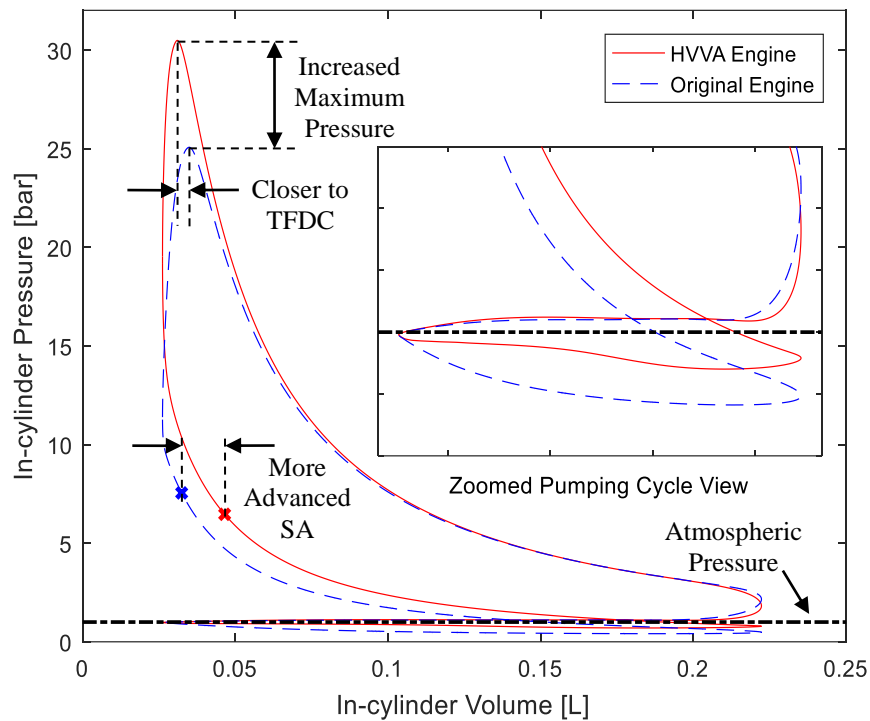
Figure 6.12 Engine cycle P-V diagram at 7Nm/3600rpm

6.3 Optimized Results for Improving Fuel Economy at Partial Load Operations via Adoption to the Proposed VAC

In order to identify the overall tendency of the distinct ACs for achieving different partial engine load operations when running the HVVA engine in VAC, the optimized solutions to all the considered variables found by the proposed GA scheme are drawn in Figure 6.13 over a meshed grid of the engine's sampling speed-load operating points.
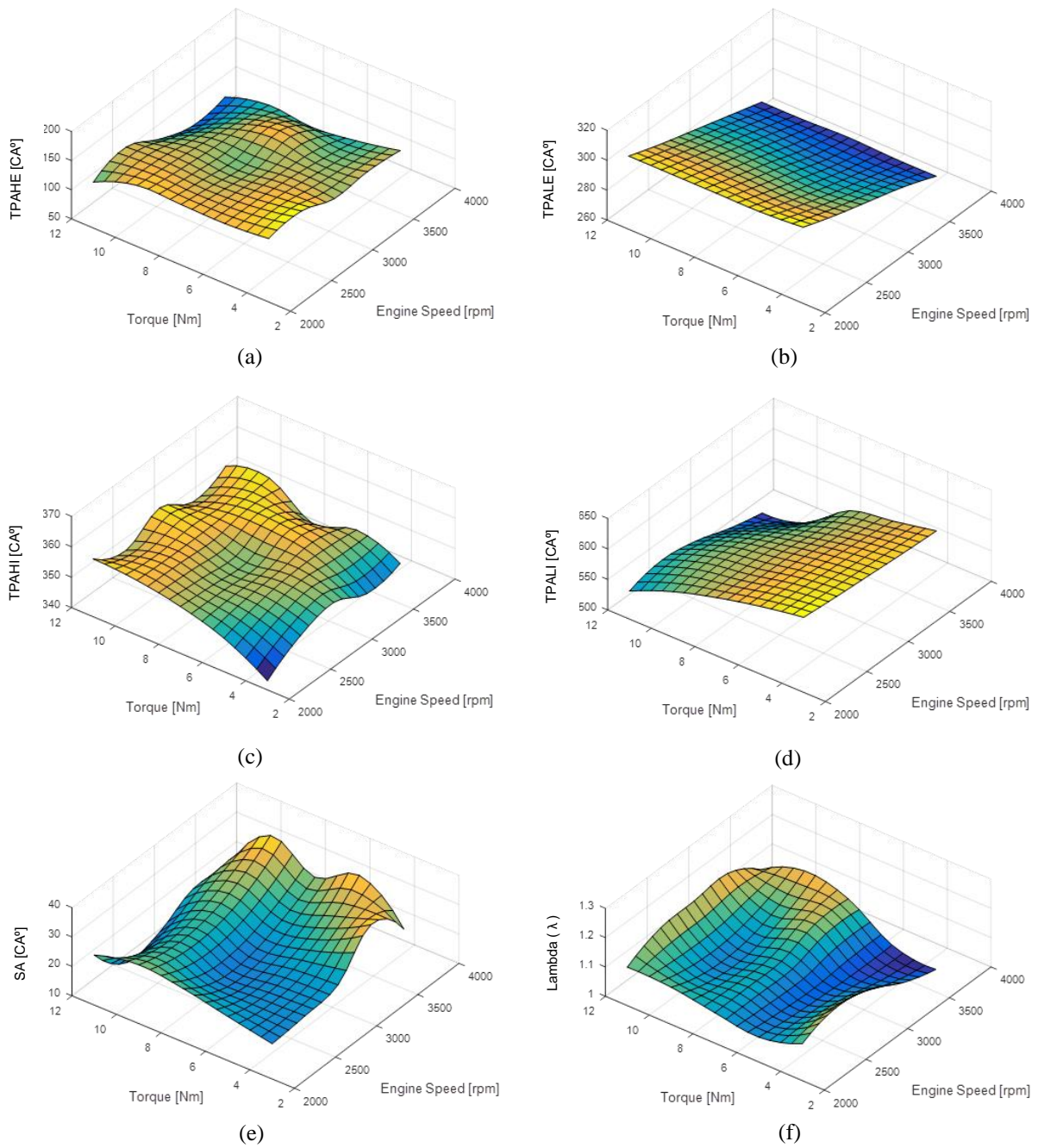
Figure 6.13 Optimized variables for partial load engine operations achieved by VAC

(a) TPAHE (b) TPALE (c) TPAHI (d) TPALI (e) SA (f) Lambda

By running the HVVA engine in the proposed VAC mode with the optimized variables for fulfilling the desired partial loads at different engine speeds, the fuel efficiency can be globally

84

improved comparing to the throttled baseline engine. Figure 6.14 and Figure 6.15 present a contrast on the resulted BSFC of the HVVA engine from adopting the optimized VAC to that of the baseline engine from using throttling.
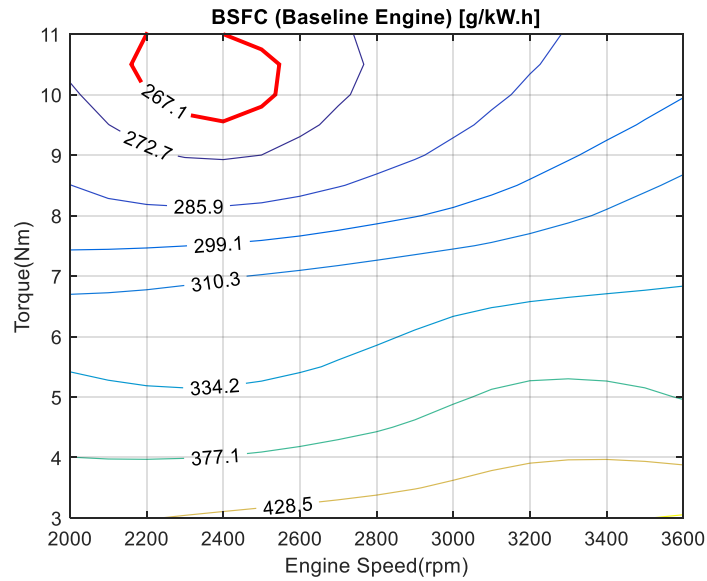
Figure 6.14 Resulted BSFC plots of the baseline engine across the speed-load map of the partial engine load operations via throttling control
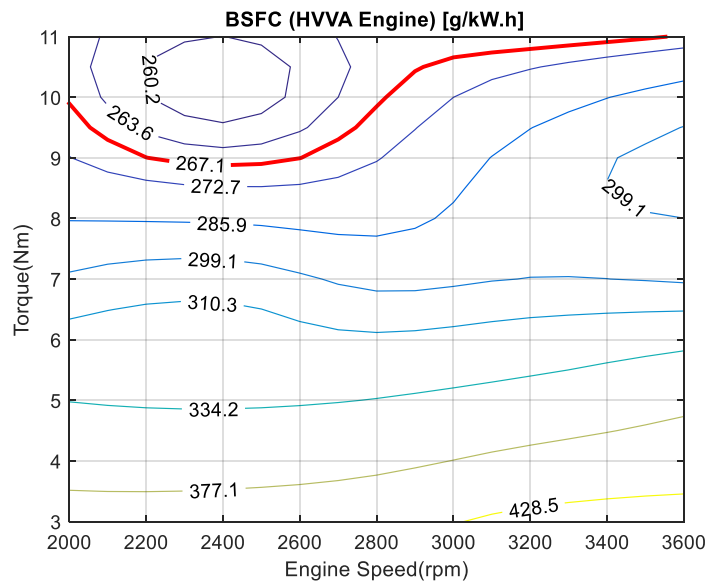
Figure 6.15 Resulted BSFC plots of the HVVA engine across the speed-load map of the partial engine load operations via VAC

As can be clearly noticed in Figure 6.14 and Figure 6.15, the highlighted contour, which encloses the most fuel efficient operation domain of the baseline engine, is considerably enlarged by the HVVA engine and covering almost the entire operating speed range, while the BSFC at the most fuel efficient operating domain of the baseline engine is further reduced. As a matter of fact, the resulted improvements to the fuel efficiency are not localized to specific regions, but in a global scale across the entire speed-load map. This can be more obviously observed in Figure 6.16, which visualizes the savings of the BSFC in percentage achieved by the HVVA engine running in VAC with respect to the baseline engine with throttling.
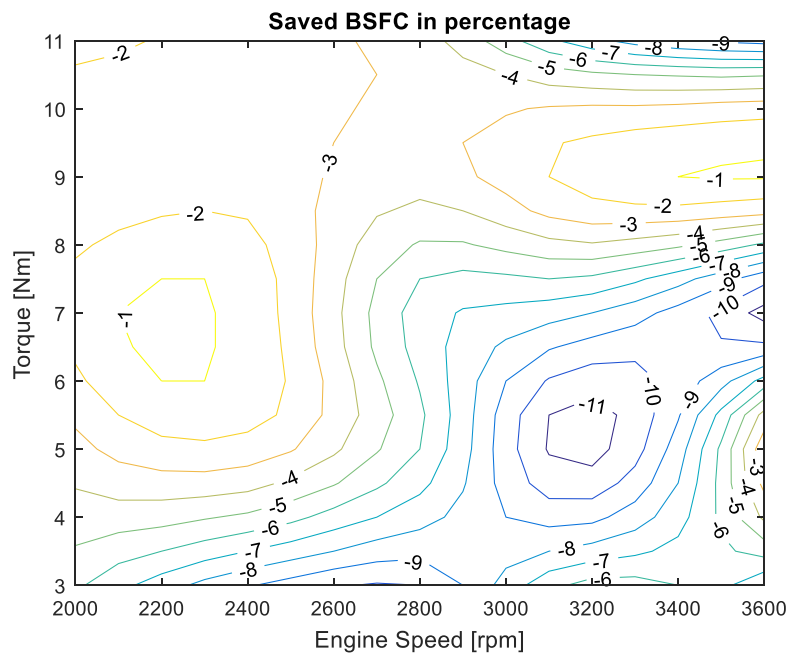
Figure 6.16 Resulted decrements on the BSFC shown in percentage achieved by running the HVVA engine in VAC

It can be seen from Figure 6.16 that greater improvements on the engine's fuel economy can be realized at relatively high-speed and low-load operating domains by running the HVVA engine in the optimized VAC, with a maximum saving of 11% on the BSFC noticed at the med-high-speed and mid-low-load operating domain. By retrieving the actual fuel consumptions achieved by the HVVA engine from all the sampling operating points, an average saving of the resulted BSFC over the entire sampling grid of the speed-load map is calculated at 16.1g/kW·h. The resulted better fuel economy is in fact mainly benefited from the lowered pumping losses and the increased thermal efficiency of the unthrottled over-expansion engine cycles of the VAC.

6.4 Advanced Complex Implementations

With all the proposed HVVA valve motion strategies in this research for realizing the unthrottled engine control, the HVVA engine is granted with the potential of carrying out different highly configurable engine operation schemes over difference preferences. Moreover, the engine operation schemes are not necessarily permanent and fixed to a tuned engine once been adopted, in fact, the HVVA engine can easily switch between different viable schemes or update its tunings upon requirements without performing any modification to the engine parts or the components of the HVVA system. Hence, knowing these potentials and benefits, some possible advanced complex implementations that could be performed by the HVVA engine are discussed hereinafter.

6.4.1 Realization to Variable Otto-Atkinson Cycle (VOAC)

With the proposed VOC and VAC engine operation schemes, a complex implementation of the realization to a variable Otto-Atkinson cycle (VOAC), which makes the HVVA engine to carry out a VOC at full load operations and a VAC at partial load operations via the continuous variations of the valve motions, is proposed. By running in VOAC, the HVVA engine can be granted the capability of delivering higher outputs at full load while being more fuel economical at partial load.

In order to take an overall inspection and analysis over the related tendencies of the corresponding engine cycle variations when performing the optimized VOAC, the resulted EER and the EER-to-ECR ratio at any given engine operation point are used for identifying and describing that specific engine cycle realized by the HVVA engine. It is easy to understand that the VOAC engine would be considered as running in OCs if the EER-to-ECR ratio is equal to 1, and in ACs if greater than 1, in theoretical.

According to the previously presented VOC optimization results, Figure 6.17 shows the EER, ECR and EER-to-ECR ratio resulted from the optimized valve motion events at full load operations. As can tell from the figure, the value of the EER-to-ECR ratio is fairly stabled at 1 over the entire speed range, with only very tiny variations within the neighboring regions, which indicates that the HVVA engine is running in OCs. Actually, these variations are caused by the optimized HVVA valve motion events found by the proposed GA optimizer that could contribute to further improvements to the engine's overall indicated work. Take the sampling points at 3200rpm and 3600rpm for instance, the corresponding EER-to-ECR ratios are in fact less than 1, which implies that the EER has become smaller than the ECR under the optimized operations. The reason that the ECR is becoming smaller

and smaller as the engine speed increases is the fact that the IVC needs to be further retarded for achieving greater VE at high engine speeds has been picked up by the proposed GA optimizations. However, the optimizer also captured the principle of the work trade-off demonstrated in Figure 3.5, and recognized an optimized solution accordingly that eventually resulted in an even further advanced EVO. Consequently, the resultant EER-to-ECR ratio turns out to be actually possible to become less than 1. It should be noted that despite the EER-to-ECR ratio is moderately maintained as 1 under the VOC operations, the EER and ECR have been changed substantially in order to make a better match of the current engine cycle to the engine speed, which could be comprehended as the effective displacement of the engine can be virtually altered when running in VOC, and this feature also reflects the major difference between the VOC and the conventional OC.
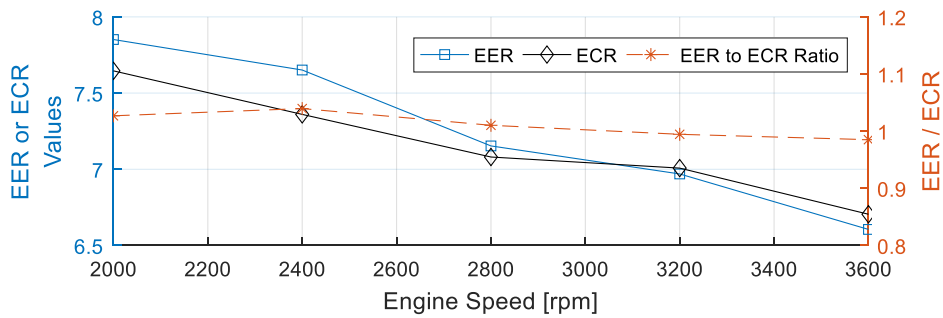
Figure 6.17 Resulted EER, ECR and EER-to-ECR ratio of the HVVA engine running at optimized full load operations in VOC

Similarly, according to the optimized results of the engine running in VAC, the corresponding EER and EER-to-ECR ratio maps over the entire sampled speed-load operation domain for partial load operations are presented in Figure 6.18 and Figure 6.19, respectively. It is worth to mention that the magnitudes of the EER and the EER-to-ECR ratio at any speed-load operation point can characteristically represent the resultant AC that the HVVA engine is currently running, and a realized AC with a greater EER-to-ECR ratio basically infers that the degree of the Atkinson effect is higher. Therefore, for realizing different partial load operations by performing the VAC, the engine can actually be treated as equal as a group of AC engines with different displacements and degrees of the Atkinson effect are operating at their own WOT conditions, and each of them covers only 1 single speed-load operating points. In another word, the HVVA engine is able to be virtually converted into any specific type of AC engine with different displacements and degrees of the Atkinson effect when

operating in VAC, by means of the EER indicating the equivalent displacement and the EER-to-ECR ratio implying the degree of the Atkinson effect.
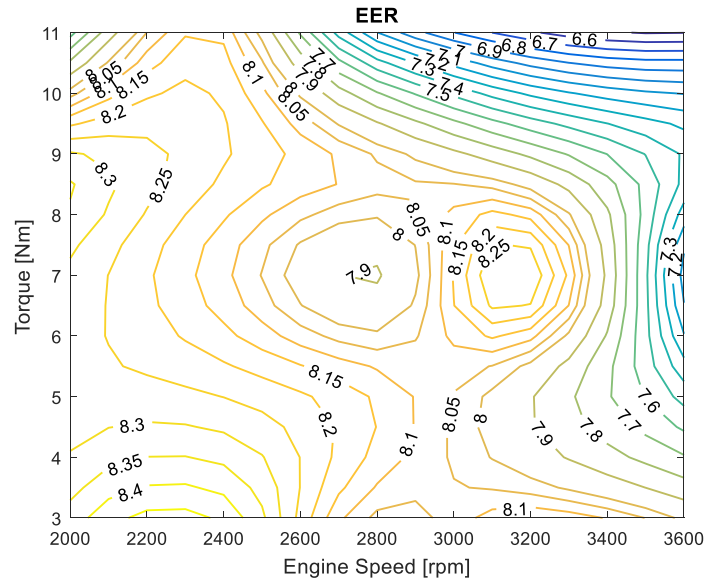
Figure 6.18 Resulted EER of the HVVA engine running at optimized partial load operations while in VAC mode
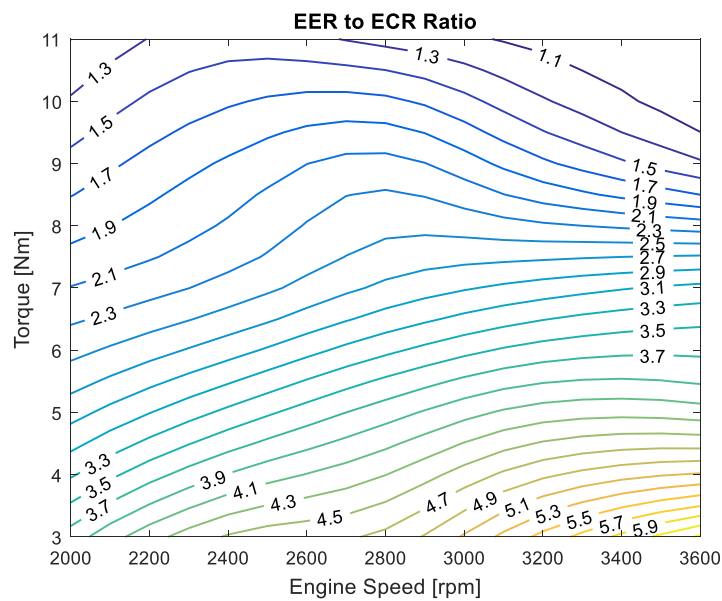
Figure 6.19 Resulted EER-to-ECR ratio of the HVVA engine running at optimized partial load operations while in VAC mode

It can also be observed from Figure 6.18 and Figure 6.19 that the EER varies from 6.6 to 8.4 across the speed-load map, with a general tendency of incrementing as the engine speed or load drops. Moreover, unlike the VOC operations, the EER-to-ECR ratio can reach up to 6.1 in VAC operations in order to meet the desired outputs of the HVVA engine at different engine speeds.

Hence, by adopting the proper mode with the suitable optimized EER and ECR that summarized in above, the HVVA engine can realize a VOAC that could carry out different speed-load operations by running the engine in VOC or VAC that is featured by the capability of virtually altering the engine's effective displacement in a continuous manner.

6.4.2 Achieving Partial Load Operations by Sectionalized Implementations to the Proposed HVVA Engine Operation Schemes

Another possible complex implementation to the introduced HVVA engine operation schemes is to achieve different required partial load operations by adopting both the proposed tunable IEGR scheme and the VAC scheme over different speed-load operation zones of the same engine to achieve an even better overall fuel economy under partial loads.

For instance, if a specific engine could only perform the tunable IEGR scheme at mid-load operations due to high knock probability at high-load regions and unstable combustion processes at low-load regions that could be resulted by the inappropriate IEGR ratios, the HVVA engine could easily switch over to the VAC scheme over those inapplicable regions of the IEGR scheme to maintain the unthrottled load control of the engine. On the contrary, whenever there was a section of the entire speed-load operation region that the VAC scheme would be considered as inapplicable (e.g. possible interference of the SA and IVC) or the fuel economy turned out to be worse than that from adopting the tunable IEGR scheme, the ECU of the HVVA engine can be programmed to adopt the tunable IEGR scheme whenever the engine is operating within this section while having the rest of the speed-load sections still running in VAC.

As a matter of fact, by sectioning the entire speed-load operation map of a specific engine into multiple regions and adopting the only viable or the preferred better scheme out of the proposed two choices, respectively, the HVVA engine could receive a further optimized fuel economy with respect to the overall speed-load range of the engine. And theoretically speaking, the number of these sectionalized regions could go up to as many as desired.

Furthermore, it should be mentioned that the way of sectioning the speed-load operation map can also be determined according to functional preferences. For example, since the tunable IEGR scheme could benefit in lowing emissions (HC and NO_x) [104] because of the EGR effect, for those engines that might have unacceptable emissions over certain speed-load operation regions, the HVVA engine could force an adoption to the tunable IEGR scheme to make the performance with respect to emissions as the top priority over such regions instead of the fuel economy.

6.5 Summary

In this chapter, the resulted engine performances from adopting the optimized operating parameters of the HVVA engine under different proposed operating schemes are presented and compared with those resulted by the baseline engine. Analyses to the observed improvements are also conducted for providing better explanations and proofs by principles. In addition, the discussions over the advanced complex implementations of the HVVA engine are made, which further reveals the potential of the HVVA engine from flexibly utilizing its extraordinary configurability for achieving better engine performance upon specific preferences in terms of power, fuel economy, and even emissions, for different speed-load operations regions.

Chapter 7

Experimental Studies[1]

7.1 The HVVA Engine Test Bench Assembly

Based on the abovementioned studies of this research, a testing HVVA engine is converted from a single-cylinder gasoline engine and assembled together with the designed engine test bench[1]. Seen by the illustrative structure of the HVVA system set up shown in Figure 7.1, two sets of the HVVA system are adopted for controlling the intake and exhaust valve of the engine, respectively, with the rotational motions of all the spool valves acquired from the crankshaft of the engine.

As shown in Figure 7.2, which is the actual assembly of HVVA system, four servo motors are attached to each of the spool valves through worm gears for adjusting the TPA timings. In addition, sensors are hooked up to the spool valves for identifying their rotational positions.
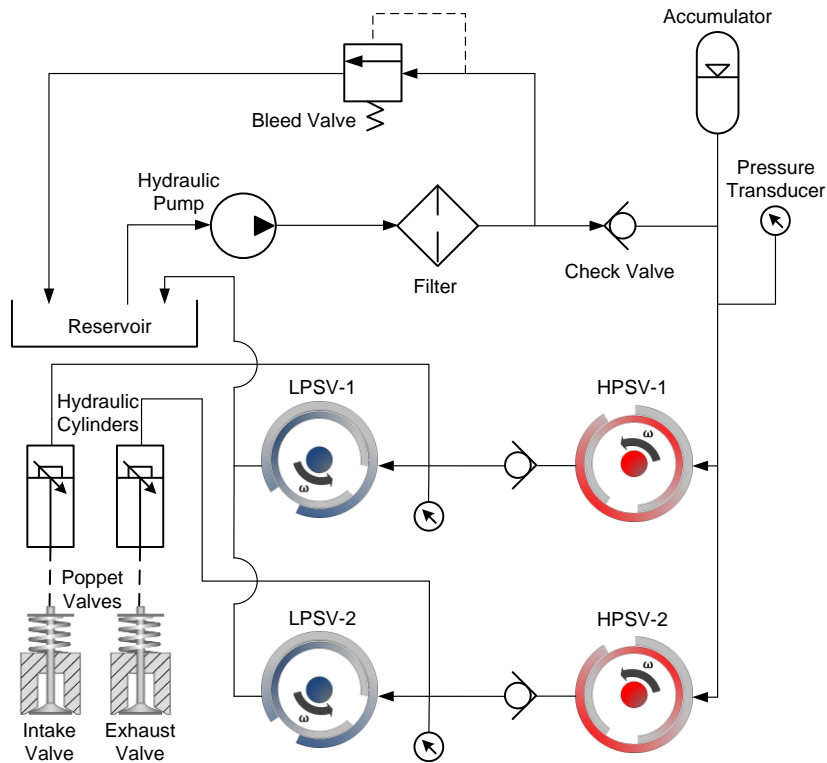
Figure 7.1 Illustrative layout of the HVVA system for the test engine

_____

[1] Refer to the "Statement of Contributions" for detailed dedications of the contents in this chapter.
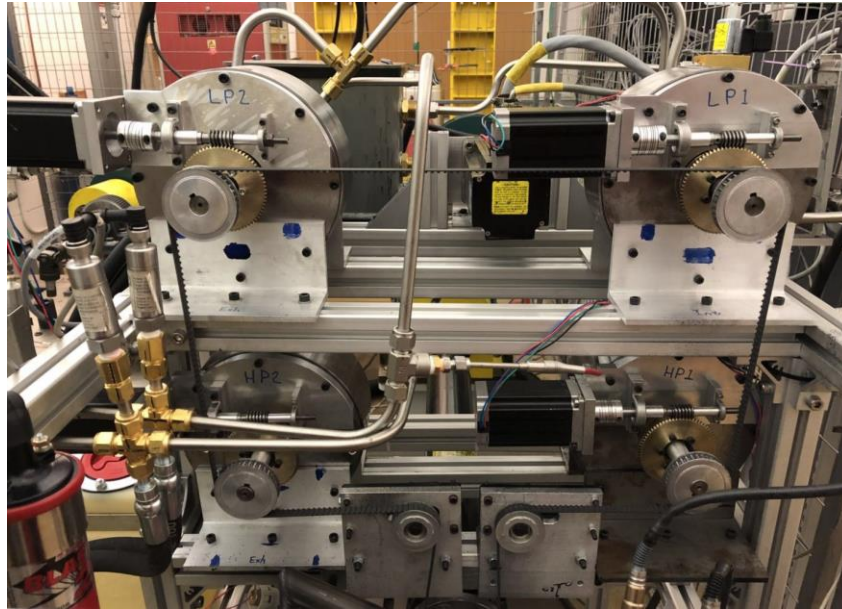
Figure 7.2 Actual assembly of the HVVA system for the test engine

The original single-cylinder gasoline engine, which was equipped with a mechanical system for ignitions, a carburetor for fuel feeding, and a butterfly throttle for load control, has been significantly modified and become capable of performing unthrottled engine control with variable spark timing and AFR functionalities.
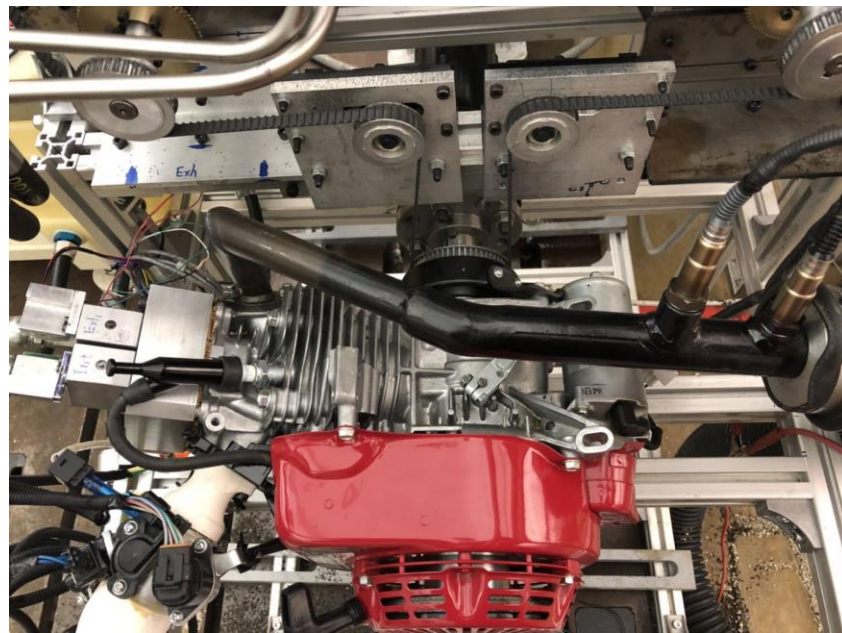
Figure 7.3 The modified single-cylinder gasoline engine

As shown in Figure 7.3 of the converted HVVA engine, instead of the original cam-based valve system with push rods and rocker arms, the engine is now mounted with the hydraulic actuators at the cylinder head, which are attached with position sensors to each of them for monitoring the valve lifts, for driving the engine valves. Moreover, the original carburetor is replaced by an electric fuel injection (EFI) system that could feed the engine with any desired amount of fuel per engine cycle to achieve AFR control. In addition, a digital spark ignition (DSI) system is adopted for configuring the SA for providing the capability of adopting different spark timings, and a knock sensor is attached to the engine body for picking up possible cylinder knock.

(a) (b) (c)

(d) (e)
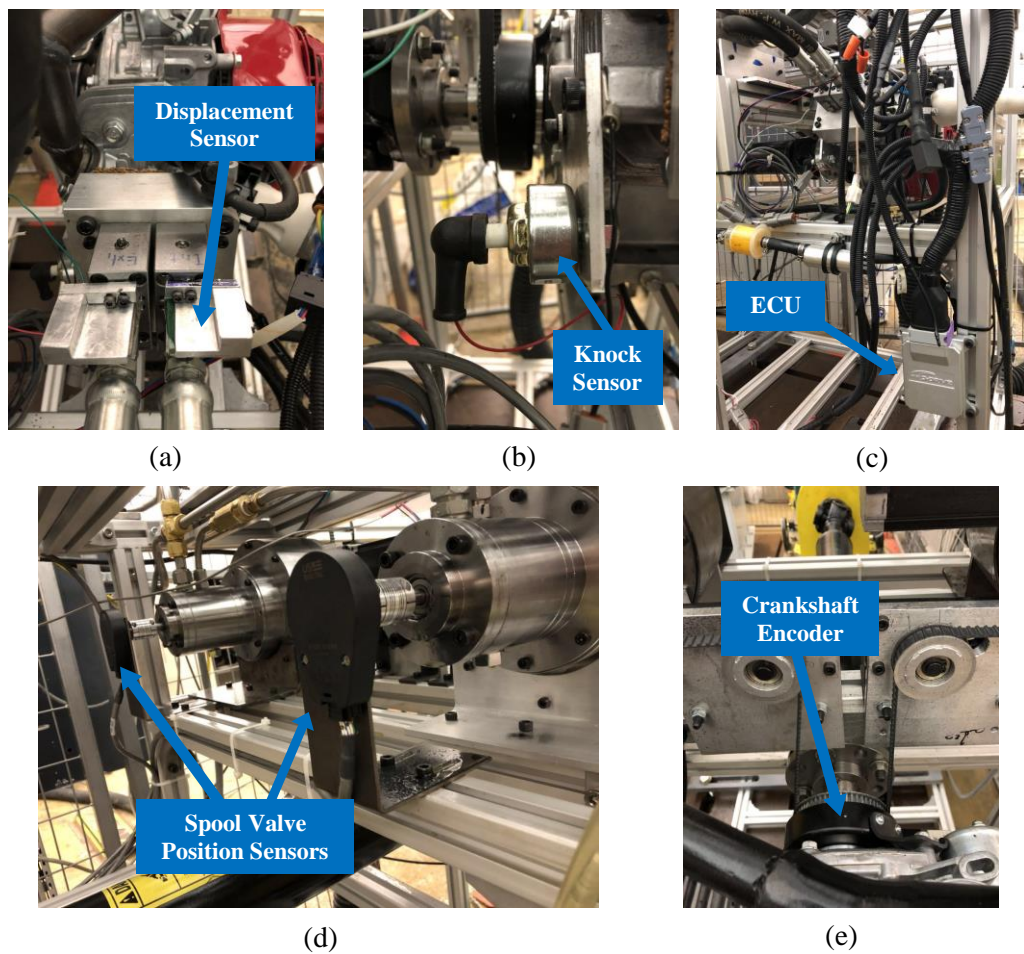
Figure 7.4 Detailed demonstrations to some of the key components
(a) Hydraulic cylinders and valve displacement sensors, (b) Knock sensor, (c) ECU
and signal cables, (d) Spool valve position sensors, (e) Crankshaft encoder

Both the EFI system and the DSI system are hooked up to a newly added configurable ECU along with other related components, such as the crankshaft encoder, the exhaust temperature sensor and the oxygen sensor. To show better the details of the converted HVVA engine in this experiment and its specialized components, more pictures are demonstrated in Figure 7.4 showing some of the components and related sensors of the HVVA engine in zoomed views.

By having all the sensors, servo motors, and the ECU connected to an open-access control desk, known as the dSPACE, the engine test bench can be digitally controlled and the readings from all installed sensors can be monitored in real-time. In addition, the engine crankshaft is also connected to a dynamometer for observing the engine output.

Finally, the overall experimental set up for conducting the HVVA engine tests is constructed as shown in Figure 7.5.

Figure 7.5 Overall set up of the HVVA engine test bench

7.2 Running the HVVA Engine with Proposed Valve Motion Strategies

With the constructed HVVA engine test bench, the proposed HVVA strategies are carried out one by one via designed experiments to realize the corresponding engine operations. However, due to the prototype nature of the HVVA system, the assembled HVVA test engine is not suitable for long-time running and high-speed operations, hence, the engine testing speed is set at 1000rpm for all the designed experiments in this section.

Besides, for the same reason, the overall mechanical loss caused by the prototype HVVA system adopted in the current test bench set up is also greater than expected. Therefore, in order to exclude this exaggerated overall mechanical loss of the prototype HVVA system, which could actually be significantly reduced in an improved HVVA system for real applications, the corresponding mechanical loss of the adopted HVVA system at 1000rpm engine speed is estimated experimentally by driving the engine with only the dynamometer while leaving both intake and exhaust valves open, and is ruled out from the acquired experimental results.

7.2.1 Full Engine Load Operations

For validating the potentials of granting improvements to the engine's power performance from utilizing the HVVA system, the following experiments and results are performed and shown.

By tuning the TPA timings of the HVVA engine, a set of the resulted valve lift profiles, which is deliberately adjusted via experiments to match its valve timings to those of the cam-based baseline engine, are used as a base reference and shown in Figure 7.6. The reason that these specific valve timings are adopted by the baseline engine is that they are considered as optimized with respect to a specific or a certain range of the engine speed that the designer thinks the baseline engine would most likely to run at for most of its practical operations. However, since the baseline engine is designed for an operating speed range of 2000rpm to 3600rpm, it is clear that these valve timings are not the optimized ones for the full load engine operation at the exemplary testing speed of 1000rpm.

Therefore, by implementing the proposed VOC power optimization strategy of the HVVA system that alters the valve timings and opening durations according the engine speed, a set of optimized TPA timings, which would lead to optimized valve motions for realizing the full load operation of the HVVA engine at the exemplary 1000rpm speed, is identified by the proposed GA optimizer and listed in Table 7.
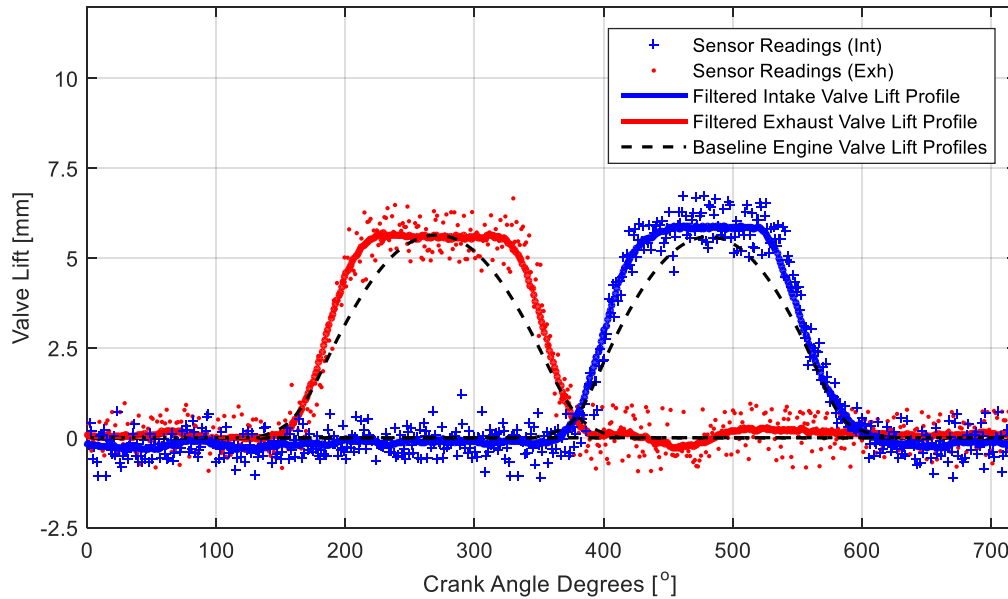
Figure 7.6 Experimentally tuned valve lift profiles for matching the valve timings to those of the baseline engine at 1000rpm

Table 7 Optimized TPA timings for full load operations at 1000rpm

Optimized TPA timings for full load operations at 1000rpm

TPAHE	146 CA⁰
TPALE	308 CA⁰
TPAHI	347 CA⁰
TPAHE	486 CA⁰

In order to make fair comparisons and avoid the risk of causing cylinder knock, the HVVA engine is running at the stoichiometric AFR of 14.7 for both the tests of utilizing the base valve timings and the optimized valve timings at 1000rpm/full load operation. The measured torques at the dynamometer from both the tests are compared and shown in Table 8 with the observed optimized engine valve lift profiles demonstrated in Figure 7.7.

Table 8 Comparisons over the engine outputs for 1000rpm/full load operations between the two tests

Comparisons over the engine outputs for 1000rpm/full load operations between the two tests

Measured torque with base valve timings	3.2 Nm
Measured torque with optimized VOC valve timings	4.1 Nm
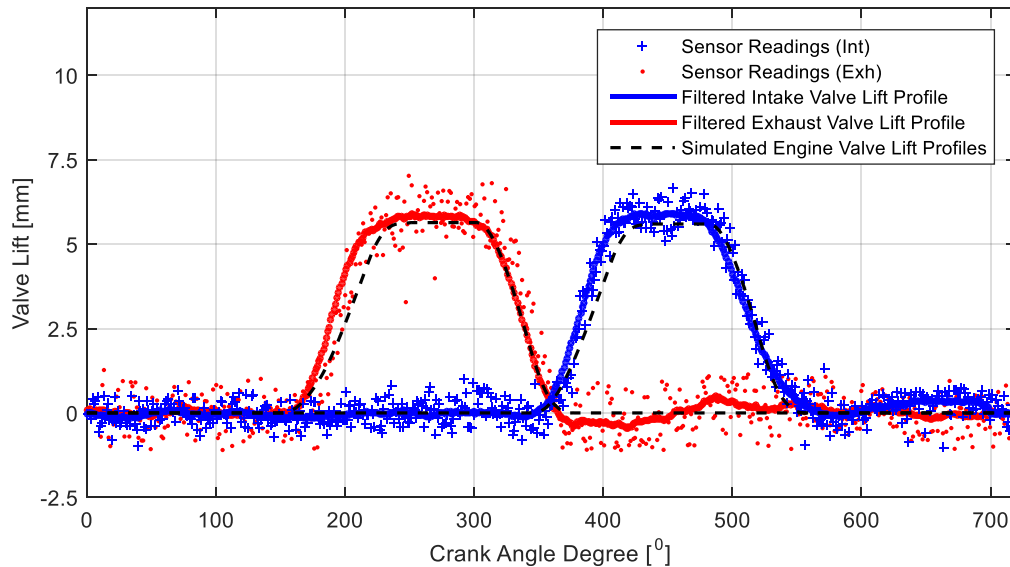
Figure 7.7 Simulated and observed valve lift profiles with the optimized valve timings for 1000rpm/full load operation

By subtracting the equivalent resistance torque corresponding to the aforementioned mechanical loss of the HVVA system from the mean torque measured by the dynamometer, the effective HVVA engine output at 1000 rpm/full load operation with the optimized VOC valve motions is calculated at around 8.2 Nm, an increment 12.3% with respect to the calculated 7.3 Nm of the engine running with the fixed default valve timings under the same AFR. This increment is mainly contributed by a less advanced EVO, which made the expansion process more complete and efficient at such low engine speed, and a reduced LIVC, which eliminated the undesired gas backflow at the intake and increased the VE. Also, it should be again pointed out that such noticed performance improvement is not achieved by simply shifting the timings of the intake and exhaust valves, but altering their timings as well as their opening durations independently, which is able to be performed by the HVVA system but not able to achieve by the cam-based mechanism of the baseline engine. In another word, even granting the cam-based valve system of the baseline engine with a VVT technology that allows the cam to make shifts of the valve timings, the potential improvements to the power performance that could be gained by the same engine would not be as great as that from using the HVVA system with the proposed VOC strategy.

7.2.2 Unthrottled Partial Load Operations

Similarly, for partial engine load operations, both the proposed IEGR scheme and the VAC scheme are performed via bench tests of running the HVVA engine at the chosen exemplary engine speed of 1000rpm. To validate the potential benefit of gaining better fuel economy via implementing the unthrottled engine load control from adopting these proposed valve motion strategies, the following experiments are conducted.

Same as the previous-mentioned experiments for power improvement validations, for fair comparison reasons, a base reference is set by running the engine under a certain partial load via throttle control under the same base valve motions that shown in Figure 7.6 at also the stoichiometric AFR of 14.7. With a 46% throttle opening, the measured output at the dynamometer of 1.1 Nm under the test engine speed of 1000rpm, which indicates a 5.2 Nm effective engine output after excluding the estimated mechanical loss, is determined as the reference partial load operation.

Then, to achieve the same partial engine load of the reference operation via the proposed HVVA valve motion strategies for unthrottled engine load control, corresponding GA optimizations are conducted. **Error! Reference source not found.** and Table 10 list the identified TPA timings of implementing the IEGR scheme and the VAC scheme for realizing the reference partial engine load operation, while the resultant valve lift profiles from both the simulations and experiments are shown in Figure 7.8 and Figure 7.9, respectively.

Table 9 Optimized TPA timings for partial load operations at 1000rpm/5.2 Nm using IEGR scheme

Optimized TPA timings for partial load operations at 1000rpm/5.2 Nm using IEGR scheme	
TPAHE	122 CA$^\mathbf{o}$
TPALE	372 CA$^\mathbf{o}$
TPAHI	355 CA$^\mathbf{o}$
TPAHE	443 CA$^\mathbf{o}$

It should be noticed that the throttle positions are always maintaining at WOT when conducting the IEGR scheme and the VAC scheme experiments for achieving the same reference partial load of 1000rpm/5.2 Nm since the engine load is no longer controlled by the throttle position. However, the engine is now able to run at leaner mixtures under both proposed strategies, with an AFR of 16.1 for the IEGR scheme and 16.3 for the VAC scheme, which are satisfactorily close to the optimized Lambda values of 1.13 and 1.16, respectively, that identified by the GA optimizer. The mean torque

measured at the dynamometer is at 1.3 Nm for the IEGR scheme, and 1.0 Nm for the VAC scheme, which are indicating an effective engine output of 5.4 Nm and 5.1 Nm, respectively.

Table 10 Optimized TPA timings for partial load operations at 1000rpm/5.2 Nm using VAC scheme

Optimized TPA timings for partial load operations at 1000rpm/5.2 Nm using VAC scheme

TPAHE	118 CA^o
TPALE	279 CA^o
TPAHI	346 CA^o
TPAHE	545 CA^o

Moreover, it is worth to explain that since the nozzle of the EFI system feeds the fuel at a fix frequency while under the same engine speed that inject only once per engine cycle, and the amount of fuel that are fed to the engine per engine cycle is controlled by the duty cycle of a fuel injection square wave embedded in the built-in EFI controller that automatically adapts according to the calculated real-time measurements from the oxygen sensor at the exhaust and ensures the AFR is always maintained at the desired value. Hence, the resulted lean mixture in the performed experiments are not achieved by taking excessive fresh air charge, but reducing the fuel feeding rate, which means the engine's fuel consumption is actually lowered while running with lean mixture than stoichiometric.
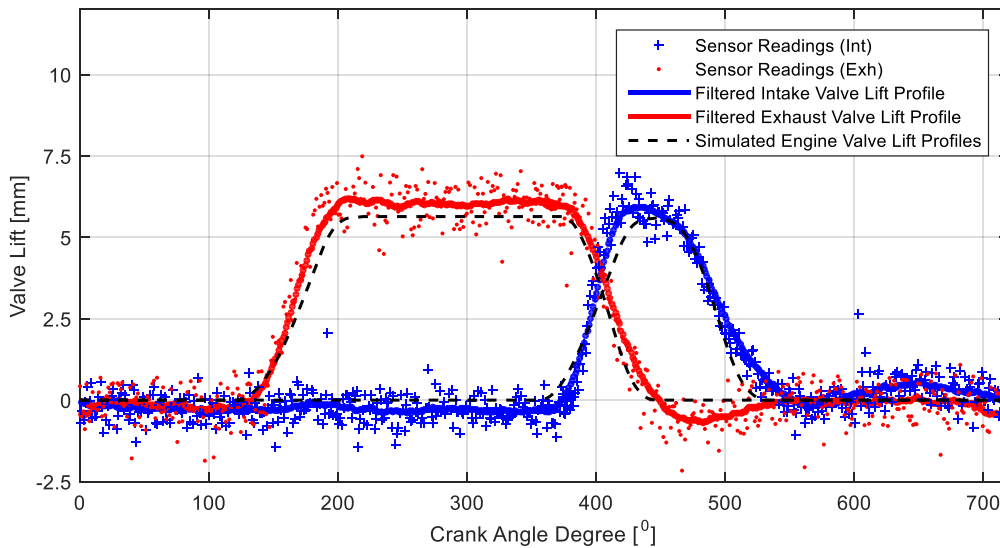
Figure 7.8 Simulated and observed valve lift profiles with the optimized valve timings for 1000rpm/5.2 Nm operation achieved by IEGR scheme

100

To better understand the results of the performed experiments, the following explanations are provided. On one hand, as been explained in the previous chapter, the proved better fuel economy at partial load operations from utilizing the IEGR scheme in this experiment is mainly benefited from the lowered pumping loss, which improves the engine's mechanical efficiency, and the increased in-cylinder temperature and pressure after compression, which increases the engine's thermal efficiency, resulted by the IEGR process. On the other hand, beside the same reason of the lowered pumping losses, the experimentally revealed potentials to the improvements on the engine's fuel economy when running the HVVA engine with the VAC scheme is the realization to the over-expansion effect.
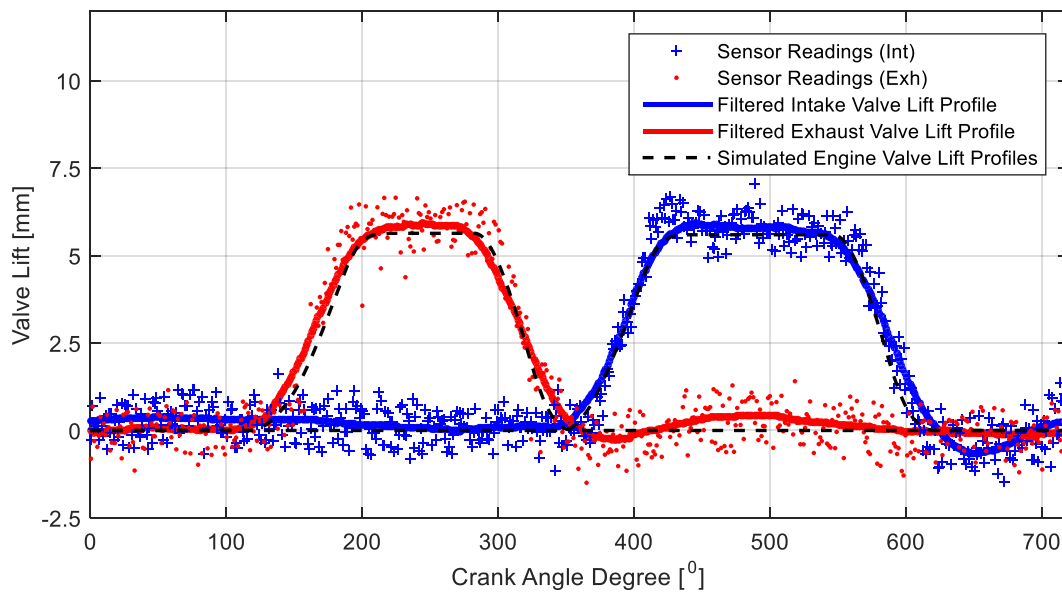
Figure 7.9 Simulated and observed valve lift profiles with the optimized valve timings for 1000rpm/5.2 Nm operation achieved by VAC scheme

In all, by conducting all the partial load test experiments, it can be concluded that these performed experiments demonstrated the HVVA engine with the unthrottled engine load control valve motion strategies is not only able to realize the reference partial engine load operations without throttling, but also proved that the engine could actually run at leaner air-fuel mixtures and gain better fuel economy comparing to the throttling approach of the baseline engine for fulfilling the same partial engine load operation.

7.3 Summary

In this chapter, the actual build of the prototype HVVA engine and the engine test bench are introduced. The prototype HVVA engine is firstly tested with the valve timings of the baseline engine to verify that the HVVA system is able to operate properly on the test engine.

Then, by conducting the designed exemplary experiments, not only that the proposed GA optimization methodologies have been verified as valid for identifying the considered operating parameters of the HVVA engine, but also the experiment results have qualitatively proved that the HVVA engine could actually achieve higher power performance for full load operations by running in the proposed VOC scheme, and gain better fuel economy for partial load operations by adopting the unthrottled engine load control strategies of the IEGR and VAC schemes.

Chapter 8

Conclusions and Future Work

8.1 Conclusions

In this research, by replacing the cam-based valve train with the HVVA system of a single-cylinder gasoline engine, improving potentials for the power and fuel economy performances of the engine were explored. The converted single-cylinder engine was carefully modeled in GT-Suite for physically simulating the resultant engine performance and the behavior of the HVVA system. Thanks to the high adjustability provided by the HVVA system in terms of its continuously variable valve motions, several base HVVA valve motion strategies for full load and partial load operations were developed, and together evolved into the proposed VOC scheme, tunable IEGR scheme, and the VAC scheme.

Corresponding to each of the proposed engine operation schemes, a series of GA optimizations were developed considering all the constraints using co-simulation of MATLAB-Simulink and GT-Suite to identify the optimal operating parameters of the HVVA engine for achieving different objectives under different engine working conditions. In order to make the unthrottled HVVA engine run at different desired engine operations, the proposed GA-based optimization schemes were implemented for optimizing the corresponding HVVA valve motion events, as well as the SA and AFR of the engine for both the full load and partial load operations. With these optimized operating parameters, the HVVA engine was then able to perform all the proposed operation schemes upon different choices of preferences, featuring noticeable improvements on the maximum outputs and overall efficiency of the engine.

In summary, the following benefits and improvements were achieved from using the HVVA system and the proposed methods discussed in this thesis over a cam-based naturally aspirated engine:

❖ *Unthrottled load control.* The engine load is no longer controlled by choking the intake processes with throttle but by adopting the proposed engine operation schemes, namely the VOC, the VAC, and the tunable IEGR schemes, which can grant the engine with the potentials of achieving greater power performance at full load operations and gaining higher efficiency at partial load operations.

❖ *Variable Otto cycle*. By running the HVVA engine in VOC at full load operations with the optimized operating parameters found by the proposed MATLAB-Simulink and GT-Suite coupling GA optimizations, a calculated average of 13.5% improvement to the engine's output across the operating speed range was revealed. The resulted BSFCs, however, were even slightly reduced. A maximum output increment of 16.6% was recognized at 3600 rpm engine speed by the simulations while having the corresponding BSFC been lowered by 5.6% comparing to those of the baseline engine.

❖ *Tunable IEGR feature.* With the unthrottled load control realized by the proposed HVVA strategy with IEGR, the engine's fuel economy at partial load operations can be improved. The simulation results at the 7Nm load point were presented as an example, showing an average saving of 13.1% on the resulted BSFC can be achieved over the entire speed range of the engine with a maximum reduction of 15.8% at 3600 rpm when adopting the operating parameters optimized by the proposed GA approach.

❖ *Variable Atkinson cycle*. The alternative operation scheme for fulfilling partial engine load operations beside the proposed tunable IEGR implementations is the proposed VAC, which could contribute to an average saving on the resulted BSFC at approximately 16.1g/kW·h over the entire sampled speed-load map according to the simulated results. The resulted BSFC of the HVVA engine running at all the sampled speed-load operations while in the VAC mode were found by the simulations and showed the potential improvement to the engine's fuel economy could reach up to 11% when the engine runs at around the mid-high speed and mid-low load operations.

❖ *High flexibility on achieving different engine tunings and convenient way for their implementations.* Running in either the proposed VOC, tunable IEGR or VAC schemes, the HVVA engine is able to continuously adjust its valve motions, EER and EER-to-ECR ratio for fulfilling the desired speed-load operations upon different preferences of the engine performances. With such high flexibility, it could become much easier when the engine needs to update its current tuning or switch among up to as many as is needed pre-tuned modes with different specialized characteristics, since there is no need for hardware modifications or common types of complex mechanisms for realizing IEGR, VVT or VCR. Furthermore, the characteristics of the engine can even be easily updated by re-programming the ECU to meet better with any possible new requirement towards different performance preferences of the engine, e.g., maximizing the

engine outputs at full load operations while considering the fuel efficiency to be maintained at above a certain level, or switching to a priority of achieving lower emissions under certain specified speed-load operation regions. Also, the related parameters, such as the HVVA valve motion events and other considered engine operating parameters, could be identified by using the proposed GA structure with specific-purpose-customized individuals, fitness function and constraints etc.

8.2 Future Work

Based on the work of this research, potential future work could be focused on the following tasks:

- To take better account of the turbulence and swirl variations of the gas flow, and provide more realistic estimations to the combustion process, the work of enclosing both a 3-D combustion model and a set of 3-D manifold models into the current HVVA engine model for acquiring more accurate and detailed combustion estimations could be conducted. By using the 3-D models, the pressure wave actions along the intake and exhaust manifolds could be more accurately noticed, as well as their subsequent impacts to the engine combustion processes. This would result in an acquisition to a set of better-optimized parameters after conducting the GA optimizations, which could diminish the error between the simulated and the actual performances of the engine.

- Apart from the proposed tunable IEGR scheme in this research, which adopts LEVCs to realize the IEGR effect, the alternative approach for achieving the IEGR functionality via EEVCs and LIVOs could also be studied and enclosed as another IEGR implementation scheme of the HVVA engine. By knowing and comparing the pros and cons of these two IEGR schemes, the engine would be able to benefit more by intelligently switching between these two schemes over different engine working conditions when IEGR is required.

- By adopting a more detailed and more accurate combustion model, and having the estimations to the emissions been well calibrated with the access to the specialized equipments for retrieving qualified data of measured emissions, new GA schemes for achieving the specific focus on lowing the engine emissions could be developed. Furthermore, by taking separate considerations on both the warm-engine scenario and the cold-start scenario, this new HVVA engine operation scheme for lowing the engine emissions could be better developed and could be used for constructing new complex implementations.

- Since the work of this research was conducted on the basis of naturally aspirated SI engines, the developments to the proper operation schemes for turbo-charged engines and even for compression ignition engines could also be considered as valuable objectives in the future. In addition, for multi-cylinder engines, even more complexed valve motion strategies could be implemented that may allow the cylinders adopt different strategies while running at the same time.

Bibliography

[1] Amir Khajepour, Mohammad Pournazeri, "Systems and Methods for Variable Valve Actuation", US 9194264 B2 (Patent), issued 2015-11-24.

[2] Michael K. Hidrue, George R. Parsons, "Is there a near-term market for vehicle-to-grid electric vehicles?," Applied Energy, Volume 151, 1 August 2015, Pages 67–76.

[3] João Ribau, Carla Silva, Francisco P. Brito, Jorge Martins, "Analysis of four-stroke, Wankel, and microturbine based range extenders for electric vehicles," Energy Conversion and Management, Volume 58, June 2012, Pages 120–133.

[4] Hong Wang, Yanjun Huang, Hongwen He, Chen Lv, Wei Liu, Amir Khajepour, "Chapter 5 - Energy Management of Hybrid Electric Vehicles, In Modeling," Dynamics and Control of Electrified Vehicles, 2018, Pages 159-206, ISBN 9780128127865, https://doi.org/10.1016/B978-0-12-812786-5.00005-7.

[5] J. Wang, "Hybrid Robust Air-path Control for Diesel Engines Operating Conventional and Low Temperature Combustion Modes," IEEE Transactions of Control Systems Technology, 2008.

[6] Lyle E. Kocher, "Physically-Based Modeling, Estimation and Control of the Gas Exchange and Combustion Processes for Diesel Engines Utilizing Variable Intake Valve Actuation," PhD thesis of Purdue University, West Lafayette, Indiana, 2012.

[7] Devesh Upadhyay, Vadim I. Utkin, Giorgio Rizzoni, "Multivariable Control Design for Intake Flow Regulation of A Diesel Engine Using Sliding Mode," Proc. IFAC 15th Triennial World Congress, pages 1389–1394, 2002.

[8] Robert Fairbrother, Thomas Leifert, Rudolf Gande, Georg Salentinig, "Accurate Gas Exchange and Combustion Analysis Directly at the Test Bed," ASME Internal Combustion Engine Division Fall Technical Conference, ICEF2012-92194, 2012.

[9] Heywood J. B., "Internal Combustion Engine Fundamentals," Mc Graw-Hill, 1988.

[10] George A. Goodenough, John B. Baker, "A Thermodynamic Analysis of Internal-combustion Engine Cycles," Bulletin No. 160, Engineering Experiment Station, University of Illinois, 1927.

[11] J.Y. Pan, G.Q. Shu, H.Q. Wei, "Interaction of Flame Propagation and Pressure Waves During Knocking Combustion in Spark-ignition Engines," Combustion Science and Technology. 186 (2014) 192–209, 2014.

[12] Y. Yang, J.E. Dec, N. Dronniou, M. Sjöberg, "Partial Fuel Stratification to Control HCCI Heat Release Rates: Fuel Composition and Other Factors Affecting Pre-ignition Reactions of Two-stage Ignition Fuels," SAE Technical Paper, 2011–01–1359, 2011.

[13] C. Stovell, J. Chiu, R. Hise, P. Swenson, "Effect of Reduced Boost Air Temperature on Knock Limited Brake Mean Effective Pressure (BMEP)," SAE Technical Paper, 2001–01–3682, 2001.

[14] J.Y. Pan, G.Q Shu, H.Q. Wei, "Research on In-cylinder pressure Oscillation Characteristic During Knocking Combustion in Spark-ignition Engine," Fuel 120 (2014) 150–157, 2014

[15] Jiaying Pan, Gequn Shu, Peng Zhao, Haiqiao Wei, Zheng Chen, "Interactions of Flame Propagation, Auto-ignition and Pressure Wave During Knocking Combustion," Combustion and Flame, 000(2015)1-10, 2015

[16] Wladyslaw Mitianiec, Krzysztof Sliwinski, "Combustion Process of Oxygen Enriched Mixture in SI Engine with EGR System," ResearchGate Conference Paper, 2014.

[17] Sanjeet Limbu, "Swirling Flow for Engine Combustion," ResearchGate Artical, 2014.

[18] Charles Fayette Taylor, "The Internal-Combustion Engine in Theory and Practice," The M.I.T. Press, Cambridge, Massachusetts USA, 1986.

[19] J. Chauvin, N. Petit, P. Rouchon, G. Corde, C. Vigild, "Air Path Estimation on Diesel HCCI Engine," SAE 2006-01-1085, 2006.

[20] T. Leroy, G. ALix, J. Chauvin, A. Duparchy, F. Le Berr, "Modelling Fresh Air Charge and Residual Gas Fraction on A Dual Independent Variable Valve Timing SI Engine," SAE 2008-01-0983, 2008.

[21] E. Hendricks, A. Chevalier, M. Jensen, S. Sorenson, D. Trumpy, J. Asik, "Modelling of the Intake Manifold Filling Dynamics." SAE 960037, 1996.

[22] Ove F. Storset, Anna G. Stefanopoulou, Roy Smith, "Adaptive Air Charge Estimation for Turbocharged Diesel Engines Without Exhaust Gas Recirculation," ASME Journal of Dynamic Systems, 126:633–643, 2004.

[23] Mrdjan Jankovic, Stephen W. Magner, "Variable Cam Timing: Consequences to Automotive Engine Control Design," IFAC 15th Trigeminal World Congress, Barcelona, Spain, 2002.

[24] G. De Nicolao, R. Scattolini, C. Siviero, "Modelling the Volumetric Efficiency of IC Engines: Parametric, Non-parametric and Neural Techniques," Control Engineering Practice, 4(10):1405-1415, 1996.

[25] Hamid B. Servati, Robert G. DeLosh, "A Regression Model for Volumetric Efficiency," SAE 860328, 1986.

[26] Alexander Stotsky, Ilya Kolmanovsky, "Application of Input Estimation Techniques to Charge Estimation and Control In Automotive Engines," Control Engineering Practice, 10:1371-1383, 2002.

[27] Gilles Corde, Yvan Bianco, Yves Lecluse, "Air Mass Flow Rate Observer Applied to SI AFR Control," SAE 952460, 1995.

[28] L. Kocher, E. Koeberlein, D. G. Van Alstine, K. Stricker, G. Shaver, "Physically Based Volumetric Efficiency Model for Diesel Engines Utilizing Variable Intake Valve Actuation," International Journal of Engine Research, doi: 10.1177/1468087411424378, 2011.

[29] Turin, R., Zhang, R., and Chang, M., "Volumetric Efficiency Model for Variable Cam-Phasing and Variable Valve Lift Applications," SAE Technical Paper 2008-01-0995, 2008.

[30] Gray C., "A Review of Variable Engine Valve Timing," SAE paper 880386, 1988.

[31] Dresner, T. and Barkan, P., "A Review and Classification of Variable Valve Timing Mechanisms," SAE Technical Paper 890674, 1989.

[32] Ahmad, T. and Theobald, M.A., "A Survey of Variable-Valve-Actuation Technology," SAE paper 891674, 1989.

[33] Mitsubishi Motors Corporation. "Mitsubishi innovative valve timing electronic control system," Available at http://www.mitsubishi-motors.com/en/innovation/technology/library/mivec.html, 2011.

[34] A. AG, "Audi valvelift system," Audi, 2011. [Online]. Available at: http://www.audi-technology-portal.de/en/drivetrain/fsi-tsi-engines/audivalvelift-system_en/.

[35] D. S. C. Brustle, "VarioCam Plus–A Highlight of the Porsche 911 Turbo Engine," SAE Technical Paper Series, vol. 01, no. 0245, p. 2, 2001.

[36] K. Colwell, "Timing Changes: How Honda's VTEC Variable-Timing System Works," Car and Driver, 7 August 2015. [Online]. Available at: http://blog.caranddriver.com/timing-changes-how-hondas-vtec-variabletiming-system-works/.

[37] Bimmertips, "The basics of bmw vanos variable valve timing system," Available at: http://bimmertips.com/basics-bmw-vanos-variable-valve-timing/, 2016.

[38] Division on Engineering National Research Council and Physical Sciences, "Assessment of Fuel Economy Technologies for Light-Duty Vehicles," National Academies Press, 2010.

[39] Schechter, M., Levin, M., "Camless Engine," SAE Technical Paper 960581, 1996.

[40] Trajkovic, S., Tunestal, P., Johansson, B., "Investigation of Different Valve Geometries and Valve Timing Strategies and Their Effect on Regenerative Efficiency for A Pneumatic Hybrid with Variable Valve Actuation," SAE Int. J. Fuels Lubr. 1(1):1206-1223, 2008.

[41] Cope, D., Wright, A., "Electromagnetic Fully Flexible Valve Actuator," SAE Technical Paper 2006-01 -0044, 2006.

[42] Shiao, Y., Dat, L. V., "Actuator Control for A New Hybrid Electromagnetic Valvetrain in Spark Ignition Engines." Journal of Automobile Engineering, 227(6), 789, 2013.

[43] Mohammad Pournazeri, "Development of a New Fully Flexible Hydraulic Variable Valve Actuation System," PhD thesis in Mechanical Engineering, University of Waterloo, 2012.

[44] Øyvind Gundersen, "Free Valve Technology," Master of Science thesis, Stockholm Sweden, 2009.

[45] Allan Geert Nielsen, "Free valve technology," Available at http://www.freevalve.com/technology/freevalve-technology/, 2017.

[46] Tufail Habib, "Modeling and investigation of electromechanical valve train actuator at simulated pressure conditions," Proceedings of NordDesign 2012, the 9th NordDesign conference, Aarlborg University, Denmark. 22-24.08.2012, 2012.

[47] Mohammad Pournazeri, Amir Khajepour, "Precise lift control in a new variable valve actuation system using discrete-time sliding mode control," Mechanism and Machine Theory, Volume 99, May 2016, Pages 217-235, ISSN 0094-114X.

[48] Stein, R.A., Galietti, K.M. and Leone, T.G., "Dual Equal VCT – A Variable Camshaft Timing Strategy for Improved Fuel Economy and Emissions," SAE paper 950975, 1995.

[49] Leone, T.G., Christenson, E.J. and Stein, R.A., "Comparison of Variable Camshaft Timing Strategies at Part Load," SAE paper 960584, 1996.

[50] Inoue, K., Nagahiro, K., Ajiki, Y. and Kishi, N., "A High Power, Wide Torque Range Efficient Engine with A Newly Developed Variable Valve Lift and Timing Mechanism," SAE paper 890675, 1989.

[51] Kreuter, P., Heuser, P., and Schebitz, M., "Strategies to Improve SI-Engine Performance by Means of Variable Intake Lift, Timing and Duration," SAE Technical Paper 920449, 1992, doi:10.4271/920449.

[52] Nan Li, Hui Xie, Tao Chen, Le Li, Hua Zhao, "The effects of intake backflow on in-cylinder situation and auto ignition in a gasoline controlled auto ignition engine," Applied Energy, Volume 101, January 2013, Pages 756-764, ISSN 0306-2619.

[53] Hatano, K., Iida, K., Higashi, H., and Murata, S., "Development of a New Multi-Mode Variable Valve Timing Engine," SAE Technical Paper 930878, 1993, doi:10.4271/930878.

[54] G. Fontana, E. Galloni, "Variable valve timing for fuel economy improvement in a small spark-ignition engine," Applied Energy, Volume 86, Issue 1, January 2009, Pages 96-105, ISSN 0306-2619.

[55] F. Bonatesta, G. Altamore, J. Kalsi, M. Cary, "Fuel economy analysis of part-load variable camshaft timing strategies in two modern small-capacity spark ignition engines," Applied Energy, Volume 164, 15 February 2016, Pages 475-491, ISSN 0306-2619.

[56] Jinxing Zhao, Min Xu, "Fuel economy optimization of an Atkinson cycle engine using genetic algorithm," Applied Energy, Volume 105, May 2013, Pages 335-348, ISSN 0306-2619.

[57] Yun-long Bai, Zhi Wang and Jian-xin Wang, "Part-load characteristics of direct injection spark ignition engine using exhaust gas trap," Applied Energy, Volume 87, Issue 8, August 2010, Pages 2640-2646, ISSN 0306-2619.

[58] Haiqiao Wei, Tianyu Zhu, Gequn Shu, Linlin Tan, Yuesen Wang, "Gasoline engine exhaust gas recirculation – A review," Applied Energy, Volume 99, 2012, Pages 534-544, ISSN 0306-2619.

[59] V. De Bellis, A. Gimelli, M. Muccillo, "Effects of Pre-Lift Intake Valve Strategies on the Performance of a DISI VVA Turbocharged Engine at Part and Full Load Operation," Energy Procedia, Volume 81, 2015, Pages 874-882, ISSN 1876-6102.

[60] Xiangyu Zhang, Hu Wang, Zunqing Zheng, Rolf D. Reitz, Mingfa Yao, "Effects of late intake valve closing (LIVC) and rebreathing valve strategies on diesel engine performance and emissions at low loads," Applied Thermal Engineering, Volume 98, 5 April 2016, Pages 310-319, ISSN 1359-4311.

[61] Xiangyu Zhang, Hu Wang, Zunqing Zheng, Rolf Reitz, Mingfa Yao, "Experimental investigations of gasoline partially premixed combustion with an exhaust rebreathing valve strategy at low loads," Applied Thermal Engineering, Volume 103, 25 June 2016, Pages 832-841, ISSN 1359-4311.

[62] Manuel A., Gonzalez D., "Late Intake Valve Closing and Exhaust Rebreathing in a V8 Diesel Engine for High Efficiency Clean Combustion," DEER Conference, GM-DOE Agreement No. DE-FC26-05NT42415, 2010.

[63] Lenz, H., Wichart, K., and Gruden, D., "Variable Valve Timing-A Possibility to Control Engine load without Throttle," SAE Technical Paper 880388, 1988, doi:10.4271/880388.

[64] Urushihara, T., Hiraya, K., Kakuhou, A., and Itoh, T., "Expansion of HCCI Operating Region by the Combination of Direct Fuel Injection, Negative Valve Overlap and Internal Fuel Reformation," SAE Technical Paper 2003-01-0749, 2003, doi:10.4271/2003-01-0749.

[65] Cairns, A., Blaxill, H., and Irlam, G., "Exhaust Gas Recirculation for Improved Part and Full Load Fuel Economy in a Turbocharged Gasoline Engine," SAE Technical Paper 2006-01-0047, 2006, doi:10.4271/2006-01-0047.

[66] Tuttle, J., "Controlling Engine Load by Means of Early Intake-Valve Closing," SAE Technical Paper 820408, 1982, doi:10.4271/820408.

[67] Shiga S, Hirooka Y, Yagi S., "Effects of over-expansion cycle in a spark-ignition engine using late-closing of intake valve and its thermodynamic consideration of the mechanism," International Journal of Automotive Technology, 2001; 2(1): 1-7.

112

[68] Tuttle, J., "Controlling Engine Load by Means of Late Intake-Valve Closing," SAE Technical Paper 800794, 1980, doi:10.4271/800794.

[69] Blakey, S., Saunders, R., Ma, T., and Chopra, A., "A Design and Experimental Study of an Otto Atkinson Cycle Engine Using Late Intake Valve Closing," SAE Technical Paper 910451, 1991, doi:10.4271/910451.

[70] Tie Li, Yi Gao, Jiasheng Wang, Ziqian Chen, "The Miller cycle effects on improvement of fuel economy in a highly boosted, high compression ratio, direct-injection gasoline engine: EIVC vs. LIVC," Energy Conversion and Management, Volume 79, March 2014, Pages 59-65, ISSN 0196-8904.

[71] Hara, S., Nakajima, Y., and Nagumo, S., "Effects of intake-Valve Closing Timing on Spark-Ignition Engine Combustion," SAE Technical Paper 850074, 1985, doi:10.4271/850074.

[72] Battistoni, M. and Mariani, F., "Fluid Dynamic Study of Unthrottled Part Load SI Engine Operations with Asymmetric Valve Lifts," SAE Technical Paper 2009-24-0017, 2009, doi:10.4271/2009-24-0017.

[73] Jinxing Zhao, "Research and application of over-expansion cycle (Atkinson and Miller) engines – A review," Applied Energy, Volume 185, Part 1, 1 January 2017, Pages 300-319, ISSN 0306-2619.

[74] R. Patel, N. Ladommatos, P.A. Stansfield, G. Wigley, C.P. Garner, G. Pitcher, J.W.G. Turner, H. Nuglisch, J. Helie, "Un-throttling a direct injection gasoline homogeneous mixture engine with variable valve actuation," International Journal of Engine Research, Vol-11, Issue 6, pp. 391 - 411, 2010.

[75] E. Sher, T. Bar-Kohany, "Optimization of variable valve timing for maximizing performance of an unthrottled SI engine—a theoretical study," Energy, Volume 27, Issue 8, August 2002, Pages 757-775, ISSN 0360-5442.

[76] Xudong Zhen, Yang Wang, Shuaiqing Xu, Yongsheng Zhu, Chengjun Tao, Tao Xu, Mingzhi Song"The engine knock analysis – An overview," Applied Energy, Volume 92, April 2012, Pages 628–636.

[77] Vichi, G., Romani, L., Ferrara, G., Carmignani, L. et al., "Improvement of the Specific Fuel Consumption at Partial Load in SI Engines by Design Strategies based on High Compression Ratio," SAE Technical Paper 2014-32-0060, 2014, doi:10.4271/2014-32-0060.

[78] Rodrigo C. Costa, José R. Sodré, "Compression ratio effects on an ethanol/gasoline fuelled engine performance," Applied Thermal Engineering, Volume 31, Issues 2–3, February 2011, Pages 278–283.

[79] Nilsson, Y., Eriksson, L., and Gunnarsson, M., "A Model for Fuel Optimal Control of a Spark-Ignited Variable Compression Engine," SAE Technical Paper 2006-01-0399, 2006, doi:10.4271/2006-01-0399.

[80] Thiago Hoeltgebaum, Roberto Simoni, Daniel Martins, "Reconfigurability of engines: A kinematic approach to variable compression ratio engines," Mechanism and Machine Theory, Volume 96, Part 2, February 2016, Pages 308–322.

[81] Shuhn-Shyurng Hou, "Comparison of performances of air standard Atkinson and Otto cycles with heat transfer considerations," Energy Conversion and Management, Volume 48, Issue 5, May 2007, Pages 1683–1690.

[82] J. Atkinson, "Gas Engine," US 367496 A (Patent), issued 1887-08-02.

[83] Miller Ralph, "Supercharged Engine," US 2817322 A (Patent), issued 1957-12-24.

[84] Pertl, P., Trattner, A., Abis, A., Schmidt, S. et al., "Expansion to Higher Efficiency - Investigations of the Atkinson Cycle in Small Combustion Engines," SAE Technical Paper 2012-32-0059, 2012, doi:10.4271/2012-32-0059.

[85] Tie Li, Yi Gao, Jiasheng Wang, Ziqian Chen, "The Miller cycle effects on improvement of fuel economy in a highly boosted, high compression ratio, direct-injection gasoline engine: EIVC vs. LIVC," Energy Conversion and Management, Volume 79, March 2014, Pages 59–65.

[86] Feng, R., Li, Y., Yang, J., FU, J. et al., "Investigations of Atkinson Cycle Converted from Conventional Otto Cycle Gasoline Engine," SAE Technical Paper 2016-01-0680, 2016, doi:10.4271/2016-01-0680.

[87] Luria, D., Taitel, Y., and Stotter, A., "The Otto-Atkinson Engine - A New Concept in Automotive Economy," SAE Technical Paper 820352, 1982, doi:10.4271/820352.

[88] Blakey, S., Saunders, R., Ma, T., and Chopra, A., "A Design and Experimental Study of an Otto Atkinson Cycle Engine Using Late Intake Valve Closing," SAE Technical Paper 910451, 1991, doi:10.4271/910451.

[89] Boggs, D., Hilbert, H., and Schechter, M., "The Otto-Atkinson Cycle Engine-Fuel Economy and Emissions Results and Hardware Design," SAE Technical Paper 950089, 1995, doi:10.4271/950089.

[90] Saunders, R. and Abdul-Wahab, E., "Variable Valve Closure Timing for Load Control and the Otto Atkinson Cycle Engine," SAE Technical Paper 890677, 1989, doi:10.4271/890677.

[91] Eid Mohamed, "Modeling and performance evaluation of an electromechanical valve actuator for a camless IC engine," International Journal of Energy and Environment, 2012; 3(2)275-294.

[92] A-F.M. Mahrous, A. Potrzebowski, M.L. Wyszynski, H.M. Xu, A. Tsolakis, P. Luszcz, "A modelling study into the effects of variable valve timing on the gas exchange process and performance of a 4-valve DI homogeneous charge compression ignition (HCCI) engine," Energy Conversion and Management, Volume 50, Issue 2, February 2009, Pages 393-398, ISSN 0196-8904.

[93] G. D'Errico, T. Cerri, G. Pertusi, "Multi-objective optimization of internal combustion engine by means of 1D fluid-dynamic models, Applied Energy," Volume 88, Issue 3, March 2011, Pages 767-777, ISSN 0306-2619.

[94] Necla Kara Togun, Sedat Baysec, "Prediction of torque and specific fuel consumption of a gasoline engine by using artificial neural networks," Applied Energy, Volume 87, Issue 1, January 2010, Pages 349-355, ISSN 0306-2619.

[95] Mustafa Gölcü, Yakup Sekmen, Perihan Erduranlı, M. Sahir Salman, "Artificial neural-network based modeling of variable valve-timing in a spark-ignition engine," Applied Energy, Volume 81, Issue 2, June 2005, Pages 187-197, ISSN 0306-2619.

[96] Donghoon Lee, Li Jiang, Hakan Yilmaz, Anna G. Stefanopoulou, "Preliminary Results on Optimal Variable Valve Timing and Spark Timing Control via Extremum Seeking," IFAC Proceedings Volumes, Volume 43, Issue 18, 2010, Pages 377-384, ISSN 1474-6670.

[97] George Thomas, Dan Simon, John Michelini, "Biogeography-based optimization of a variable camshaft timing system," Engineering Applications of Artificial Intelligence, Volume 45, October 2015, Pages 376-387, ISSN 0952-1976.

[98] K. Atashkari, N. Nariman-Zadeh, M. Gölcü, A. Khalkhali, A. Jamali, "Modelling and multi-objective optimization of a variable valve-timing spark-ignition engine using polynomial neural networks and evolutionary algorithms," Energy Conversion and Management, Volume 48, Issue 3, March 2007, Pages 1029-1041, ISSN 0196-8904.

[99] Necla Togun, Sedat Baysec, "Genetic programming approach to predict torque and brake specific fuel consumption of a gasoline engine," Applied Energy, Volume 87, Issue 11, November 2010, Pages 3401-3408, ISSN 0306-2619.

[100] Ugur Kesgin, "Genetic algorithm and artificial neural network for engine optimisation of efficiency and NOx emission," Fuel, Volume 83, Issues 7–8, May 2004, Pages 885-895, ISSN 0016-2361.

[101] Y.G. Li, P. Pilidis, "GA-based design-point performance adaptation and its comparison with ICM-based approach," Applied Energy, Volume 87, Issue 1, 2010, Pages 340-348, ISSN 0306-2619.

[102] Yangtao Li, Amir Khajepour, Cécile Devaud, Kaimin Liu, "Power and fuel economy optimizations of gasoline engines using hydraulic variable valve actuation system," Applied Energy, Volume 206, 2017, Pages 577-593, ISSN 0306-2619.

[103] Ganesan, "Internal Combustion Engines (4th Edition)," McGraw Hill Education (India) Pvt Ltd., 2012.

[104] Shizuo Sasaki, Daisaku Sawada, Takanori Ueda, Hiroyuki Sami, "Effects of EGR on direct injection gasoline engine," JSAE Review, Volume 19, Issue 3, 1998, Pages 223-228, ISSN 0389-4304.

[105] Sara McAllister, Jyh-Yuan Chen, A. Carlos Fernandez-Pello, "Fundamentals of Combustion Processes," Springer Science & Business Media, 2011.

[106] Gunnar Stiesch, "Modeling Engine Spray and Combustion Processes," Springer Science & Business Media, 2013.

[107] H. N. Gupta, "Fundamentals of Internal Combustion Engines," PHI Learning Pvt. Ltd., 2012.

[108] M. C. Ramaswamy, "I.C. Engines and Combustion," in Anna University, Chennai-600 025, India, Allied Publishers, 1997.

[109] Mohammad S. Siddiqui, "Hydraulic Variable Valve Actuation on a Single Cylinder Engine," Master of Applied Science thesis, University of Waterloo, Ontario, Canada, 2017.

[110] Gamma Technologies, "GT-Suite reference manual - context help for engine reference templates," GT-SUITE, Version 2016.

[111] Douaud, A. and Eyzat, P., "Four-Octane-Number Method for Predicting the Anti-Knock Behavior of Fuels and Engines," SAE Technical Paper 780080, 1978, doi:10.4271/780080.

Appendix A

The simplified valve-lift-profile-based gas exchange model is able to estimate the resultant VE, EGR rate and total pumping losses under the given inputs, which are the engine speed, valve lift profiles and the in-cylinder pressure at EVO. The governing equations for describing the relationships among the key variables are written in Eqs. (9.1-9.4) with the definitions to the parameters listed in Table 11.

$$V = \frac{\pi d^2 x}{4} + V_C \quad and \quad x = r\left[(1-\cos\theta) + \frac{l}{r}\left(1 - \sqrt{1-\left(\frac{r}{l}\right)^2 \sin^2\theta}\right)\right] \tag{9.1}$$

$$\dot{m}_{exh} = A_{exh}Cd_1\sqrt{2\rho_1 P_{up}\left(\frac{k}{k-1}\right)\left[\left(\frac{P_{down}}{P_{up}}\right)^{\frac{2}{k}} - \left(\frac{P_{down}}{P_{up}}\right)^{\frac{k+1}{k}}\right]} \tag{9.2}$$

$$\dot{m}_{int} = A_{int}Cd_2\sqrt{2\rho_2 P_{up}\left(\frac{k}{k-1}\right)\left[\left(\frac{P_{down}}{P_{up}}\right)^{\frac{2}{k}} - \left(\frac{P_{down}}{P_{up}}\right)^{\frac{k+1}{k}}\right]} \tag{9.3}$$

$$P_C = f(\dot{m}_{int}, \dot{m}_{exh}, V) \tag{9.4}$$

Table 11 Nomenclatures for Eqs. (9.1-9.4)
Nomenclatures for Eqs. (9.1-9.4)

V	Total In-cylinder Volume	P_{up}	Upstream Pressure
d	Diameter of the Piston	P_{down}	Downstream Pressure
V_C	Cylinder Dead Volume	k	Specific heat capacity ($k = C_P / C_V = 1.4$)
x	Piston Displacement	θ	Crank Angle Degree
A_{exh}	Effective Valve Opening Area of the Exhaust Valve	A_{int}	Effective Valve Opening Area of the Intake Valve
l	Length of the Connecting Rod	Cd_1	Discharge Coefficient of the Exhaust Valve
r	Length of the Crank Arm	Cd_2	Discharge Coefficient of the Intake Valve
$\dot{m}_{exh}$	Gas Mass Flow at Exhaust Valve	ρ_1	Average Density of the Gas that Flows Through the Exhaust Valve under Upstream Conditions
$\dot{m}_{int}$	Gas Mass Flow at Intake Valve	ρ_2	Average Density of the Gas that Flows Through the Intake Valve under Upstream Conditions

In this model, apart from all the prerequisite calculations and all the geometric specifications of the engine components, the inputs are the valve lift profiles, engine speed and in-cylinder initial exhaust pressure. In order to make a better capture to the gas exchange processes of any specific engine, the model is embedded with several look-up tables, such as discharge coefficient maps and in-cylinder gas temperature increment map, which are obtained from experimental tests and could indicate some of the unique characteristics of the engine. A simplified illustrative chart of the model is shown in Figure A.1.
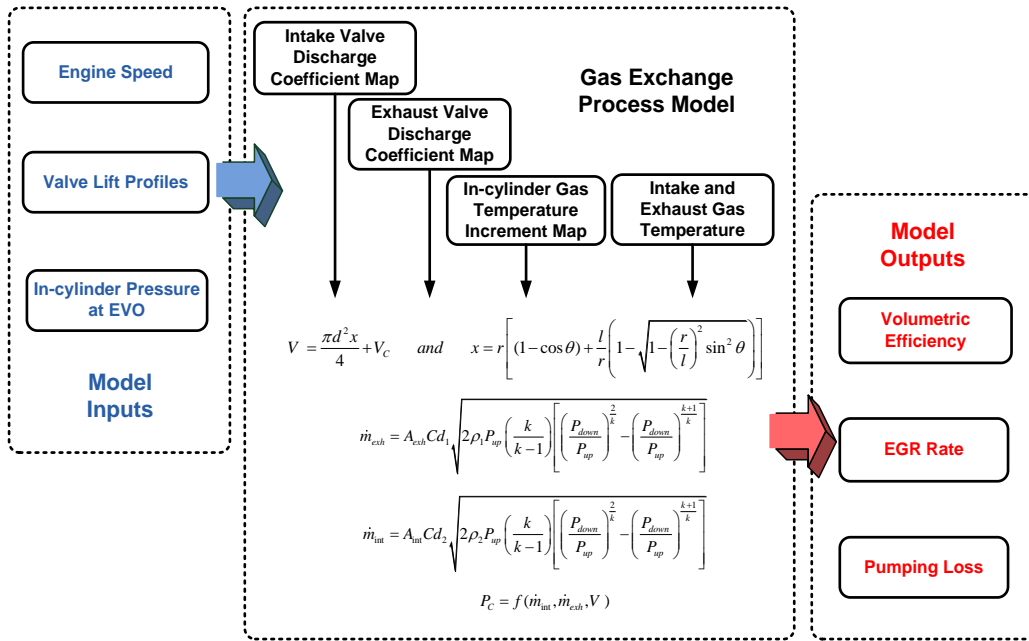

Figure A.1 Simplified illustrative chart of the model

The model was validated by a set of experimental data acquired from a 4-cylinder engine tests. Figure A.2 shows the tendencies of the simulated volumetric efficiency and the experimental measurements of the test engine, and it can be observed that they are fairly in agreement to each other.
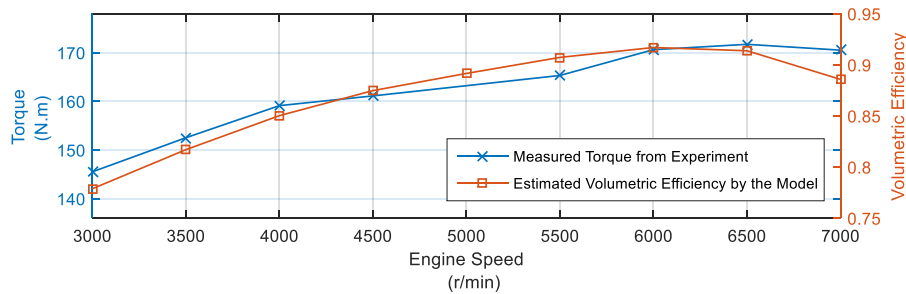

Figure A.2 Model validation result by experimental data of the 4-cylinder test engine

Appendix B

As the effective power of the engine P_e can be expressed as a function of the engine output torque T and engine speed n:

$$P_e = \frac{2\pi nT}{60} \times 10^{-3} = \frac{nT}{9550} \tag{9.5}$$

and also can be calculated by

$$P_e = \frac{P_{me}iV_hn}{30\tau} \tag{9.6}$$

where P_{me}, V_h, i and τ indicate the mean effective pressure, piston displacement, number of cylinders and number of strokes per engine cycle, respectively. By equating Eq. (9.5) and Eq. (9.6), and solving for T, Eq. (9.7) and Eq. (9.8) are derived.

$$\frac{P_{me}iV_hn}{30\tau} = \frac{nT}{9550} \tag{9.7}$$

$$T = \frac{318.33P_{me}iV_h}{\tau} \tag{9.8}$$

Table 12 Nomenclatures for Appendix B
Nomenclatures for Appendix B

T	Engine output torque	Q_{fuel}	Total energy contained by the fuel injected per cylinder per engine cycle
V_h	Piston displacement	η_i	Indicated thermal efficiency
n	Engine speed	g_b	Mass of the injected fuel per cylinder per engine cycle
τ	Number of strokes per engine cycle	H_u	Fuel heating value
P_e	Effective power of the engine	α	Excess air coefficient
P_{me}	In-cylinder mean effective pressure	m_l	Actual intake gas mass per cylinder per engine cycle
i	Number of cylinders	l_0	Theoretical air-fuel ratio ($l_0 = c_1 : c_2$)
P_{mi}	Mean indicated pressure	η_v	Volumetric efficiency
η_m	Mechanical efficiency	ρ_s	Density of the fresh gas under the status of the intake manifold
W_i	Indicated work per cylinder per engine cycle	m_0	Theoretical total fresh gas mass for filling up the displacement volume

Then, with the nomenclatures listed in Table 12, the in-cylinder mean effective pressure P_{me} can be calculated as:

$$P_{me} = P_{mi}\eta_m = \frac{W_i}{V_h}\eta_m = \frac{Q_{fuel}\eta_i}{V_h}\eta_m \tag{9.9}$$

By substituting the expression of Q_{fuel} for gasoline engines, which is found by

$$Q_{fuel} = g_b H_u = m_l \frac{c_2}{\alpha c_1 + c_2} H_u = \frac{\eta_v m_0 c_2}{\alpha c_1 + c_2} H_u = \frac{\eta_v V_h \rho_s c_2}{\alpha c_1 + c_2} H_u \tag{9.10}$$

into Eq. (9.9), respectively, it becomes

$$P_{me} = \frac{H_u \rho_s \eta_i \eta_m \eta_v c_2}{\alpha c_1 + c_2} \tag{9.11}$$

Eventually, by substituting Eq. (9.11) into Eq. (9.8), the relationship between the engine output torque and the volumetric efficiency are found:

$$T = \frac{318.33 H_u \rho_s \eta_i \eta_m \eta_v c_2 i V_h}{\tau \alpha c_1 + \tau c_2} \tag{9.12}$$

Since for the same engine running under a certain type of engine cycle, all the other variables remain as constants in Eq. (9.12) except for η_v and η_i. However, η_i is majorly affected by α, and only has a negligible varying due to the change of η_v, hence,

$$\frac{318.33 H_u \rho_s \eta_i \eta_m c_2 i V_h}{\tau \alpha c_1 + \tau c_2} \approx \text{Constant} \tag{9.13}$$

Therefore, it can be considered that the engine output torque is directly proportional to the volumetric efficiency.

$$T \propto \eta_v \tag{9.14}$$